

## CLUSTER STRUCTURES IN SCHUBERT VARIETIES IN THE GRASSMANNIAN

K. SERHIYENKO, M. SHERMAN-BENNETT, AND L. WILLIAMS

ABSTRACT. In this article we explain how the coordinate ring of each (open) Schubert variety in the Grassmannian can be identified with a cluster algebra, whose combinatorial structure is encoded using (target labelings of) Postnikov’s *plabic graphs*. This result generalizes a theorem of Scott [Sco06] for the Grassmannian, and proves a folklore conjecture for Schubert varieties that has been believed by experts since [Sco06], though the statement was not formally written down until Müller-Speyer explicitly conjectured it [MS16a]. To prove this conjecture we use a result of Leclerc [Lec16], who used the module category of the preprojective algebra to prove that coordinate rings of many Richardson varieties in the complete flag variety can be identified with cluster algebras. Our proof also uses a construction of Karpman [Kar16] to build plabic graphs associated to reduced expressions. We additionally generalize our result to the setting of skew Schubert varieties; the latter result uses *generalized* plabic graphs, i.e. plabic graphs whose boundary vertices need not be labeled in cyclic order.

## CONTENTS

1. Introduction	1
2. Background on cluster structures and plabic graphs	6
3. The rectangles seed associated to a skew Schubert variety	10
4. Obtaining the rectangles seed from a bridge graph	11
5. Obtaining the rectangles seed from Leclerc’s categorical cluster structure	17
6. The proofs of Theorem 1.5 and Theorem 1.6	34
7. Applications	38
Appendix A. Skew Schubert varieties	40
Appendix B. A cluster structure not realizable by generalized plabic graphs	42
References	43

## 1. INTRODUCTION

The main goal of this paper is to show that the coordinate ring of (the affine cone over) any (open) Schubert variety of the Grassmannian (embedded into projective space via the Plücker embedding) can be identified with a cluster algebra, whose combinatorial structure is described explicitly in terms of plabic graphs. *Cluster algebras* are a class of commutative rings which were introduced by Fomin and Zelevinsky [FZ02]; they are connected to many fields of mathematics including Teichmüller theory and quiver representations, and their generators satisfy many nice properties, including the *Laurent phenomenon* [FZ02] and *positivity theorem* [LS15, GHKK14]. *Plabic graphs* are certain planar bicolored graphs which were introduced by Postnikov [Pos]; plabic graphs (or rather an equivalent object, namely alternating strand diagrams) were subsequently used by Scott [Sco06] to show that the coordinate ring of the affine cone over the Grassmannian in its Plücker embedding *admits a cluster algebra structure*, i.e. it can be identified with a cluster algebra.

There is a natural plabic graph generalization of Scott’s construction which experts have believed for some time should give a cluster structure for (open) Schubert varieties (and more generally, open positroid

---

*Date:* December 15, 2024.

*Key words and phrases.* Grassmannians, cluster algebras.

varieties). This construction was stated explicitly as a conjecture in a recent paper of Müller-Speyer [MS16b], who provided some evidence in [MS16a]. The conjecture can be stated roughly as follows.

**Conjecture 1.1.** *Let  $G$  be a reduced plabic graph corresponding to an (open) Schubert (or more generally an open positroid) variety. Then the target labeling of the faces of  $G$  (which we identify with a collection of Plücker coordinates) together with the dual quiver of  $G$  gives rise to a seed for a cluster structure on the coordinate ring of the open Schubert (or positroid) variety.*

Meanwhile, Leclerc [Lec16] constructed a subcategory  $\mathcal{C}_{v,w}$  of the module category of the preprojective algebra, that has a cluster structure, to show that the coordinate ring of each open Richardson variety  $\mathcal{R}_{v,w}$  of the complete flag variety contains a subalgebra which is a cluster algebra; when  $w$  has a factorization of the form  $w = xv$  with  $\ell(w) = \ell(x) + \ell(v)$ , he showed that this subalgebra coincides with the coordinate ring. Because open Schubert varieties are isomorphic to open Richardson varieties with the above property, Leclerc’s result implies that their coordinate rings admit a cluster structure. However, Leclerc’s description of the cluster structure is very different from the plabic graph description and is far from explicit: e.g. his cluster quiver is defined in terms of morphisms of modules of the preprojective algebra.

In this paper we prove Conjecture 1.1 for Schubert varieties by relating Leclerc’s cluster structure to the conjectural one coming from plabic graphs. We also generalize our result to construct cluster structures in skew Schubert varieties; interestingly, these cluster structures for skew Schubert varieties depart from the one in Conjecture 1.1, since they use *generalized* plabic graphs (with boundary vertices which are not longer cyclically labeled).

Once we have proved that the coordinate rings of (open) Schubert and skew Schubert varieties have cluster structures, we obtain a number of results “for free” from the cluster theory, including the Laurent phenomenon and the Positivity theorem for cluster variables. As a consequence of our results we also obtain many combinatorially explicit cluster seeds for each (open) Schubert and skew Schubert variety. Note that (open) Schubert varieties provide examples of cluster structures of all the finite type simply-laced cluster types (*ADE*), see Section 7. Combining our main results with [MS16b, Theorem 3.3] and [Mul13], we find that the coordinate rings of (open) Schubert and skew Schubert varieties (viewed as cluster algebras) are *locally acyclic*, which implies that each one is finitely generated, normal, locally a complete intersection, and equal to its own upper cluster algebra. Combining our result with [FS18, Theorem 1.2], we find that the quivers giving rise to the cluster structures for Schubert and skew Schubert varieties admit *green-to-red sequences*, which by [GHKK14] implies that the cluster algebras have *Enough Global Monomials* and hence each coordinate ring has a canonical basis of theta functions, parameterized by the lattice of  $g$ -vectors. Finally we obtain applications to the structure of indecomposable summands of cluster-tilting modules in  $\mathcal{C}_{v,w}$  and the morphisms between them.

**1.1. Notation for the flag variety.** Let  $\mathrm{GL}_n$  denote the general linear group,  $B$  the Borel subgroup of lower triangular matrices,  $B^+$  the opposite Borel subgroup of upper triangular matrices, and  $W = S_n$  the Weyl group (which is in this case the symmetric group on  $n$  letters).  $W$  is generated by the simple reflections  $s_i$  for  $1 \leq i \leq n-1$ , where  $s_i$  is the transposition exchanging  $i$  and  $i+1$ , and it contains a longest element, which we denote by  $w_0$ , with  $\ell(w_0) = \binom{n}{2}$ . The *complete flag variety*  $\mathrm{Fl}_n$  is the homogeneous space  $B \backslash \mathrm{GL}_n$ . Concretely, each element  $g$  of  $\mathrm{GL}_n$  gives rise to a flag of subspaces  $\{V_1 \subset V_2 \subset \cdots \subset V_n\}$ , where  $V_i$  denotes the span of the top  $i$  rows of  $g$ . The action of  $B$  on the left preserves the flag, so we can identify  $\mathrm{Fl}_n$  with the set of *flags*  $\{V_1 \subset V_2 \subset \cdots \subset V_n\}$  where  $\dim V_i = i$ .

Let  $\pi : \mathrm{GL}_n \rightarrow \mathrm{Fl}_n$  denote the natural projection  $\pi(g) := Bg$ . The Bruhat decomposition

$$\mathrm{GL}_n = \bigsqcup_{w \in W} BwB$$

projects to the Schubert decomposition

$$\mathrm{Fl}_n = \bigsqcup_{w \in W} C_w$$

where  $C_w = \pi(BwB)$  is the *Schubert cell* associated to  $w$ , isomorphic to  $\mathbb{C}^{\ell(w)}$ . We also have the Birkhoff decomposition

$$\mathrm{GL}_n = \bigsqcup_{w \in W} BwB^+,$$

which projects to the opposite Schubert decomposition

$$\mathrm{Fl}_n = \bigsqcup_{w \in W} C^w$$

where  $C^w = \pi(BwB^+)$  is the *opposite Schubert cell* associated to  $w$ , isomorphic to  $\mathbb{C}^{\ell(w_0) - \ell(w)}$ .

The intersection

$$\mathcal{R}_{v,w} := C^v \cap C_w$$

has been considered by Kazhdan and Lusztig [KL79] in relation to Kazhdan-Lusztig polynomials.  $\mathcal{R}_{v,w}$  is nonempty only if  $v \leq w$  in the Bruhat order of  $W$ , and it is then a smooth irreducible locally closed subset of  $C_w$  of dimension  $\ell(w) - \ell(v)$ . Sometimes  $\mathcal{R}_{v,w}$  is called an *open Richardson variety* [KLS13] because its closure is a *Richardson variety* [Ric92]. We have a stratification of the complete flag variety

$$\mathrm{Fl}_n = \bigsqcup_{v \leq w} \mathcal{R}_{v,w}.$$

**1.2. Notation for the Grassmannian.** Fix  $1 < k < n$ . The parabolic subgroup  $W_K = \langle s_1, \dots, s_{k-1} \rangle \times \langle s_{k+1}, s_{k+2}, \dots, s_{n-1} \rangle < W$  gives rise to a parabolic subgroup  $P_K$  in  $\mathrm{GL}_n$ , namely  $P_K = \bigsqcup_{w \in W_K} BwB$ , where  $\dot{w}$  is a matrix representative for  $w$  in  $\mathrm{GL}_n$ .  $W_K$  contains a longest element, which we denote by  $w_K$ , with  $\ell(w_K) = \binom{k}{2} + \binom{n-k}{2}$ .

The *Grassmannian*  $Gr_{k,n}$  is the homogeneous space  $P_K \backslash \mathrm{GL}_n$ . We can think of the Grassmannian  $Gr_{k,n} = P_K \backslash \mathrm{GL}_n$  more concretely as the set of all  $k$ -planes in an  $n$ -dimensional vector space  $\mathbb{C}^n$ . An element of  $Gr_{k,n}$  can be viewed as a full rank  $k \times n$  matrix of rank  $k$ , modulo left multiplication by invertible  $k \times k$  matrices. That is, two  $k \times n$  matrices of rank  $k$  represent the same point in  $Gr_{k,n}$  if and only if they can be obtained from each other by invertible row operations.

For integers  $a, b$ , let  $[a, b]$  denote  $\{a, a+1, \dots, b-1, b\}$  if  $a \leq b$  and the empty set otherwise. We use the shorthand  $[n] := [1, n]$ . Let  $\binom{[n]}{k}$  the set of all  $k$ -element subsets of  $[n]$ .

Given  $V \in Gr_{k,n}$  represented by a  $k \times n$  matrix  $A$ , for  $I \in \binom{[n]}{k}$  we let  $\Delta_I(V)$  be the maximal minor of  $A$  located in the column set  $I$ . The  $\Delta_I(V)$  do not depend on our choice of matrix  $A$  (up to simultaneous rescaling by a nonzero constant), and are called the *Plücker coordinates* of  $V$ . The Plücker coordinates give an embedding of  $Gr_{k,n}$  into projective space of dimension  $\binom{n}{k} - 1$ .

We have the usual projection  $\pi_k$  from the complete flag variety  $\mathrm{Fl}_n$  to the Grassmannian  $Gr_{k,n}$ . Let  $W^K = W_{\min}^K$  and  $W_{\max}^K$  denote the set of minimal- and maximal-length coset representatives for  $W_K \backslash W$ ; we also let  ${}^K W$  (or  ${}_{\min}^K W$ ) denote the set of minimal-length coset representatives for  $W/W_K$ . Such a permutation  $\sigma \in S_n$  is called a *Grassmannian permutation* of type  $(k, n)$ ; it has the property that it has at most one descent, and when present, that descent must be in position  $k$ , i.e.  $\sigma(k) > \sigma(k+1)$ .

Rietsch studied the projections of the open Richardson varieties in the complete flag variety to partial flag varieties [Rie98]. In particular, when  $v \in W_{\max}^K$  (or when  $w \in W_{\min}^K$ ), the projection  $\pi_k$  is an isomorphism from  $\mathcal{R}_{v,w}$  to  $\pi_k(\mathcal{R}_{v,w})$ . We obtain a stratification

$$Gr_{k,n} = \bigsqcup \pi_k(\mathcal{R}_{v,w})$$

where  $(v, w)$  range over all  $v \in W_{\max}^K$ ,  $w \in W$ , such that  $v \leq w$ . Following work of Postnikov [Pos, KLS13], the strata  $\pi_k(\mathcal{R}_{v,w})$  are sometimes called *open positroid varieties*, while their closures are called *positroid varieties*.

It follows from the definitions (see e.g. [KLS13, Section 6]) that positroid varieties include Schubert and opposite Schubert varieties in the Grassmannians, which we now define.

**Definition 1.2.** Let  $I$  denote a  $k$ -element subset of  $[n]$ . The *Schubert cell*  $\Omega_I$  is defined to be

$$\Omega_I = \{A \in Gr_{k,n} \mid \text{the lexicographically minimal nonvanishing Plücker coordinate of } A \text{ is } \Delta_I(A)\}.$$

The *Schubert variety*  $X_I$  is defined to be the closure  $\overline{\Omega_I}$  of  $\Omega_I$ .

Meanwhile the *opposite Schubert cell*  $\Omega^I$  is defined to be

$$\Omega^I = \{A \in Gr_{k,n} \mid \text{the lexicographically maximal nonvanishing Plucker coordinate of } A \text{ is } \Delta_I(A)\}.$$

The *opposite Schubert variety*  $X^I$  is defined to be the closure  $\overline{\Omega^I}$  of  $\Omega^I$ .

It's easy to see that elements  $v$  of  $W_{\max}^K$  and elements  $w$  of  $W_{\min}^K$  are also in bijection with  $k$ -element subsets of  $[n]$ , which we denote by  $I(v)$  and  $I(w)$ , respectively. When  $w \in W_{\min}^K$ ,  $\overline{\pi_k(\mathcal{R}_{e,w})}$  is isomorphic to the *opposite Schubert variety*  $X^{I(w)}$  in the Grassmannian, which has dimension  $\ell(w)$ . We therefore refer to  $\pi_k(\mathcal{R}_{e,w})$  as an *open opposite Schubert variety*. Similarly, when  $v \in W_{\max}^K$ ,  $\overline{\pi_k(\mathcal{R}_{v,w_0})}$  is isomorphic to the *Schubert variety*  $X_{I(v)}$  in the Grassmannian, which has dimension  $\ell(w_0) - \ell(v)$ . We refer to  $\pi_k(\mathcal{R}_{v,w_0})$  as an *open Schubert variety*. More generally, if  $v \in W_{\max}^K$  and  $w \in W$  has a factorization of the form  $w = xv$  which is *length-additive*, i.e. where  $\ell(w) = \ell(x) + \ell(v)$ , then we refer to  $\overline{\pi_k(\mathcal{R}_{v,w})}$  (respectively,  $\pi_k(\mathcal{R}_{v,w})$ ) as a *skew Schubert variety* (respectively, open skew Schubert variety). See Appendix A for more discussion of skew Schubert varieties, including some justification for the terminology.

Let  $\lambda$  denote a Young diagram contained in a  $k \times (n - k)$  rectangle. We can identify  $\lambda$  with the lattice path  $L_\lambda^\swarrow$  in the rectangle taking steps west and south from the northeast corner of the rectangle to the southwest corner (where the  $\swarrow$  indicates that the path “goes southwest”). If we label the steps of the lattice path from 1 to  $n$ , then the labels of the south steps give a  $k$ -element subset of  $[n]$  that we denote by  $V^\swarrow(\lambda)$  (the “vertical steps” of  $\lambda$ ). Conversely, each  $k$ -element subset  $I$  of  $[n]$  can be identified with a Young diagram, which we denote by  $\lambda^\swarrow(I)$ . Since this gives a bijection between Young diagrams contained in a  $k \times (n - k)$  rectangle and  $k$ -element subsets of  $[n]$ , we also index Schubert and opposite Schubert cells and varieties by Young diagrams, denoting them  $\Omega_\lambda$ ,  $\Omega^\lambda$ ,  $X_\lambda$ , and  $X^\lambda$ , respectively. The open Schubert and opposite Schubert varieties are denoted by  $X_\lambda^\circ$ , and  $(X^\lambda)^\circ$ . The dimension of  $\Omega_\lambda$ ,  $X_\lambda$ , and  $X_\lambda^\circ$  is  $|\lambda|$ , the number of boxes of  $\lambda$ , while the codimension of  $\Omega^\lambda$ ,  $X^\lambda$ , and  $(X^\lambda)^\circ$  is  $|\lambda|$ .

**Remark 1.3.** Throughout this paper we will be primarily working with open Schubert (and skew-Schubert) varieties. The reader should be cautioned that we will mostly drop the adjective “open” from now on but will try to consistently use the notation  $X_\lambda^\circ$  for clarity.

We also associate with a Young diagram  $\lambda$  the *Grassmannian permutation*  $\pi_\lambda^\swarrow$  of type  $(n - k, n)$ : in list notation, this permutation is obtained by first reading the labels of the horizontal steps of  $L_\lambda^\swarrow$ , and then reading the labels of the vertical steps of  $L_\lambda^\swarrow$ . (Moreover any fixed points in positions  $1, 2, \dots, n - k$  are “black” and any fixed points in positions  $n - k + 1, \dots, n$  are “white.”) Note that  $\ell(\pi_\lambda^\swarrow) = |\lambda|$ .

**Remark 1.4.** “Going northeast” along the lattice path  $L_\lambda^\swarrow$  gives rise to analogous bijections between Young diagrams in a  $k \times (n - k)$  rectangle,  $k$ -element subsets of  $n$ , and Grassmannian permutations of type  $(k, n)$ . So we can define all the notations that we did before, switching each  $\swarrow$  to a  $\nearrow$ . So a Young diagram  $\lambda$  is identified with the lattice path  $L_\lambda^\nearrow$  in the rectangle taking steps east and north from the southwest corner of the rectangle to the northeast corner. If we label the path with 1 to  $n$ , the labels of the north steps give the  $k$ -element subset  $V^\nearrow(\lambda)$ . Similarly we define  $\lambda^\nearrow(I)$ .

**1.3. The main result.** We now state the main result. Note that the definitions of plabic graph and trip permutation can be found in Section 2.

**Theorem 1.5.** *Consider the Schubert variety  $X_\lambda^\circ$  of  $Gr_{k,n}$ . Let  $G$  be a reduced plabic graph (with boundary vertices labeled clockwise from 1 to  $n$ ) with trip permutation  $\pi_\lambda^\swarrow$ . Construct the dual quiver of  $G$  and label its vertices by the Plücker coordinates given by the target labeling of  $G$ , so as to obtain a labeled seed  $\Sigma_G^{\text{target}}$  (see Definition 2.16, Figure 1, Definition 2.18). Then the coordinate ring  $\mathbb{C}[\hat{X}_\lambda^\circ]$  of the (affine cone over)  $X_\lambda^\circ$  coincides with the cluster algebra  $\mathcal{A}(\Sigma_G^{\text{target}})$ .*

Theorem 1.5 can be rephrased as follows:

- Each of the (in general, infinitely many) cluster variables in  $\mathcal{A}(\Sigma_G^{\text{target}})$  is a regular function on  $\hat{X}_\lambda^\circ$ .
- The cluster variables in  $\mathcal{A}(\Sigma_G^{\text{target}})$  generate the ring  $\mathbb{C}[\hat{X}_\lambda^\circ]$  of regular functions on  $\hat{X}_\lambda^\circ$ .

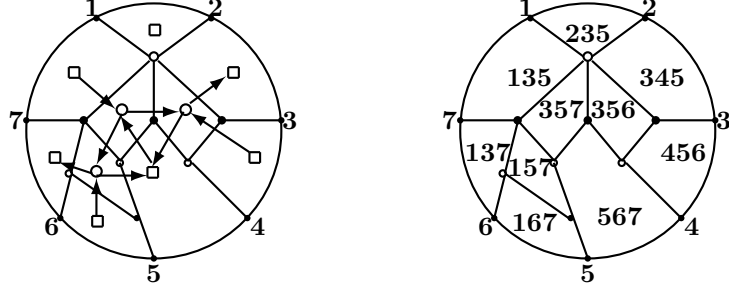


FIGURE 1. A plabic graph  $G$  for  $Gr_{3,7}$  with trip permutation  $\pi_k^\lambda = (2, 4, 6, 7, 1, 3, 5)$ , for  $\lambda = (4, 3, 2)$ , together with the dual quiver of  $G$  and the face labeling given by target labels. The associated Le-diagram is a Young diagram of shape  $\lambda$  which is filled with +’s.

We actually prove something a bit more general than Theorem 1.5; we prove the following.

**Theorem 1.6.** *Consider the skew Schubert variety  $\pi_k(\mathcal{R}_{v,w})$ , where  $v \in W_{max}^K$  and  $w$  has a length-additive factorization  $w = xv$ . Let  $G$  be a reduced plabic graph (with boundary vertices labeled clockwise from 1 to  $n$ ) with trip permutation  $vw^{-1} = x^{-1}$ , and such that boundary lollipops are white if and only if they are in  $[k]$ . Apply  $v^{-1}$  to the boundary vertices of  $G$ , obtaining the relabeled graph  $v^{-1}(G)$ , and apply the target labeling to obtain the labeled seed  $\Sigma_{v^{-1}(G)}^{\text{target}}$ . Then the coordinate ring  $\mathbb{C}[\pi_k(\mathcal{R}_{v,w})]$  of the (affine cone over) the skew Schubert variety  $\pi_k(\mathcal{R}_{v,w})$  coincides with the cluster algebra  $\mathcal{A}(\Sigma_{v^{-1}(G)}^{\text{target}})$ .*

In the case of Schubert varieties, Theorem 1.5 resolves Conjecture 1.1, which has been believed to be true by experts for some time, though it wasn’t written down explicitly as a conjecture until recently, see [MS16b, Conjecture 3.4]. Note that there is another version of the conjecture which uses the *source labeling* of  $G$  instead of the target labeling [MS16b, Remark 3.5]. Both conjectures make sense more generally for positroid varieties and arbitrary reduced plabic graphs (whose trip permutations can be arbitrary decorated permutations). However, the cluster structure that we give in Theorem 1.6 is different from either of the cluster structures proposed in [MS16b].

Our strategy of proof is to find, for each skew Schubert variety, one distinguished seed coming from Leclerc’s cluster structure, which we can describe completely explicitly. We then show that this seed agrees with a corresponding seed coming from the combinatorial construction of Theorem 1.6, and justify that mutations in both cluster structures agree. We use a (modification) of a construction of Karpman [Kar16] as a key tool in the proof.

**Remark 1.7.** In his thesis [Che12], Chevalier describes a cluster-tilting object associated to Richardson varieties  $\mathcal{R}_{v,w}$  where  $v = w_K$  and  $w \geq v$  in Bruhat order. These Richardson varieties correspond to positroid varieties in  $Gr_{k,n}$  whose J-diagrams have shape  $k \times (n - k)$ . (This case is somewhat complementary to the cases that we consider in this paper, in the sense that Chevalier treats J-diagrams of shape  $k \times (n - k)$  with arbitrary fillings, while on the other hand Schubert varieties correspond to J-diagrams of arbitrary shape whose boxes are all filled with +’s.) In the case of the big open Schubert variety in the Grassmannian (i.e. the positroid whose J-diagram is a  $k \times (n - k)$  rectangle filled with all +’s) we get the same quiver as Chevalier does, but different modules (and hence different Plücker coordinates). And in other cases of overlap (i.e. skew-Schubert varieties with  $v = w_K$ ) even our quivers are different from Chevalier’s.

**1.4. Outline of the paper.** Our paper is structured as follows. In Section 2, we give background on cluster structures, plabic graphs, and reduced expressions. While each skew Schubert variety  $\pi_k(\mathcal{R}_{v,w})$  (where  $v = w_K v' \in W_{max}^K$  and  $w \in W$  has a length-additive factorization  $\mathbf{w} = \mathbf{xv} = \mathbf{xw}_K \mathbf{v}'$  into reduced expressions for  $x$ ,  $w_K$ , and  $v'$ ) corresponds to an equivalence class of plabic graphs (more generally to a collection of cluster seeds), there is one among them which is particularly nice, which we call the *rectangles seed*. In Section 3, we give an explicit description of the rectangles seed for a skew Schubert variety  $\pi_k(\mathcal{R}_{v,w})$  as above, together with its dual cluster quiver. In Section 4 we describe a construction of Karpman [Kar16]

which produces a bridge-decomposable plabic graph associated to a pair  $(y, \mathbf{z})$ , where  $y^{-1} \in W_{\max}^K$ ,  $\mathbf{z}$  is a reduced decomposition for  $z$ , and  $y \leq z$ . And we show that if we perform her construction for the pair  $(w_K, \mathbf{xw}_K)$  and then relabel boundary vertices of the resulting plabic graph  $G$  by  $v^{-1}$ , the target labeling of the dual quiver of  $G$  gives rise to the rectangles seed for  $\pi_k(\mathcal{R}_{v,w})$ . In Section 5 we describe a construction of Leclerc [Lec16], which produces a cluster seed associated to each pair  $(v, \mathbf{w})$ , where  $v \in W_{max}^K$  and  $v \leq w$ . We also prove that for the choice  $(v, \mathbf{w} = \mathbf{xw}_K \mathbf{v}')$ , Leclerc's construction gives rise to the rectangles seed. In Section 6, we build on the results of the previous sections to prove Theorem 1.6 and then deduce Theorem 1.5 from it. Section 7 gives applications of Theorem 1.5 and Theorem 1.6, and characterizes for which Schubert varieties the cluster structure is of finite type. In Appendix A, we give a concrete description of skew Schubert varieties. And in Appendix B, we give an example showing that outside of the skew-Schubert case, the cluster subalgebra of the coordinate ring of  $\pi_k(\mathcal{R}_{v,w})$  coming from Leclerc's construction is in general impossible to realize from a plabic graph.

**Acknowledgements:** We are grateful to Bernard Leclerc for numerous helpful discussions, and for bringing the work of Chevalier [Che12] to our attention. K.S. acknowledges support from the National Science Foundation Postdoctoral Fellowship MSPRF-1502881. M.S.B acknowledges support by an NSF Graduate Research Fellowship No. DGE-1752814. L. W. was partially supported by the NSF grant DMS-1600447. Any opinions, findings and conclusions or recommendations expressed in this material are those of the authors and do not necessarily reflect the views of the National Science Foundation.

## 2. BACKGROUND ON CLUSTER STRUCTURES AND PLABIC GRAPHS

**2.1. Background on cluster structures.** Cluster algebras are a class of rings with a particular combinatorial structure; they were introduced by Fomin and Zelevinsky in [FZ02].

**Definition 2.1** (Quiver). A *quiver*  $Q$  is a directed graph; we will assume that  $Q$  has no loops or 2-cycles. Each vertex is designated either *mutable* or *frozen*.

**Definition 2.2** (Quiver Mutation). Let  $q$  be a mutable vertex of quiver  $Q$ . The quiver mutation  $\mu_q$  transforms  $Q$  into a new quiver  $Q' = \mu_q(Q)$  via a sequence of three steps:

- (1) For each oriented two path  $r \rightarrow q \rightarrow s$ , add a new arrow  $r \rightarrow s$  (unless  $r$  and  $s$  are both frozen, in which case do nothing).
- (2) Reverse the direction of all arrows incident to the vertex  $q$ .
- (3) Repeatedly remove oriented 2-cycles until unable to do so.

We say that two quivers  $Q$  and  $Q'$  are *mutation equivalent* if  $Q$  can be transformed into a quiver isomorphic to  $Q'$  by a sequence of mutations.

**Definition 2.3** (Labeled seeds). Choose  $M \geq N$  positive integers. Let  $\mathcal{F}$  be an *ambient field* of rational functions in  $N$  independent variables over  $\mathbb{C}(x_{N+1}, \dots, x_M)$ . A *labeled seed* in  $\mathcal{F}$  is a pair  $(\tilde{\mathbf{x}}, Q)$ , where

- $\tilde{\mathbf{x}} = (x_1, \dots, x_M)$  forms a free generating set for  $\mathcal{F}$ , and
- $Q$  is a quiver on vertices  $1, 2, \dots, N, N+1, \dots, M$ , whose vertices  $1, 2, \dots, N$  are *mutable*, and whose vertices  $N+1, \dots, M$  are *frozen*.

We refer to  $\tilde{\mathbf{x}}$  as the (labeled) *extended cluster* of a labeled seed  $(\tilde{\mathbf{x}}, Q)$ . The variables  $\{x_1, \dots, x_N\}$  are called *cluster variables*, and the variables  $c = \{x_{N+1}, \dots, x_M\}$  are called *frozen* or *coefficient variables*. We often view the labeled seed as a quiver  $Q$  where each vertex  $i$  is labeled by the corresponding variable  $x_i$ .

**Definition 2.4** (Seed mutations). Let  $(\tilde{\mathbf{x}}, Q)$  be a labeled seed in  $\mathcal{F}$ , and let  $q \in \{1, \dots, N\}$ . The *seed mutation*  $\mu_q$  in direction  $q$  transforms  $(\tilde{\mathbf{x}}, Q)$  into the labeled seed  $\mu_q(\tilde{\mathbf{x}}, Q) = (\tilde{\mathbf{x}}', \mu_q(Q))$ , where the cluster  $\tilde{\mathbf{x}}' = (x'_1, \dots, x'_M)$  is defined as follows:  $x'_j = x_j$  for  $j \neq q$ , whereas  $x'_q \in \mathcal{F}$  is determined by the *exchange relation*

$$(2.1) \quad x'_q x_q = \prod_{q \rightarrow r} x_r + \prod_{s \rightarrow q} x_s,$$

where the first product is over all arrows  $q \rightarrow r$  in  $Q$  which start at  $q$ , and the second product is over all arrows  $s \rightarrow q$  which end at  $q$ .

**Remark 2.5.** It is not hard to check that seed mutation is an involution.

**Remark 2.6.** Note that arrows between two frozen vertices of a quiver do not affect seed mutation (they do not affect the mutated quiver or the exchange relation). For that reason, one may omit arrows between two frozen vertices.

**Definition 2.7** (*Patterns*). Consider the  $N$ -regular tree  $\mathbb{T}_N$  whose edges are labeled by the numbers  $1, \dots, N$ , so that the  $N$  edges emanating from each vertex receive different labels. A *cluster pattern* is an assignment of a labeled seed  $\Sigma_t = (\tilde{\mathbf{x}}_t, Q_t)$  to every vertex  $t \in \mathbb{T}_N$ , such that the seeds assigned to the endpoints of any edge  $t \xrightarrow{q} t'$  are obtained from each other by the seed mutation in direction  $q$ . The components of  $\tilde{\mathbf{x}}_t$  are written as  $\tilde{\mathbf{x}}_t = (x_{1;t}, \dots, x_{N;t})$ .

Clearly, a cluster pattern is uniquely determined by an arbitrary seed.

**Definition 2.8** (*Cluster algebra*). Given a cluster pattern, we denote

$$(2.2) \quad \mathcal{X} = \bigcup_{t \in \mathbb{T}_N} \tilde{\mathbf{x}}_t = \{x_{i,t} : t \in \mathbb{T}_N, 1 \leq i \leq N\},$$

the union of clusters of all the seeds in the pattern. The elements  $x_{i,t} \in \mathcal{X}$  are called *cluster variables*. The *cluster algebra*  $\mathcal{A}$  associated with a given pattern is the  $\mathbb{C}[x_{N+1}^{\pm 1}, \dots, x_M^{\pm 1}]$ -subalgebra of the ambient field  $\mathcal{F}$  generated by all cluster variables:  $\mathcal{A} = \mathbb{C}[c^{\pm 1}][\mathcal{X}]$ . We denote  $\mathcal{A} = \mathcal{A}(\tilde{\mathbf{x}}, Q)$ , where  $(\tilde{\mathbf{x}}, Q)$  is any seed in the underlying cluster pattern. In this generality,  $\mathcal{A}$  is called a *cluster algebra from a quiver*, or a *skew-symmetric cluster algebra of geometric type*. We say that  $\mathcal{A}$  has *rank*  $N$  because each cluster contains  $N$  cluster variables.

**Remark 2.9.** One of the earliest definitions of cluster algebra defined it as  $\mathcal{A} = \mathbb{C}[c][\mathcal{X}]$  instead of  $\mathcal{A} = \mathbb{C}[c^{\pm 1}][\mathcal{X}]$ . This is the definition Scott worked with in proving that the coordinate ring of the Grassmannian is a cluster algebra [Sco06]. If one uses Definition 2.8 instead, then the statement is that the coordinate ring of the open Schubert variety in the Grassmannian is a cluster algebra.

**2.2. Background on plabic graphs.** In this section we review Postnikov’s notion of *plabic graphs* [Pos], which we will then use to define cluster structures in Schubert varieties.

**Definition 2.10.** A *plabic* (or *planar bicolored*) graph is an undirected graph  $G$  drawn inside a disk (considered modulo homotopy) with  $n$  *boundary vertices* on the boundary of the disk, labeled  $1, \dots, n$  in clockwise order, as well as some colored *internal vertices*. These internal vertices are strictly inside the disk and are colored in black and white. An internal vertex of degree one adjacent to a boundary vertex is a *lollipop*. We will always assume that no vertices of the same color are adjacent, and that each boundary vertex  $i$  is adjacent to a single internal vertex.

See Figure 2 for an example of a plabic graph.

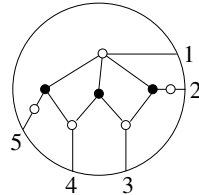


FIGURE 2. A plabic graph

**Definition 2.11.** A *generalized plabic graph* is a plabic graph with boundary vertices are labeled by  $1, \dots, n$  in some order, not necessarily clockwise.

Generalized plabic graphs naturally arise in the course of our arguments. Though we state all of the following definitions for plabic graphs for clarity, they can equally be made for generalized plabic graphs.

There is a natural set of local transformations (moves) of plabic graphs, which we now describe. Note that we will always assume that a plabic graph  $G$  has no isolated components (i.e. every connected component contains at least one boundary vertex). We will also assume that  $G$  is *leafless*, i.e. if  $G$  has an internal vertex of degree 1, then that vertex must be adjacent to a boundary vertex.

(M1) SQUARE MOVE (Urban renewal). If a plabic graph has a square formed by four trivalent vertices whose colors alternate, then we can switch the colors of these four vertices (and add some degree 2 vertices to preserve the bipartiteness of the graph).

(M2) CONTRACTING/EXPANDING A VERTEX. Any degree 2 internal vertex not adjacent to the boundary can be deleted, and the two adjacent vertices merged. This operation can also be reversed. Note that this operation can always be used to change an arbitrary square face of  $G$  into a square face whose four vertices are all trivalent.

(M3) MIDDLE VERTEX INSERTION/REMOVAL. We can always remove or add degree 2 vertices at will, subject to the condition that the graph remains bipartite.

See Figure 3 for depictions of these three moves.

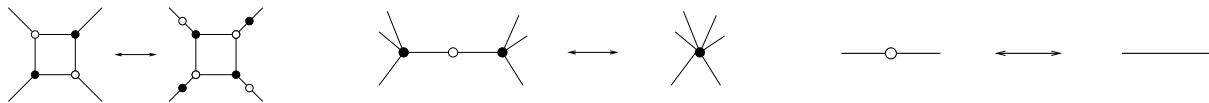


FIGURE 3. A square move, an edge contraction/expansion, and a vertex insertion/removal.

(R1) PARALLEL EDGE REDUCTION. If a plabic graph contains two trivalent vertices of different colors connected by a pair of parallel edges, then we can remove these vertices and edges, and glue the remaining pair of edges together.



FIGURE 4. Parallel edge reduction

**Definition 2.12.** Two plabic graphs are called *move-equivalent* if they can be obtained from each other by moves (M1)-(M3). The *move-equivalence class* of a given plabic graph  $G$  is the set of all plabic graphs which are move-equivalent to  $G$ . A leafless plabic graph without isolated components is called *reduced* if there is no graph in its move-equivalence class to which we can apply (R1).

**Definition 2.13.** A *decorated permutation*  $\pi^\cdot$  is a permutation  $\pi \in S_n$  together with a coloring  $\{i \mid \pi(i) = i\} \rightarrow \{\text{black, white}\}$ .

**Definition 2.14.** Given a reduced plabic graph  $G$ , a *trip*  $T$  is a directed path which starts at some boundary vertex  $i$ , and follows the “rules of the road”: it turns (maximally) right at a black vertex, and (maximally) left at a white vertex. Note that  $T$  will also end at a boundary vertex  $j$ ; we then refer to this trip as  $T_{i \rightarrow j}$ . Setting  $\pi(i) = j$  for each such trip, we associate a (decorated) *trip permutation*  $\pi_G = (\pi(1), \dots, \pi(n))$  to each reduced plabic graph  $G$ , where a fixed point  $\pi(i) = i$  is colored white (black) if there is a white (black) lollipop at boundary vertex  $i$ . We say that  $G$  has *type*  $\pi_G$ .

As an example, the trip permutation associated to the reduced plabic graph in Figure 2 is  $(3, 4, 5, 1, 2)$ .

**Remark 2.15.** Note that the trip permutation of a plabic graph is preserved by the local moves (M1)-(M3), but not by (R1). For reduced plabic graphs the converse holds, namely it follows from [Pos, Theorem 13.4] that any two reduced plabic graphs with the same trip permutation are move-equivalent.



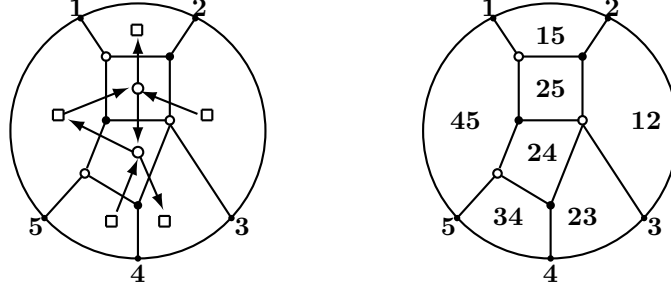


FIGURE 5. A plabic graph  $G$  together with  $Q(G)$  and its face labeling  $\mathcal{F}_{\text{source}}(G)$ . Here  $\pi_G = (3, 4, 5, 1, 2)$ .

Now we use the notion of trips to label each face of  $G$  by a Plücker coordinate. Towards this end, note that every trip will partition the faces of a plabic graph into two parts: those on the left of the trip, and those on the right of a trip.

**Definition 2.16.** Let  $G$  be a reduced plabic graph with  $b$  boundary vertices. For each one-way trip  $T_{i \rightarrow j}$  with  $i \neq j$ , we place the label  $i$  (respectively,  $j$ ) in every face which is to the left of  $T_{i \rightarrow j}$ . If  $i = j$  (that is,  $i$  is adjacent to a lollipop), we place the label  $i$  in all faces if the lollipop is white and in no faces if the lollipop is black. We then obtain a labeling  $\mathcal{F}_{\text{source}}(G)$  (respectively,  $\mathcal{F}_{\text{target}}(G)$ ) of faces of  $G$  by subsets of  $[b]$  which we call the *source* (respectively, *target*) labeling of  $G$ . We identify each  $a$ -element subset of  $[b]$  with the corresponding Plücker coordinate.

The right-hand side of Figure 5 shows a plabic graph with the face labeling  $\mathcal{F}_{\text{source}}(G)$ .

We next associate a quiver to each plabic graph, and relate quiver mutation to moves on plabic graphs.

**Definition 2.17.** Let  $G$  be a reduced plabic graph. We associate a quiver  $Q(G)$  as follows. The vertices of  $Q(G)$  are labeled by the faces of  $G$ . We say that a vertex of  $Q(G)$  is *frozen* if the corresponding face is incident to the boundary of the disk, and is *mutable* otherwise. For each edge  $e$  in  $G$  which separates two faces, at least one of which is mutable, we introduce an arrow connecting the faces; this arrow is oriented so that it “sees the white endpoint of  $e$  to the left and the black endpoint to the right” as it crosses over  $e$ . We then remove oriented 2-cycles from the resulting quiver, one by one, to get  $Q(G)$ . See Figure 5.

**Definition 2.18.** Given a reduced plabic graph  $G$ , we let  $\Sigma_G^{\text{target}}$  (respectively,  $\Sigma_G^{\text{source}}$ ) be the labeled seed consisting of the quiver  $Q(G)$  with vertices labeled by the Plücker coordinates  $\mathcal{F}_{\text{target}}(G)$  (respectively,  $\mathcal{F}_{\text{source}}(G)$ ). Given a plabic graph  $G$  on  $n$  vertices and a permutation  $v \in S_n$ , we will sometimes use relabeled plabic graphs  $v^{-1}(G)$  (where the boundary vertices have been modified by applying  $v^{-1}$  to them). We will refer to the corresponding seeds with the induced target labelings by e.g.  $\Sigma_{v^{-1}(G)}^{\text{target}}$ .

The following lemma is straightforward, and is implicit in [Sco06].

**Lemma 2.19.** *If  $G$  and  $G'$  are related via a square move at a face, then  $\Sigma_G^{\text{target}}$  and  $\Sigma_{G'}^{\text{target}}$  are related via mutation at the corresponding vertex. Similarly for  $\Sigma_G^{\text{source}}$  and  $\Sigma_{G'}^{\text{source}}$ .*

Because of Lemma 2.19, we will subsequently refer to “mutating” at a nonboundary face of  $G$ , meaning that we mutate at the corresponding vertex of quiver  $Q(G)$ . Note that in general the quiver  $Q(G)$  admits mutations at vertices which do not correspond to moves of plabic graphs. For example,  $G$  might have a hexagonal face, all of whose vertices are trivalent; in that case,  $Q(G)$  admits a mutation at the corresponding vertex, but there is no move of plabic graphs which corresponds to this mutation.

**Remark 2.20.** The open positroid varieties  $\pi_k(\mathcal{R}_{v,w}) \subseteq Gr_{k,n}$  are in bijection with a variety of combinatorial objects introduced by Postnikov in [Pos], including the decorated permutations on  $n$  letters with  $k$  *antiexcedances*. Here we say that  $i \in [n]$  is an *antiexcedance* if  $\pi_{v,w}^{-1}(i) > \pi_{v,w}(i)$  or  $i$  is a white lollipop.

As pointed out in [Wil07], the trip permutation of  $\pi_k(\mathcal{R}_{v,w})$  is  $\pi_{v,w} := v^{-1}w$  with all white fixed points lying in  $v^{-1}([k])$  (see [Kar16, Section 2.4, Equation 2.27] for phrasing that is closer to ours). The set of antiexcedances is exactly  $v^{-1}([k])$ . Clearly one can recover the pair  $(v, w)$  from  $\pi_{v,w}$  since  $v \in W_{\max}^K$ .

1	5	8	10
2	6	9	11
3	7		
4			

$s_4$	$s_5$	$s_6$	$s_7$
$s_3$	$s_4$	$s_5$	$s_6$
$s_2$	$s_3$		
$s_1$			

FIGURE 6. Let  $x = (2, 4, 7, 8, 1, 3, 5, 6) \in {}^K W$ , and  $\lambda^\rceil(x([k])) = (4, 4, 2, 1)$ . On the left, the *columnar* reading order for the boxes of  $\lambda^\rceil(x([k]))$ ; on the right, the filling of  $\lambda^\rceil(x([k]))$  with simple transpositions. This reading order produces the reduced expression  $\mathbf{x} = s_6 s_7 s_5 s_6 s_3 s_4 s_5 s_1 s_2 s_3 s_4$  for  $x \in {}^K W$ , and the reduced expression  $s_4 s_3 s_2 s_1 s_5 s_4 s_3 s_6 s_5 s_7 s_6$  for  $x^{-1} \in W^K$ .

**2.3. A fact about permutations.** We will need the following lemma on reduced expressions for permutations in  ${}^K W$  and  $W^K$ . It is illustrated in Figure 6.

**Lemma 2.21.** [Ste96] *Let  $x \in {}^K W$  and let  $\lambda := \lambda^\rceil(x([k]))$ . Choose a “reading order” for the boxes of  $\lambda$  such that each box is read before the box immediately below it and the box immediately to its right (that is, choose a standard Young tableau of shape  $\lambda$ ). Fill each box with a simple transposition; the box in row  $r$  and column  $c$  is filled with  $s_{k-c+r}$ . Then reading the fillings of the boxes according to the reading order gives a reduced expression for  $x$  (written from right to left).*

Since the elements of  $W^K$  are just the inverses of the elements of  ${}^K W$ , one can also obtain reduced expressions for  $y \in W^K$  by the process described in Lemma 2.21, using the partition  $\lambda^\rceil(y^{-1}([k]))$ . The only difference is the resulting reduced expression for  $y$  is written down from left to right.

**Remark 2.22.** For simplicity, we will always use the *columnar* reading order, which reads the columns of  $\lambda$  from top to bottom, moving left to right (see Figure 6). We will call the resulting reduced expressions *columnar expressions*.

We will be particularly concerned with pairs  $(v, w)$  where  $v \in W_{\max}^K$  and  $w$  has a *length-additive factorization*  $w = xv$ , i.e.  $\ell(w) = \ell(x) + \ell(v)$ . We will often use reduced expressions for such permutations  $w$  that reflect their length-additive factorizations.

**Definition 2.23.** Let  $v \leq w$ , with  $v \in W_{\max}^K$  and  $w = xv$  length-additive. Let  $v = w_K v'$  be length-additive, where  $v'$  is necessarily in  $W_{\min}^K$ . Then a *standard reduced expression* for  $w$  is a reduced expression  $\mathbf{w} = \mathbf{x} \mathbf{w}_K \mathbf{v}'$ , where  $\mathbf{x}$  and  $\mathbf{v}'$  are the columnar expressions for  $x$  and  $v'$ , respectively, and  $\mathbf{w}_K$  is an arbitrary reduced expression for  $w_K$ .

### 3. THE RECTANGLES SEED ASSOCIATED TO A SKEW SCHUBERT VARIETY

Definition 3.1 explains how to associate to a pair of permutations a quiver whose vertices are labeled by Plücker coordinates. The construction is illustrated in Figure 7.

**Definition 3.1** (*The rectangles seed  $\Sigma_{v,w}$* ). Let  $v \leq w$ , where  $v \in W_{\max}^K$  and  $w = xv$  is a length-additive factorization. Let  $\lambda := \lambda^\rceil(x([k]))$ . If  $b$  is a box of  $\lambda$ , let  $\text{Rect}(b)$  be the largest rectangle contained in  $\lambda$  whose lower right corner is  $b$ .

We obtain a quiver  $Q_{v,w}$  as follows: place one vertex in each box of  $\lambda$ . A vertex is mutable if it lies in a box  $b$  of the Young diagram and the box immediately southeast of  $b$  is also in  $\lambda$ . We add arrows between vertices in adjacent boxes, with all arrows pointing either up or to the left. Finally, in every  $2 \times 2$  rectangle in  $\lambda$ , we add an arrow from the upper left box to the lower right box. Equivalently, we add an arrow from the vertex in box  $a$  to the vertex in box  $b$  if

- $\text{Rect}(b)$  is obtained from  $\text{Rect}(a)$  by removing a row or column.
- $\text{Rect}(b)$  is obtained from  $\text{Rect}(a)$  by adding a hook shape.

We then remove all arrows between two frozen vertices.

To obtain the *rectangles seed*  $\Sigma_{v,w}$ , we label each vertex of  $Q_{v,w}$  with a Plücker coordinate. For  $b$  a box of  $\lambda$ , let  $J(b) := V^\wedge(\text{Rect}(b))$ . The label of the vertex in  $b$  is  $\Delta_{v^{-1}(J(b))}$ . This labeled quiver  $\Sigma_{v,w}$  gives a seed as in Definition 2.3, where the Plücker coordinates labeling the vertices give the extended cluster.

**Definition 3.2.** Let  $\lambda$  be a partition and let  $b$  be a box of  $\lambda$ . We say that  $\text{Rect}(b)$  is *frozen* for  $\lambda$  or  $\lambda$ -*frozen* if  $b$  touches the south or east boundary of  $\lambda$  (either along an edge or at the southeast corner).

Note that the  $\lambda$ -frozen rectangles correspond to the frozen vertices of  $\Sigma_{v,w}$ .

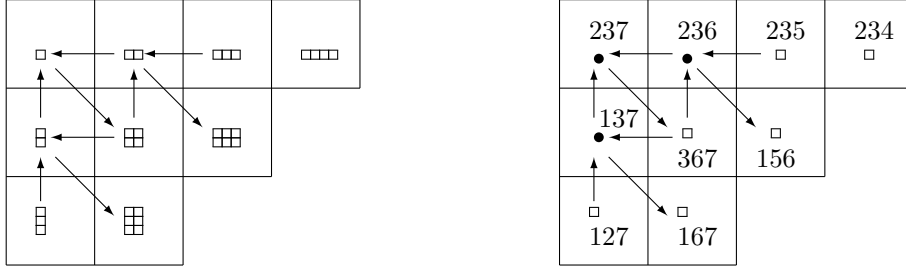


FIGURE 7. An example of  $\Sigma_{v,w}$  for  $k = 3$ ,  $n = 7$ ,  $v = w_K$  and  $x = wv^{-1} = (3, 5, 7, 1, 2, 4, 6)$ . At the left, the  $\lambda$ -frozen rectangles are  $\square\square\square$ ,  $\square\square$ ,  $\square\square$ ,  $\square$ ,  $\square$ ,  $\square$ . On the right, the same quiver is shown but rectangles have been replaced by the corresponding 3-element subsets of  $[7]$ , which should be interpreted as Plücker coordinates.

**Proposition 3.3.** Let  $\pi_k(\mathcal{R}_{v,w})$  be a skew Schubert variety. Then the rectangles seed  $\Sigma_{v,w}$  is a seed for a cluster structure on the coordinate ring of (the affine cone over)  $\pi_k(\mathcal{R}_{v,w})$ , i.e.  $\mathbb{C}[\pi_k(\mathcal{R}_{v,w})] = \mathcal{A}(\Sigma_{v,w})$ .

This result follows as an immediate corollary from Theorem 5.18, whose proof is the focus of Section 5.

In the following section, we discuss the generalized plabic graph whose dual quiver (with the target labeling) coincides with  $\Sigma_{v,w}$ , as well as the connections of this theorem to Conjecture 1.1.

Recall that if  $v \in W_{max}^K$  and  $\lambda = \lambda^\vee(v^{-1}([k]))$ , then  $\pi_k(\mathcal{R}_{v,w_0})$  is the open Schubert variety  $X_\lambda^\circ$ . So as an immediate corollary to this result, we obtain the following.

**Corollary 3.4.** Let  $v \in W_{max}^K$  and let  $\lambda := \lambda^\vee(v^{-1}([k]))$ . Then the rectangles seed  $\Sigma_{v,w_0}$  is a seed for the cluster structure on  $X_\lambda^\circ$ , i.e.  $\mathbb{C}[X_\lambda^\circ] = \mathcal{A}(\Sigma_{v,w_0})$ .

#### 4. OBTAINING THE RECTANGLES SEED FROM A BRIDGE GRAPH

Here we give a construction of a special kind of plabic graph – a *bridge graph* – from a pair of permutations [Kar16], and explain how to use this construction to produce the rectangles seed.

**4.1. Bridge graphs.** One can obtain a plabic graph with arbitrary trip permutation by successively adding “bridges” (see Figure 8) to a graph consisting entirely of lollipops. The plabic graphs created this way are *bridge graphs*. We will define them below, after reviewing the notion of (bounded) affine permutations.

An *affine permutation* of order  $n$  is a bijection  $f : \mathbb{Z} \rightarrow \mathbb{Z}$  such that  $f(i + n) = f(i) + n$  for all  $i \in \mathbb{Z}$ .

**Definition 4.1** (The bounded affine permutation associated to a decorated permutation). If  $\sigma$  is a decorated permutation of  $[n]$ , we define the bounded affine permutation  $\tilde{\sigma}$  on  $[n]$  as

$$\tilde{\sigma}(i) := \begin{cases} \sigma(i) & \text{if } \sigma(i) > i \text{ or } i \text{ is a black fixed point} \\ \sigma(i) + n & \text{if } \sigma(i) < i \text{ or } i \text{ is a white fixed point} \end{cases}$$

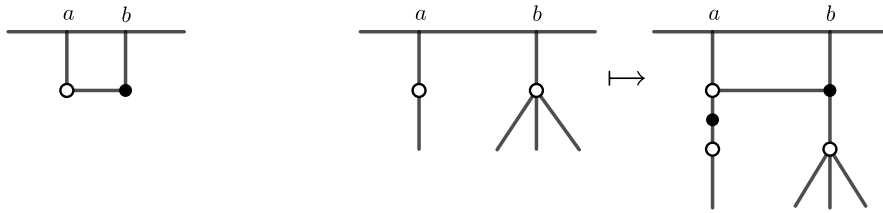


FIGURE 8. On the left, an  $(a\ b)$ -bridge. On the right, an example of adding an  $(a\ b)$ -bridge to a plabic graph.

and extend periodically to  $\mathbb{Z}$ . In other words, to obtain a bounded affine permutation, add  $n$  to all antiexcedances of  $\sigma$  and then extend periodically to  $\mathbb{Z}$ .

An  $(a\ b)$ -bridge is a collection of two vertices and three edges inserted at boundary vertices  $a$  and  $b$  as in the left of Figure 8. Let  $G$  be a plabic graph with (bounded affine) trip permutation  $\tilde{\sigma}_G$ . For a pair of boundary vertices  $a < b$ , we say that the  $(a\ b)$ -bridge is *valid* if  $\tilde{\sigma}_G(a) > \tilde{\sigma}_G(b)$ , all boundary vertices  $c$  between  $a$  and  $b$  are lollipops, and if  $a$  (resp.  $b$ ) is a lollipop it is white (resp. black).

To add a bridge to  $G$ , choose boundary vertices  $a, b$  such that the  $(a\ b)$ -bridge is valid. Place a white (resp. black) vertex in the middle of the edge adjacent to  $a$  (resp.  $b$ ) and put an edge between these two vertices; if  $a$  (resp.  $b$ ) is a lollipop, we use the boundary leaf as the white (resp. black) vertex of the bridge. We then add degree two vertices as necessary to make the resulting graph bipartite. A plabic graph obtained by successively adding valid bridges to a lollipop graph is called a *bridge graph*.

Adding a bridge changes the trip permutation in a predictable way.

**Lemma 4.2** ([Kar16, Proposition 2.5]). *Suppose  $G$  is a reduced plabic graph with (bounded affine) trip permutation  $\tilde{\sigma}_G$ . Let  $1 \leq a < b \leq n$  be vertices such that the  $(a\ b)$ -bridge is valid and let  $G'$  be the plabic graph obtained by adding an  $(a\ b)$ -bridge to  $G$ . Then  $G'$  is reduced and has trip permutation  $\tilde{\sigma}_G \circ (a\ b)$ .*

**Remark 4.3.** Let  $G_0$  be a lollipop graph,  $(a_1\ b_1), \dots, (a_r\ b_r)$  a sequence of bridges, and  $G_i$  the graph obtained from adding bridge  $(a_i\ b_i)$  to  $G_{i-1}$ . We also assume that  $(a_i\ b_i)$  is a valid bridge for  $G_{i-1}$ . In the construction given above, new bridges are always added at the boundary and “push” the existing faces towards the center of the disk (see Example 4.7). One can also obtain  $G_r$  from an empty graph by adding bridges in the opposite order, placing new bridges “below” existing bridges, and adding lollipops at the end if necessary. We will always use the former algorithm, but the latter can be useful as well.

If  $G'$  is obtained from a plabic graph  $G$  by adding a valid bridge, all faces of  $G'$  correspond to faces in  $G$ , except for the face bounded by the bridge.

**Lemma 4.4.** *Suppose  $G$  is a reduced plabic graph,  $1 \leq a < b \leq n$  vertices such that the  $(a\ b)$ -bridge is valid, and  $G'$  the plabic graph resulting from adding an  $(a\ b)$ -bridge to  $G$ . Then, using the target labeling, the labels of faces in  $G$  coincide with the labels of corresponding faces in  $G'$ .*

It is not hard to find the (target) label of the remaining face of  $G'$ .

**Definition 4.5.** Let  $\sigma$  be a decorated permutation of  $[n]$ . The *Grassmann necklace* of  $\sigma$  is a sequence  $\mathcal{J} = (J_1, J_2, \dots, J_n)$  of subsets of  $[n]$  where  $J_1 := \{i \in [n] \mid \sigma^{-1}(i) > i \text{ or } i \text{ is a white fixed point}\}$  and

$$J_{i+1} := \begin{cases} (J_i \setminus \{i\}) \cup \{\sigma(i)\} & \text{if } i \in J_i \\ J_i & \text{else.} \end{cases}$$

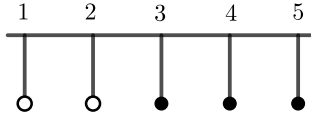
If  $\sigma_{G'}$  is the trip permutation of  $G'$ , the boundary faces of  $G'$  are labeled with the Grassmann necklace of  $\sigma_{G'}$  [OPS15]. So the label of the face bounded by the  $(a\ b)$ -bridge is just the  $(a + 1)^{st}$  entry of the Grassmann necklace of  $\sigma_{G'}$ .

**4.2. Bridge graphs from pairs of permutations.** In [Kar16], Karpman gives an algorithm for producing a bridge graph with trip permutation  $vw^{-1}$  from a pair  $(v, \mathbf{w})$ , where  $v^{-1} \in W_{\max}^K$  and  $\mathbf{w}$  is a reduced expression for some permutation  $w \geq v$ . We use a special case of her construction in the following definition.

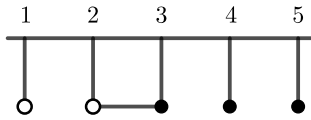
**Definition 4.6.** Let  $w \in W$  with a length-additive factorization  $w = xw_K$ , where  $x \in {}^K W$ . Let  $\mathbf{x} = s_{i_r} \dots s_{i_1}$  be the columnar expression for  $x$  (see Remark 2.22) and let  $\mathbf{w}$  be a standard reduced expression for  $w$  (Definition 2.23). We define  $B_{w_K, \mathbf{w}}$  to be the bridge graph obtained from the lollipop graph with white lollipops  $[k]$  and black lollipops  $[k+1, n]$  with bridge sequence  $s_{i_1}, s_{i_2}, \dots, s_{i_r}$ .

By [Kar16],  $B_{w_K, \mathbf{w}}$  is a reduced plabic graph. By Lemma 4.2,  $B_{w_K, \mathbf{w}}$  has (decorated) trip permutation  $x^{-1}$  with fixed points in  $[k]$  colored white.

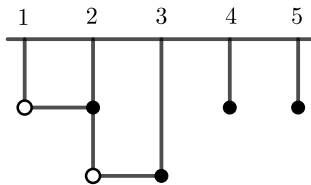
**Example 4.7.** Let  $k = 2$ ,  $n = 5$ ,  $x = (3, 5, 1, 2, 4)$  and  $w = xw_K$ . The partition  $\lambda^\nearrow(x([2]))$  corresponding to  $x([2]) = \{x(1), x(2)\}$  is  $(3, 2)$ , and the columnar expression for  $x$  is  $\mathbf{x} = s_4 s_2 s_3 s_1 s_2$ . So the bridge sequence for  $B_{w_K, \mathbf{w}}$  is  $(2\ 3), (1\ 2), (3\ 4), (2\ 3), (4\ 5)$ . To build  $B_{w_K, \mathbf{w}}$ , we start with the lollipop graph



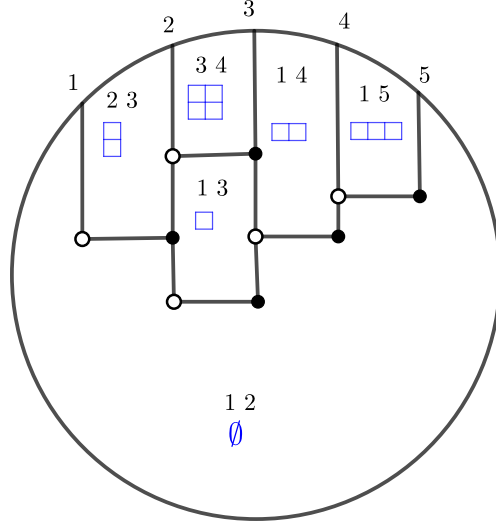
then add the bridge  $(2\ 3)$ ,



the bridge  $(1\ 2)$ ,



and the bridges  $(3\ 4), (2\ 3), (4\ 5)$  to obtain the following graph.



Note that the (target) face labels of  $B_{w_K, \mathbf{w}}$  correspond to rectangles that fit inside of  $\lambda^\nearrow(x([2]))$ .

The structure of  $B_{w_K, \mathbf{w}}$  will follow entirely from the structure of its Grassmann necklace. First, we need the following simple lemma.

**Lemma 4.8.** *Let  $x \in {}^K W$ .*

- (1) *The fixed points of  $x$  are  $[p] \cup [q, n]$  for some  $0 \leq p \leq k < q \leq n + 1$ .*
- (2) *For  $i \in [k]$ ,  $x(i) \geq i$ .*

*Proof.* For the first statement, recall that  $x \in {}^K W$  implies  $x(1) < x(2) < \dots < x(k)$  and  $x(k+1) < \dots < x(n)$ . Suppose  $x(j) = j$  for some  $j \in [k]$ . Since for  $i < j$ ,  $x(i) < x(j)$ , we must have that  $x([j]) = [j]$ . The increasing condition described above then implies that  $x(i) = i$  for  $i < j$ . An analogous argument shows that if  $x(j) = j$  for some  $j \in [k+1, n]$ , then  $x(\ell) = \ell$  for all  $\ell > j$ .

The second statement is clear from the condition that  $x(1) < x(2) < \dots < x(k)$ .  $\square$

Proposition 4.9 shows that the Young diagrams associated to the Grassmann necklace of  $y \in W_{\min}^K$  are the rectangles which are frozen for  $\lambda := \lambda^\nearrow(y^{-1}[k])$  (cf Definition 3.2), together with  $\emptyset$ .

**Proposition 4.9.** *Let  $y \in W_{\min}^K$  with fixed points  $[p] \cup [q, n]$ , and let  $\lambda := \lambda^\nearrow(y^{-1}[k])$ . We color the fixed points of  $y$  in  $[k]$  white and all others black. Let  $\mathcal{J} = (J_1, \dots, J_n)$  be the Grassmann necklace of  $y$ . Then  $\lambda^\nearrow(J_i) = \emptyset$  for  $i \in [p+1] \cup [q, n]$ . For other  $i$ ,  $\lambda^\nearrow(J_i)$  is a rectangle which is frozen for  $\lambda$ , and  $\lambda^\nearrow(J_{i+1})$  can be obtained from  $\lambda^\nearrow(J_i)$  by adding a column to  $\lambda^\nearrow(J_i)$  if the resulting rectangle fits inside of  $\lambda$  (that is, if  $y(i) > k$ ) or removing a row from  $\lambda^\nearrow(J_i)$  if it does not (that is, if  $y(i) \leq k$ ). In particular, every  $\lambda$ -frozen rectangle occurs as one of the  $\lambda^\nearrow(J_i)$ .*

*Proof.* We induct on the length of  $y$ . If  $y = e$ , the white fixed points of  $y$  are  $[k]$ , so  $J_i = [k]$  for all  $i$ , corresponding to the empty set.

Now, consider  $y \neq e$ . Note that by Lemma 4.8, if  $i \in [k]$  is not a fixed point of  $y$ , then  $y^{-1}(i) > i$ . This together with our choice of decoration implies that the antiexcedance set of  $y$  is  $[k]$ .

Suppose the columnar expression for  $y$  ends in  $s_j$ . Then  $z := ys_j$  is an element of  $W^K$  corresponding to the partition  $\lambda' := \lambda^\nearrow(z^{-1}([k]))$ , which is  $\lambda$  with the bottom box of the rightmost column removed. In other words, in  $\lambda$ , the  $j^{\text{th}}$  step is horizontal and the  $(j+1)^{\text{th}}$  step is vertical, and vice versa in  $\lambda'$ . Again, we color the fixed points of  $z$  in  $[k]$  white and the fixed points in  $[k+1, n]$  black, and let  $\mathcal{I} = (I_1, \dots, I_n)$  be the Grassmann necklace of  $z$ .

Note that  $J_r = I_r$  for  $r \leq j$ , since the antiexcedances of both permutations are  $[k]$  and  $y(r) = z(r)$  for  $r \neq j, j+1$ . Note also that since  $\ell(y) > \ell(z)$ ,  $y(j) > y(j+1)$ . As  $y$  is a minimum length right

coset representative, this implies  $y(j) > k \geq y(j+1)$ . From this, we can conclude neither  $j$  nor  $j+1$  are fixed by  $y$ ; otherwise, Lemma 4.8 would lead to a contradiction. So  $J_{j+1} = (I_j \setminus \{j\}) \cup \{y(j)\}$  and  $J_{j+2} = (J_{j+1} \setminus \{j+1\}) \cup \{y(j+1)\}$ .

By definition,  $z(j+1) > k \geq z(j)$ . By induction,  $\lambda^\vee(I_j)$  is a rectangle, so  $I_j = [a] \cup [b, c]$  for  $0 \leq a \leq b, c \leq n$ . There are 4 cases, depending on if  $j$  or  $j+1$  is fixed by  $z$ . The cases in which at least one of  $j$  and  $j+1$  is fixed are straightforward, so we just prove the last.

Suppose neither  $j$  nor  $j+1$  are fixed by  $z$ , so  $\lambda'$  is obtained from  $\lambda$  by removing a box that is not in the left column or top row. Suppose  $I_j = [a] \cup [b, c]$ . Since  $z(j) \leq k$ ,  $\lambda^\vee(I_{j+1})$  is obtained from  $\lambda^\vee(I_j)$  by removing a row, and we have that  $I_{j+1} = [a+1] \cup [b+1, c]$ . In other words,  $j = b$  and  $z(j) = a+1$ .  $\lambda^\vee(I_{j+2})$  is obtained from  $\lambda^\vee(I_{j+1})$  by adding a column, so  $I_{j+2} = [a+1] \cup [b+2, c+1]$ ; that is,  $z(j+1) = c+1$ . So  $J_{j+1} = [a] \cup [b+1, c+1]$ , which means that  $\lambda^\vee(J_{j+1})$  is the rectangle obtained from  $\lambda^\vee(J_j)$  by adding a column. This rectangle fits inside of  $\lambda$  because of where we added a box and is also  $\lambda$ -frozen, since its lower right corner touches the southeastern boundary of  $\lambda$ . Computation shows that  $J_{j+2} = I_{j+2}$ , and thus  $\lambda^\vee(J_{j+2})$  is obtained from  $\lambda^\vee(J_{j+1})$  by removing a row. Since  $I_r = J_r$  for  $r \neq j+1$ , and all of the rectangles  $\lambda^\vee(I_r)$  are  $\lambda$ -frozen for  $r \neq j+1$ , we are done.  $\square$

As a corollary, we obtain the structure of the face labels of the plabic graphs we are interested in.

**Corollary 4.10.** *Let  $w \in W$  with a length-additive factorization  $w = xw_K$ , where  $x \in {}^K W$ . Let  $\mathbf{x} = s_{i_r} \dots s_{i_1}$  be the columnar expression for  $x$  and  $\mathbf{w}$  be a standard reduced expression for  $w$ . Let  $\lambda := \lambda^\vee(x([k]))$ . Then the set of face labels of  $B_{w_K, \mathbf{w}}$  (see Definition 4.6) with respect to the target labeling is  $\{V^\vee(\text{Rect}(b)) \mid b \text{ a box of } \lambda\} \cup \{V^\vee(\emptyset)\}$ . The boundary face labels correspond to the  $\lambda$ -frozen rectangles and the empty set.*

*Proof.* Recall that the bridge sequence of  $B_{w_K, \mathbf{w}}$  is exactly the simple transpositions in the columnar expression for  $x^{-1}$ ; that is  $s_{i_1}, \dots, s_{i_r}$ . After placing the  $j^{\text{th}}$  bridge, we get a plabic graph with trip permutation  $s_{i_1} \dots s_{i_j}$  with fixed points in  $[k]$  colored white. Since  $s_{i_1} \dots s_{i_j} \in W_{\min}^K$ , by Proposition 4.9, its Grassmann necklace consists of rectangles that are frozen for the partition corresponding to  $s_{i_1} \dots s_{i_j}$ . The face labels of the boundary faces are the Grassmann necklace of the trip permutation, with  $I_j$  labeling the face immediately to the left of  $j$ . When we add the  $(j+1)^{\text{th}}$  bridge, we introduce a new boundary face (whose label is a rectangle that is frozen for the partition corresponding to  $s_{i_1} \dots s_{i_{j+1}}$ ) and the labels of all other faces stay the same. An old boundary face may be pushed off of the boundary by the new face; this occurs precisely when its label is not frozen for the new partition. Further, it is clear that every rectangle that fits into  $\lambda$  is frozen for a partition corresponding to some prefix of  $s_{i_1} \dots s_{i_r}$ .  $\square$

We can also describe the dual quiver of  $B_{w_K, \mathbf{w}}$ .

**Proposition 4.11.** *Let  $w, x$ , and  $\mathbf{w}$  be as in Corollary 4.10, and let  $\lambda := \lambda^\vee(x([k]))$ . Let  $\mu, \nu$  be rectangles contained in  $\lambda$  which are not the empty partition. In the dual quiver of  $B_{w_K, \mathbf{w}}$ , there is an arrow from the face labeled  $V^\vee(\mu)$  to the face labeled  $V^\vee(\nu)$  if*

- $\nu$  is obtained from  $\mu$  by removing a row or column
- $\nu$  is obtained from  $\mu$  by adding a hook shape

*unless both faces are on the boundary, in which case there is no arrow between them. There is also an arrow from the face labeled  $V^\vee(\mu)$ , where  $\mu$  is a single box, to the face labeled  $[k]$ .*

*Proof.* This follows from the proof of Corollary 4.10 by induction on the number of bridges.

To make the proof more uniform, we color all boundary vertices of  $B_{w_K, \mathbf{w}}$  adjacent to white (black) internal vertices black (white) and add arrows appropriately in the dual quiver. To obtain the statement of the proposition, just remove all arrows between frozen vertices.

Let  $\mathbf{x} = s_{i_r} \dots s_{i_1}$  be the columnar expression for  $x$ , so that  $s_{i_1}, \dots, s_{i_r}$  is the bridge sequence for  $B_{w_K, \mathbf{w}}$ . Note that  $s_{i_1} = s_k$ .

If there is only one single bridge, then  $B_{w_K, \mathbf{w}}$  has two faces, one face  $f$  labeled with  $[k] = V^\vee(\emptyset)$  and the other face  $f'$  labeled with  $V^\vee(\mu)$ , where  $\mu$  is a single box. From the coloring of vertices in a bridge, it is clear that the dual quiver has one arrow from  $f'$  to  $f$ .

We examine what occurs after we place the final bridge  $s_{i_r} = (j \ j+1)$ . Let  $f'$  be the new face created by this bridge. Note that  $j$  and  $j+1$  cannot both be lollipops. Indeed, it is easy to see from the definition of the columnar reading order for  $\lambda$  that  $s_{i_r}$  is preceded by either a  $s_{i_r-1}$  or a  $s_{i_r+1}$  in the bridge sequence. If  $j$  or  $j+1$  is a lollipop, then the face  $f'$  shares 2 edges with  $f$ , the face labeled with  $[k]$ . This means there are no edges between these faces in the dual quiver, since 2 shared edges results in an oriented 2-cycle.

Note also that we do not have to add additional vertices of degree 2 after placing the bridge to make the graph bipartite; this is clear from the previous paragraph if  $j$  or  $j+1$  is a lollipop. If neither is a lollipop, from the columnar reading order, it is clear that there is a  $s_{j-1}$  and a  $s_{j+1}$  between each occurrence of  $s_j$  in the sequence  $s_{i_1}, \dots, s_{i_r}$ , so  $j$  is adjacent to a black internal vertex and  $j+1$  is adjacent to a white internal vertex. This means that there is an arrow in the dual quiver between  $f'$  and all adjacent faces that are not labeled with  $[k]$ . We discuss these arrows in the case when neither  $j$  nor  $j+1$  are lollipops, as the other cases are similar.

We know that  $f'$  is labeled by (the vertical steps of)  $\text{Rect}(b)$ , where  $b$  is the last box of  $\lambda$  in the columnar reading order. According to the proof of Corollary 4.10, to its right is the face labeled by (the vertical steps of) a partition  $\nu$  obtained from  $\text{Rect}(b)$  by removing a row (since the partition obtained from  $\text{Rect}(b)$  by adding a column does not fit in  $\lambda$ ). Similarly, to the left of  $f'$  is the face labeled by (the vertical steps of) a partition  $\nu'$  obtained from  $\text{Rect}(b)$  by removing a column. Below  $f'$  is the face labeled by the partition obtained from  $\text{Rect}(b)$  by removing a hook shape. This, together with the color of vertices in bridges, gives the proposition. □

**4.3. Obtaining the rectangles seed from a plabic graph.** The goal of this section is to verify Lemma 4.12, which will be used in Section 6.2 to deduce Theorem 1.5 from Theorem 1.6.

In what follows, when we say “reflect a (generalized) plabic graph in the mirror”, we mean the operation shown in Figure 9.

Now, we return to the setup of Section 3.

**Lemma 4.12.** *Let  $v \leq w$  where  $v \in W_{\max}^K$  and  $w = xv$  is length-additive and let  $\mathbf{w}'$  be a standard reduced expression for  $xw_K$ . Consider the following generalized plabic graphs, with the indicated face labeling.*

- $G_{v,w}$ , obtained by applying  $v^{-1}$  to the boundary vertices of  $B_{w_K, \mathbf{w}'}$ , with target labels.
- $G_{v,w}^{\text{mir}}$ , obtained by applying  $v^{-1}$  to the boundary vertices of  $B_{w_K, \mathbf{w}'}$  and reflecting in the mirror, with source labels.
- $H_{v,w}$ , obtained by applying  $w^{-1}$  to the boundary vertices of  $B_{w_K, \mathbf{w}'}$ , with source labels.
- $H_{v,w}^{\text{mir}}$ , obtained by applying  $w^{-1}$  to the boundary vertices of  $B_{w_K, \mathbf{w}'}$  and reflecting in the mirror, with target labels.

*The labeled dual quiver of each of these graphs, with the vertex labeled  $v^{-1}([k])$  deleted, is  $\Sigma_{v,w}$  (up to reversing all arrows).*

*Proof.* Clearly  $G_{v,w}$  and  $H_{v,w}$  have the same (unlabeled) dual quiver as  $B_{w_K, \mathbf{w}'}$ ; reflecting in the mirror reverses all arrows in the dual quiver. By Proposition 4.11, the dual quiver of all of these graphs is  $Q_{v,w}$  (see Definition 3.1), up to reversal of all arrows.

Since the face labels of  $G_{v,w}$  are obtained from those of  $B_{w_K, \mathbf{w}'}$  by applying  $v^{-1}$ , it is clear from Corollary 4.10 that the labeled dual quiver of  $G_{v,w}$  is  $\Sigma_{v,w}$ . So it suffices to show that the face labels of  $G_{v,w}$  agree with the face labels of the 3 other graphs.

Recall that the trip permutation of  $B_{w_K, \mathbf{w}'}$  is  $x^{-1}$ . This implies that applying  $v^{-1}$  to a target face label of  $B_{w_K, \mathbf{w}'}$  gives the same set as applying  $v^{-1}x^{-1} = w^{-1}$  to a source face label of  $B_{w_K, \mathbf{w}'}$ . Thus the face labels of  $H_{v,w}$  are the same as the face labels of  $G_{v,w}$ .

Note that reflecting a generalized plabic graph in the mirror reverses all trips and also exchanges left and right. As a result, the target labels of  $G_{v,w}$  are the same as the source labels of  $G_{v,w}^{\text{mir}}$ , and the source labels of  $H_{v,w}$  are the same as the target labels of  $H_{v,w}^{\text{mir}}$ . □



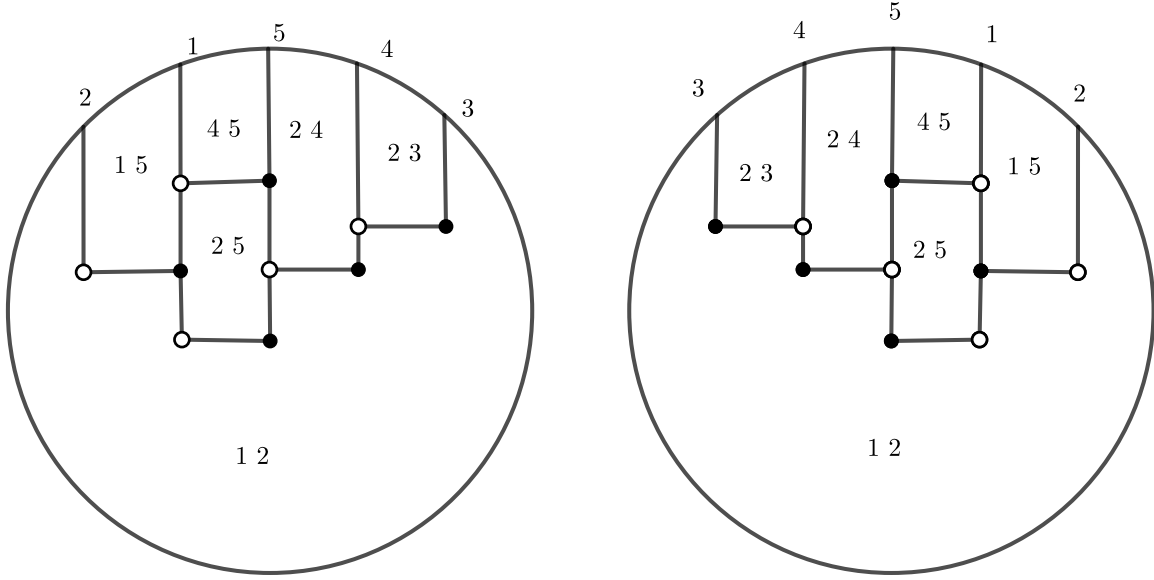


FIGURE 9. Let  $k = 2$ ,  $n = 5$ ,  $x = (3, 5, 1, 2, 4)$  and  $w = xw_K$  as in Example 4.7. On the left, we have applied  $w_K^{-1}$  to the boundary vertices of  $B_{w_K, \mathbf{w}}$  to obtain  $G_{w_K, w}$  (shown with target labels). On the right, we have “reflected  $G_{w_K, w}$  in the mirror” to obtain  $G_{w_K, w}^{\text{mir}}$  (shown with source labels).

**Remark 4.13.** Since we are actually interested in the affine cone over  $\pi(\mathcal{R}_{v, w})$ , we always assume that  $\Delta_{v^{-1}([k])}$ , the lexicographically minimal nonvanishing Plücker coordinate, is equal to 1. This is why we delete the vertex labeled by  $v^{-1}([k])$  in Lemma 4.12.

Note that if  $v = w_K$ ,  $G_{v, w}^{\text{mir}}$  is a “usual” plabic graph (that is, its boundary vertices are  $1, \dots, n$  going clockwise). Similarly, if  $w = w_0$ ,  $H_{v, w}^{\text{mir}}$  is a usual plabic graph. So in these cases, the rectangles seed  $\Sigma_{v, w}$  gives rise to the cluster structure conjectured in [MS16b, Conjecture 3.4]. In general,  $\Sigma_{v, w}$  gives rise to a different cluster structure; the cluster variables may differ and the frozen variables generally do not agree with the labels of the boundary faces (with either source or target labels) of a plabic graph corresponding to the positroid variety. However, the cluster structure given by  $\Sigma_{v, w}$  is *quasi-isomorphic* to the cluster structure conjectured in [MS16b, Conjecture 3.4]. This means roughly that seeds in one cluster algebra can be obtained from seeds in the other by rescaling variables by Laurent monomials in frozen variables, in a way that is compatible with mutation (see [Fra16]). Details will appear in [FSB19].

**Remark 4.14.** Applying  $v^{-1}$  or  $w^{-1}$  to the boundary vertices of  $B_{w_K, \mathbf{w}}$  is a mysterious operation. This relabeling takes a plabic graph associated to  $\pi_k(\mathcal{R}_{w_K, w_K x^{-1}})$  to one associated to  $\pi_k(\mathcal{R}_{v, xv})$ , and hence these positroid varieties are isomorphic. We can describe the association of these two positroid varieties combinatorially in terms of J-diagrams: to obtain the J-diagram of  $\pi_k(\mathcal{R}_{v, xv})$ , rotate the J-diagram of  $\pi_k(\mathcal{R}_{e, x^{-1}})$  by  $180^\circ$ , cut off boxes so it has shape  $\lambda^\vee(v^{-1}([k]))$ , and then perform J-moves until it satisfies the J-property (see Appendix A).

## 5. OBTAINING THE RECTANGLES SEED FROM LECLERC’S CATEGORICAL CLUSTER STRUCTURE

**5.1. The categorical cluster structure for Richardson varieties.** We describe the categorical cluster structure on the coordinate ring of the Richardson variety  $\mathcal{R}_{v, w}$  obtained in [Lec16]. It involves representation theory of finite-dimensional algebras, see [ASS06, Sch14] for some background. As we are only interested in the case of Grassmannians, we restrict our discussion to the construction in type  $A$ .

Let  $\Lambda$  be the *preprojective algebra* over  $\mathbb{C}$  of type  $A$  and rank  $n - 1$ . It is the finite-dimensional path algebra of the *double quiver*

$$\overline{Q} = 1 \begin{array}{c} \xrightarrow{\alpha_1} \\ \xleftarrow{\alpha_1^*} \end{array} 2 \begin{array}{c} \xrightarrow{\alpha_2} \\ \xleftarrow{\alpha_2^*} \end{array} 3 \begin{array}{c} \xrightarrow{\alpha_3} \\ \xleftarrow{\alpha_3^*} \end{array} \cdots \begin{array}{c} \xrightarrow{\alpha_4} \\ \xleftarrow{\alpha_4^*} \end{array} n-1$$

on the vertex set  $I = \{1, \dots, n-1\}$ , subject to the relations generated by

$$\sum_i \alpha_i \alpha_i^* - \alpha_i^* \alpha_i = 0.$$

In particular, the elements of  $\Lambda$  are linear combinations of paths in the quiver modulo the relations, and multiplication is given by concatenation of paths. Any finite-dimensional module  $N$  over  $\Lambda$  has an explicit realization in terms of the quiver. In particular,  $N$  is a collection  $\{N_i\}_{i \in I}$  of finite-dimensional vector spaces over  $\mathbb{C}$  for each vertex  $i \in I$ , together with a collection of linear maps  $\phi_\beta : N_i \rightarrow N_j$  for every arrow  $\beta : i \rightarrow j$  in the quiver. Moreover, the composition of these linear maps must satisfy relations induced by the relations on the corresponding arrows.

Let  $\text{mod } \Lambda$  be the category of finite-dimensional  $\Lambda$ -modules. For any  $N \in \text{mod } \Lambda$  let  $|N|$  be the number of pairwise non-isomorphic indecomposable direct summands of  $N$ . We use  $\text{add } N$  to denote the additive closure of  $N$ , and  $\text{ind } N$  to denote the set of indecomposable direct summands of  $N$ . Given a vertex  $i$  in the quiver  $\overline{Q}$ , let  $S_i$  denote the corresponding simple module and  $Q_i$  denote the associated injective module. The simple module  $S_i$  is obtained by placing  $\mathbb{C}$ , a one-dimensional vector space, at vertex  $i$  and 0's at the remaining vertices of the quiver. In this case,  $\phi_\beta = 0$  for all arrows  $\beta$ . On the other hand, the injective  $\Lambda$ -module  $Q_i$  also has a distinct structure, and we can represent  $Q_i$  by its composition factors as follows.

$$\begin{array}{ccccccc} & & n-i & & & & \\ & & \nearrow & n-i-1 & \searrow & & \\ n-1 & \cdots & n-i+1 & & n-i & & \cdots & 1 \\ & & \searrow & & \nearrow & & & \\ & & i+1 & & i & & i-1 & \end{array}$$

In particular, when  $n = 6$  we obtain the following composition diagrams for the injective modules.

$$Q_1 = \begin{array}{c} 5 \\ 4 \\ 3 \\ 2 \\ 1 \end{array} \quad Q_2 = \begin{array}{c} 5 \\ 4 \\ 3 \\ 2 \\ 1 \end{array} \quad Q_3 = \begin{array}{c} 5 \\ 4 \\ 3 \\ 2 \\ 1 \end{array} \quad Q_4 = \begin{array}{c} 5 \\ 4 \\ 3 \\ 2 \\ 1 \end{array} \quad Q_5 = \begin{array}{c} 5 \\ 4 \\ 3 \\ 2 \\ 1 \end{array}$$

These numbers can be interpreted as basis vectors or as composition factors (see [GLS11, Section 2.4]). For example, the module  $Q_2$  is an 8-dimensional  $\Lambda$ -module with dimension vector  $(d_1, d_2, d_3, d_4, d_5) = (1, 2, 2, 2, 1)$ . In general, for every occurrence of  $j \in I$  above we obtain the corresponding one-dimensional vector space  $V_j \cong \mathbb{C}$  at vertex  $j$  of the quiver. Moreover, whenever we see a configuration  $j^{+1} \underset{j}{\cdot} \underset{j}{\cdot} j^{-1}$  then the linear map between the corresponding spaces  $V_{j+1} \rightarrow V_j$  or  $V_{j-1} \rightarrow V_j$  is the identity. We will often use this notation to denote other modules of  $\Lambda$  that have a similar structure. Moreover, in this notation, it is easy to see the top and socle of a given module  $N$ . The top (resp. socle) of  $N$  is a direct sum of simple modules  $S_i$  such that the corresponding entry  $i$  in the associated composition factor diagram lies at the top (resp. bottom). In other words, there are no  $i-1$  and no  $i+1$  appearing directly above (resp. below) this  $i$ . For more information on preprojective algebras and their representation theory see [GLS08, Rin98].

Next, for every  $i \in I$  and  $s_i \in W$  (where  $W$  is the symmetric group on  $n$  letters) we define two functors  $\mathcal{E}_i = \mathcal{E}_{s_i}$  and  $\mathcal{E}_i^\dagger = \mathcal{E}_{s_i}^\dagger$  on the category  $\text{mod } \Lambda$ . Given  $N \in \text{mod } \Lambda$  let  $\mathcal{E}_i(N)$  be the kernel of a surjection

$$N \twoheadrightarrow S_i^a$$

where  $a$  is the multiplicity of  $S_i$  in the top of  $N$ . Note that  $\mathcal{E}_i(N)$  is well-defined; it is obtained from  $N$  by removing the  $S_i$ -isotypical part of its top. Similarly, let  $\mathcal{E}_i^\dagger(N)$  be the cokernel of an injection

$$S_i^b \hookrightarrow N$$

where  $b$  is the multiplicity of  $S_i$  in the socle of  $N$ . The module  $\mathcal{E}_i^\dagger(N)$  results from  $N$  by taking away the  $S_i$ -isotypical part of its socle. In terms of the corresponding composition factor diagrams, the diagram for  $\mathcal{E}_i(N)$  (resp.  $\mathcal{E}_i^\dagger(N)$ ) is obtained from that of  $N$  by removing all entries  $i$  appearing in the top (resp. bottom). Moreover, for every  $w \in W$  we can extend the definition to  $\mathcal{E}_w, \mathcal{E}_w^\dagger$  by composing the functors associated to the simple reflections in a reduced expression for  $w$ . It was shown in [GLS08, Proposition 5.1] that this definition does not depend on the choice of a reduced expression.

Given  $w \in W$ , consider  $\mathcal{C}_w = \mathcal{E}_{w^{-1}w_0}(\text{mod } \Lambda)$  and  $\mathcal{C}^w = \mathcal{E}_{w^{-1}}^\dagger(\text{mod } \Lambda)$ , two subcategories of  $\text{mod } \Lambda$  associated to  $w$ . With this notation we can summarize the main theorem of [Lec16].

**Theorem 5.1.** [Lec16, Theorem 4.5] *For every  $v, w \in W$  with  $v \leq w$ , the subcategory  $\mathcal{C}_{v,w} := \mathcal{C}^v \cap \mathcal{C}_w$  has a cluster structure in the sense of [BIRS09]. Moreover,  $\mathcal{C}_{v,w}$  induces a cluster subalgebra in the coordinate ring  $\mathbb{C}[\mathcal{R}_{v,w}]$ , where the cardinality of the extended cluster is equal to  $\dim \mathcal{R}_{v,w}$ .*

In particular, the theorem says that  $\mathcal{C}_{v,w}$  is a Frobenius category that admits a cluster-tilting object. Given a basic cluster-tilting module  $T$  we can associate the *endomorphism quiver*  $\Gamma_T$  as follows. The vertices of  $\Gamma_T$  are in bijection with indecomposable direct summands  $T_i$  of  $T$ . The number of arrows  $T_i \rightarrow T_j$  in  $\Gamma_T$  corresponds to the dimension of the space of irreducible morphisms  $T_i \rightarrow T_j$  in  $\text{add } T$ .

Given a basic cluster-tilting module  $T \in \mathcal{C}_{v,w}$ , there is a notion of mutation of  $T$  at an indecomposable summand  $T_i$  of  $T$ , provided that  $T_i$  is not projective-injective in  $\mathcal{C}_{v,w}$ . The *mutation* of  $T$  at  $T_i$  is a new cluster-tilting module  $\mu_{T_i}(T) := T/T_i \oplus T'_i$ , obtained by replacing  $T_i$  by a unique different indecomposable module  $T'_i \in \mathcal{C}_{v,w}$ . Moreover,  $T'_i$  is defined by the two short exact sequences

$$0 \longrightarrow T'_i \longrightarrow B \xrightarrow{g} T_i \longrightarrow 0 \qquad 0 \longrightarrow T_i \xrightarrow{f} B' \longrightarrow T'_i \longrightarrow 0$$

where  $g$  and  $f$  are minimal right and left  $\text{add}(T/T_i)$ -approximations of  $T_i$ . Thus,  $B$  is a direct sum of  $T_j \in \text{ind } T$  for every arrow  $T_j \rightarrow T_i$  in  $\Gamma_T$ , and  $B'$  is a direct sum of  $T_j \in \text{ind } T$  for every arrow  $T_i \rightarrow T_j$  in  $\Gamma_T$ .

Furthermore, there is a cluster character  $\varphi : \text{obj } \mathcal{C}_{v,w} \rightarrow \mathbb{C}[\mathcal{R}_{v,w}]$  that maps modules  $N \in \mathcal{C}_{v,w}$  to functions  $\varphi_N \in \mathbb{C}[\mathcal{R}_{v,w}]$ . While the definition of  $\varphi$  is rather complicated,  $\varphi$  satisfies several nice properties. In particular, for every  $N, N' \in \mathcal{C}_{v,w}$ , we have

$$\varphi_{N \oplus N'} = \varphi_N \varphi_{N'}.$$

Moreover, for every mutation  $\mu_{T_i}$  of a cluster-tilting module  $T$ , we obtain an exchange relation in  $\mathbb{C}[\mathcal{R}_{v,w}]$ :

$$\varphi_{T_i} \varphi_{T'_i} = \varphi_B + \varphi_{B'},$$

where  $B$  and  $B'$  come from the short exact sequences above. In this way the cluster character  $\varphi$  induces a cluster algebra structure in  $\mathbb{C}[\mathcal{R}_{v,w}]$  from a categorical cluster structure in  $\mathcal{C}_{v,w}$ .

Next we want to give a more explicit version of Theorem 5.1.

**Definition 5.2.** Given  $v \leq w$  in  $W$  and a reduced expression  $\mathbf{w} = s_{i_t} \cdots s_{i_2} s_{i_1}$  for  $w$ , we construct a set of modules  $\{U_j\}$  which will give rise to a cluster in  $\mathbb{C}[\mathcal{R}_{v,w}]$ . Let  $\mathbf{v}$  be the reduced subexpression for  $v$  in  $\mathbf{w}$  that is “rightmost” in  $\mathbf{w}$ , called the *positive distinguished subexpression* for  $v$  in  $\mathbf{w}$  (see Definition B.1). Set  $w_{(j)} = s_{i_j} \cdots s_{i_2} s_{i_1}$  for  $1 \leq j \leq t$ , and let  $w_{(j)}^{-1} := (w_{(j)})^{-1}$ . Let  $v_{(j)}$  be the product of all simple reflections in  $w_{(j)}$  that are part of  $\mathbf{v}$ . Define  $J \subseteq \{1, \dots, t\}$  to be the collection of indices  $j$  such that the corresponding reflection  $s_{i_j}$  in the expression  $\mathbf{w}$  is *not* a part of  $\mathbf{v}$ .

For every  $j \in J$  we construct a module  $U_j$  from the injective module  $Q_{i_j}$ . For  $N \in \text{mod } \Lambda$  let  $\text{Soc}_{s_i}(N)$  be the direct sum of all submodules of  $N$  isomorphic to the simple module  $S_i$ . Given a reduced word  $z = s_{i_r} \cdots s_{i_2} s_{i_1}$  in  $W$ , there is a unique sequence

$$0 = N_0 \subseteq N_1 \subseteq \cdots \subseteq N_r \subseteq N$$

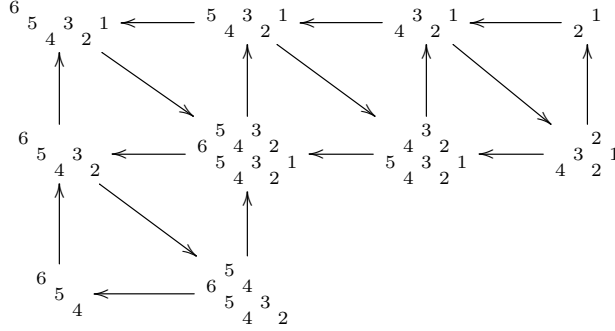
of submodules of  $N$  such that  $N_p/N_{p-1} = \text{Soc}_{s_{i_p}}(N/N_{p-1})$ . Define  $\text{Soc}_z(N) = N_r$ . For every  $j \in J$ , let

$$(5.1) \qquad V_j = \text{Soc}_{w_{(j)}^{-1}}(Q_{i_j}) \qquad \text{and} \qquad U_j = \mathcal{E}_{v_{(j)}^{-1}}^\dagger V_j.$$



$$U_{16} = \begin{matrix} 5 \\ 6 \\ 5 \\ 4 \\ 3 \\ 2 \end{matrix} \quad U_{17} = \begin{matrix} 3 \\ 4 \\ 3 \\ 2 \\ 1 \end{matrix} \quad U_{18} = \begin{matrix} 3 \\ 5 \\ 4 \\ 3 \\ 2 \\ 1 \end{matrix} \quad U_{19} = \begin{matrix} 1 \\ 2 \end{matrix} \quad U_{20} = \begin{matrix} 2 \\ 4 \\ 3 \\ 2 \\ 1 \end{matrix}$$

The projective-injective objects of  $\mathcal{C}_{v,w}$  are precisely  $U_{13}, U_{15}, U_{16}, U_{18}, U_{19}, U_{20}$ .  
The endomorphism quiver  $\Gamma_{U_{v,w}}$  is given below.



In general, it is difficult to construct the endomorphism quiver  $\Gamma_{U_{v,w}}$ , because it is difficult to determine whether a given morphism is irreducible in  $\text{add } U_{v,w}$ . For example, there is a nonzero morphism  $f : U_{15} \rightarrow U_{11}$  with image  $\begin{matrix} 5 \\ 4 \\ 3 \\ 2 \end{matrix}$  but it factors through  $U_{12}$ . Thus,  $f$  does not induce an arrow in  $\Gamma_{U_{v,w}}$ .

Our goal is to find an explicit description of the seed associated to a pair  $(v, \mathbf{w})$ , where  $v \in W_{\max}^K$ ,  $w = xv$  is a length-additive factorization, and  $\mathbf{w} = \mathbf{xv}$  is a standard expression for  $w$ . In Section 5.2 we will analyze the cluster variables coming from Theorem 5.3 (interpreting generalized minors as Plücker coordinates), and in Section 5.3 and Section 5.4 we will analyze the modules  $U_j$  and the morphisms between them, so as to obtain the quiver. The modules  $U_j$  were previously defined constructively, so we need to develop a more explicit construction, which then enables us to understand the morphisms. In the case  $v = w_K$ , the modules have a particularly nice structure, which allows us to explicitly compute the irreducible morphisms in  $\text{add } U_{w_K, \mathbf{w}}$ . Next, we use a result of [BKT14] we show that there is a bijection between morphisms  $U_i \rightarrow U_j$  in  $\text{add } U_{w_K, \mathbf{w}}$  and morphisms  $U'_i \rightarrow U'_j$  in  $\text{add } U_{w_K v', \mathbf{w} v'}$ . Then we conclude that the quiver for the pair  $(v, \mathbf{w})$  coming from this representation theoretic construction agrees with the quiver coming from a plabic graph.

**5.2. Projecting the categorical cluster variables to Grassmannians.** When  $v \leq w$  and  $v \in W_{\max}^K$ , the Richardson variety  $\mathcal{R}_{v,w}$  in the complete flag variety projects isomorphically to a positroid variety  $\pi_k(\mathcal{R}_{v,w})$  in the Grassmannian  $Gr_{k,n}$ . (Concretely, elements of this positroid variety are given by the span of rows  $v^{-1}\{1, \dots, k\} = v^{-1}[k]$  in a matrix representative  $g$  for  $Bg \in \mathcal{R}_{v,w}$ ). When additionally there is a length-additive factorization  $\mathbf{w} = \mathbf{xv}$ , the positroid variety is a skew Schubert variety, and Theorem 5.3 produces a cluster algebra which is equal to the coordinate ring  $\mathbb{C}[\mathcal{R}_{v,w}]$ . In this section we will determine how to interpret the cluster variables in  $\mathbb{C}[\mathcal{R}_{v,w}]$  as functions on the Grassmannian. In particular, since each generalized minor from Theorem 5.3 is a minor of a unipotent matrix, we can restrict that matrix to rows  $v^{-1}[k]$ , and then identify the minor with a Plücker coordinate of the resulting  $k \times n$  matrix.

For example, continuing Example 5.4 with  $v = w_K s_3$  and  $w$  given by

$$\mathbf{w} = s_5 s_6 s_4 s_5 s_2 s_3 s_4 s_1 s_2 s_3 s_1 s_2 s_1 s_4 s_5 s_4 s_6 s_5 s_4 s_3,$$

we obtain generalized minors which map to the following Plücker coordinates:

- (1)  $\Delta_{v^{-1}[3], v^{-1}s_3[3]} = \Delta_{124,247} = \Delta_{247}$ .
- (2)  $\Delta_{v^{-1}[2], v^{-1}s_3 s_2[2]} = \Delta_{24,47} = \Delta_{147}$ .
- (3)  $\Delta_{v^{-1}[1], v^{-1}s_3 s_2 s_1[1]} = \Delta_{4,7} = \Delta_{127}$ .
- (4)  $\Delta_{v^{-1}[4], v^{-1}s_3 s_2 s_1 s_4[4]} = \Delta_{1247,2476} = \Delta_{246}$ .
- (5)  $\Delta_{v^{-1}[3], v^{-1}s_3 s_2 s_1 s_4 s_3[3]} = \Delta_{124,467} = \Delta_{467}$ .
- (6)  $\Delta_{v^{-1}[2], v^{-1}s_3 s_2 s_1 s_4 s_3 s_2[2]} = \Delta_{24,67} = \Delta_{167}$ .
- (7)  $\Delta_{v^{-1}[5], v^{-1}s_3 s_2 s_1 s_4 s_3 s_2 s_5[5]} = \Delta_{12467,24567} = \Delta_{245}$ .

- (8)  $\Delta_{v^{-1}[4], v^{-1}s_3s_2s_1s_4s_3s_2s_5s_4}[4] = \Delta_{1247,4567} = \Delta_{456}$ .  
(9)  $\Delta_{v^{-1}[6], v^{-1}s_3s_2s_1s_4s_3s_2s_5s_4s_6}[6] = \Delta_{124567,234567} = \Delta_{234}$ .  
(10)  $\Delta_{v^{-1}[5], v^{-1}s_3s_2s_1s_4s_3s_2s_5s_4s_6s_5}[5] = \Delta_{12467,34567} = \Delta_{345}$ .

**Remark 5.5.** Let  $J \subseteq [n]$  with  $|J| = \ell$ . If we project an  $n \times n$  unipotent matrix  $g$  to the Grassmannian element represented by the span of rows  $v^{-1}[\ell]$  of  $g$ , the generalized minor  $\Delta_{v^{-1}[\ell], J}$  of  $g$  equals the following Plücker coordinate of  $Gr_{k, n}$ :

- If  $\ell < k$  and  $|J \cup v^{-1}([k] \setminus [\ell])| = k$ , then  $\Delta_{v^{-1}[\ell], J} = \Delta_{J \cup v^{-1}([k] \setminus [\ell])}$ .
- If  $\ell = k$  then  $\Delta_{v^{-1}[\ell], J} = \Delta_J$ .
- If  $\ell > k$  and  $|J \setminus v^{-1}([\ell] \setminus [k])| = k$ , then  $\Delta_{v^{-1}[\ell], J} = \Delta_{J \setminus v^{-1}([\ell] \setminus [k])}$ .

Using Remark 5.5, the following lemma implies that Leclerc's cluster variables in the seed corresponding to  $(v, \mathbf{w})$  coincide with those obtained from the rectangles seed defined in Section 3.

**Lemma 5.6.** Choose a Young diagram contained in a  $k \times (n - k)$  rectangle, and label its boxes by simple reflections as in the right of Figure 10. Choose a reading order for the boxes as in the left of Figure 10. Choose any box  $b$  and let  $s_\ell$  be its label. Let  $w_b$  be the word obtained by reading boxes in order up through  $b$  and recording the corresponding simple reflections. For example if  $b$  is the box indicated by the bold  $s_6$  in the right of Figure 10, then  $w_b = (s_5s_4s_3s_2)(s_6s_5s_4)(s_7s_6)$ .

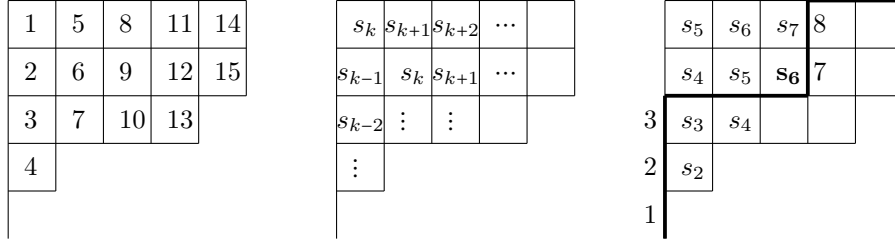


FIGURE 10.

Also let  $J(b) := V^\wedge(\text{Rect}(b))$  (see Definition 3.1). In the right of Figure 10,  $J(b) = \{1, 2, 3, 7, 8\}$ . Then for any  $b$  and  $\ell$  as above, let  $J = w_b[\ell]$ . We have that:

- (1) If  $\ell < k$ , then  $J(b) = J \cup ([k] \setminus [\ell]) = J \cup \{\ell + 1, \ell + 2, \dots, k\}$ .
- (2) If  $\ell = k$ , then  $J(b) = J$ .
- (3) If  $\ell > k$ , then  $J(b) = J \setminus ([\ell] \setminus [k]) = J \setminus \{k + 1, k + 2, \dots, \ell\}$ .

*Proof.* The proofs of the three cases are quite analogous, so we will just prove the first one, where  $\ell < k$ .

Let box  $b$  be in row  $r$  and column  $c$ , as in Figure 11, so that its label is  $s_\ell = s_{k-r+c}$ . We have that  $r > c$ .

Then  $J(b) = \{1, 2, \dots, k - r\} \cup \{k - r + c + 1, k - r + c + 2, \dots, k + c\}$ , and  $J(b) \setminus \{\ell + 1, \ell + 2, \dots, k\} = J(b) \setminus \{k - r + c + 1, k - r + c + 2, \dots, k\} = \{1, 2, \dots, k - r\} \cup \{k + 1, k + 2, \dots, k + c\}$ . We need to show that  $w_b\{1, 2, \dots, k - r + c\} = J(b) \setminus \{k - r + c + 1, k - r + c + 2, \dots, k\} = \{1, 2, \dots, k - r\} \cup \{k + 1, k + 2, \dots, k + c\}$ .

Let the labels of the simple generators in the bottom boxes of columns  $1, 2, \dots, c - 1$  be  $i_1, i_2, \dots, i_{c-1}$ , respectively. We also write  $i_c = k - r + c$ . Then we have that

$$(5.2) \quad w_b = (s_k s_{k-1} s_{k-2} \dots, s_{i_1})(s_{k+1} s_k s_{k-1} \dots, s_{i_2}) \dots (s_{k+c-2} s_{k+c-3}, \dots, s_{i_{c-1}})(s_{k+c-1} s_{k+c-2} \dots, s_{i_c}).$$

Note that

$$1 \leq i_1 < i_2 < i_3 \dots < i_{c-1} < i_c = k - r + c$$

so that  $i_s \leq k - r + s$  for all  $1 \leq s \leq c$ .

We will now explicitly analyze  $w_b(j)$  for  $1 \leq j \leq k - r + c$ . Towards this end, it's useful to observe that for  $a < b$ , the product  $s_b s_{b-1} s_{b-2} \dots s_a$  is equal to the cycle  $(b + 1, b, b - 1, \dots, a + 1, a)$  (in cycle notation).

Then looking at (5.2), we see that:

	Col 1	Col 2		Col c-1	Col c					Col n-k
Row 1	$s_k$	$s_{k+1}$	$s_{k+2}$							
Row 2	$s_{k-1}$	$s_k$	$s_{k+1}$							
	$s_{k-2}$		$s_k$							
				$s_k$						
					$s_k$					
						$s_k$				
							$s_k$			
Row r						$s_{k-r+c}$		$s_k$		
			$s_{i_3}$	$\dots$	$s_{i_{c-1}}$					
	$s_{i_1}$	$s_{i_2}$								
Row k										

FIGURE 11.

- for  $1 \leq j \leq i_1 - 1$ ,  $w_b(j) = j \in \{1, 2, \dots, k-r\}$ .
- for  $j \in \{i_1, i_2, \dots, i_c\}$ ,  $w_b(j) \in \{k+1, k+2, \dots, k+c\}$ .

We also see that

- for  $i_1 < j < i_2$ ,  $w_b(j) = j - 1$
- for  $i_2 < j < i_3$ ,  $w_b(j) = j - 2$
- $\vdots$
- for  $i_{c-1} < j < i_c$ ,  $w_b(j) = j - (c - 1)$ .

So for  $i_{s-1} < j < i_s$ , we have that  $w_b(j) = j - (s - 1) < i_s - (s - 1) \leq k - r + s - (s - 1) = k - r + 1$ , and so  $w_b(j) \leq k - r$ . This shows that for each  $j \in \{1, 2, \dots, k - r + c\}$ ,  $w_b(j) \in \{1, 2, \dots, k - r\} \cup \{k + 1, k + 2, \dots, k + c\}$ , and so  $w_b[k - r + c] = \{1, 2, \dots, k - r\} \cup \{k + 1, k + 2, \dots, k + c\}$ . This completes the proof of the lemma.  $\square$

**Corollary 5.7.** *Consider a skew Schubert variety  $\pi_k(\mathcal{R}_{v,w}) \subset Gr_{k,n}$ , where  $v \leq w$ ,  $v \in W_{max}^K$ , and with  $w = xv$  length-additive. Consider the seed for  $\mathcal{R}_{v,w}$  given by Theorem 5.3 which is associated to a standard (columnar) reduced expression  $\mathbf{w} = \mathbf{xv}$ . When we project the cluster variables to  $\pi_k(\mathcal{R}_{v,w})$ , we obtain precisely the set of Plücker coordinates from the rectangles seed (Definition 3.1). In other words, they are indexed by boxes  $b$  in  $\lambda^\vee(x([k]))$ , and are equal to the Plücker coordinates  $\Delta_{v^{-1}(J(b))}$  in the Grassmannian.*

*Proof.* Let  $\mathbf{x}$  be the columnar expression for  $x$  and  $\mathbf{w}$  be a standard reduced expression for  $w$ . Let  $b$  be a box in  $\lambda^\vee(x([k]))$ , and let  $s_\ell$ ,  $w_b$ , and  $J(b)$  be as defined in Lemma 5.6. Note that  $w_b = x_{(i)}^{-1}$  for some  $1 \leq i \leq \ell(x)$ , so  $v^{-1}w_b = w_{(j)}^{-1}$  for some  $j$ . Using Remark 5.5 and applying  $v^{-1}$  to Lemma 5.6 implies that the

generalized minor  $\Delta_{v^{-1}([\ell]), w_{(j)}^{-1}([\ell])}$  equals the Plücker coordinate  $\Delta_{v^{-1}(J(b))}$  in the Grassmannian. Each of these Plücker coordinates is irreducible in  $\mathbb{C}[\pi_k(\overline{\mathcal{R}_{v,w}})]$  (Remark 5.13), so we are done.  $\square$

It is not hard to see which Plücker coordinates are frozen in the rectangles seed.

**Lemma 5.8.** *Let  $x$  be a Grassmannian permutation of type  $(k, n)$ . Let  $b$  be a  $\lambda$ -frozen box of  $\lambda = \lambda^\wedge(x([k]))$ , and let  $s_\ell$  and  $w_b$  be as defined in Lemma 5.6. Then  $w_b([\ell]) = x^{-1}([\ell])$ . Thus  $\Delta_{v^{-1}(J(b))}$  is frozen in the rectangles seed.*

*Proof.* It is clear from the filling of  $\lambda^\wedge(x([k]))$  that the boxes in columns to the right of the column of  $b$  are filled with  $s_i$  such that  $i > \ell$ . So  $x^{-1} = w_b u$ , where  $u$  is a permutation that fixes  $[\ell]$  pointwise, so  $w_b([\ell]) = x^{-1}([\ell])$ .

Using Remark 5.5 and applying  $v^{-1}$  to Lemma 5.6 implies that  $\Delta_{v^{-1}(J(b))}$  is the projection of  $\Delta_{v^{-1}([\ell]), v^{-1}x^{-1}([\ell])}$  to the Grassmannian, which is frozen by Theorem 5.3.  $\square$

**5.3. An explicit description of the modules  $U_j$  when  $w = xv$  is length-additive.** Throughout this section we fix a pair  $(v, w)$ , where  $w = xv$  is a length additive factorization and  $v \in W_{max}^K$ . Let  $\mathbf{w}$  be a standard reduced expression for  $w$  (see Definition 2.23). Thus, we can write  $v = w_K v'$  where  $v' \in W_{min}^K$ , and choose reduced expressions  $\mathbf{x}, \mathbf{v}'$  for  $x, v'$  respectively as described in Lemma 2.21. Our goal in Section 5.3 and Section 5.4 is to prove that in this case, the quiver from Theorem 5.3 agrees with the quiver from the rectangles seed. Recall that the vertices of the quiver from Theorem 5.3 are indexed by modules  $U_j$ . In this section we will give an explicit (non-recursive) description of the composition diagrams of these modules.

Let

$$\mathbf{w} = \mathbf{x} \mathbf{w}_K \mathbf{v}' = (s_{i_t} \dots s_{i_{r+1}})(s_{i_r} \dots s_{i_{p+1}} s_{i_p} \dots s_{i_{l+1}})(s_{i_l} \dots s_{i_1})$$

where the parenthesis separate the subexpressions  $\mathbf{x}, \mathbf{w}_K, \mathbf{v}'$ . In what follows, we will define a diagram  $\mathcal{D}_{v,w}$  (see Figure 12) whose boxes are filled with simple reflections in such a way that a natural reading order of the boxes gives the reduced expression  $\mathbf{w} = \mathbf{x} \mathbf{w}_K \mathbf{v}'$ . Then to each  $j \in J$  (see Definition 5.2), we will associate a subdiagram  $D_j$  with the property that if we replace each  $s_i$  by  $i$ ,  $D_j$  is precisely the composition diagram of the module  $U_j$ . More precisely, given a subdiagram of  $\mathcal{D}_{v,w}$  the associated module is obtained as follows: for every  $s_i$  directly followed by  $s_{i+1}$  to the right (resp.  $s_{i-1}$  below) in the subdiagram we obtain  $i_{i+1}$  (resp.  $i_{i-1}$ ) in the composition factor diagram of the module (see Figure 15).

**Definition 5.9.** (Diagram  $\mathcal{D}_{v,w}$ ) Extending ideas from Lemma 2.21, we will build a diagram  $\mathcal{D}_{v,w}$  which encodes the reduced expression  $\mathbf{w}$ . We start by taking the union of diagrams  $R^*(v') \cup R(w_K) \cup R(x)$ , glued as in Figure 12, where

- $R^*(v')$  is a (rotated) Young diagram filled with simple reflections which give a reduced expression for  $v'$ , when read in the reading order indicated at the right of Figure 12;
- $R(w_K)$  is a pair of staircase Young diagrams filled with simple reflections which give a reduced expression for  $w_K$ ;
- $R(x)$  is a Young diagram filled with simple reflections which give a reduced expression for  $x$ .

We additionally embed  $R^*(v')$  into an  $(n-k) \times k$  rectangle  $D^*$  (with boxes filled with simple reflections as shown in Figure 12) and embed  $R(x)$  into a  $k \times (n-k)$  rectangle  $D$  (with boxes filled with simple reflections as shown in Figure 12). We let  $\mathcal{D}_{v,w}$  denote the union of  $D, D^*$  and  $R(w_K)$ , together with the paths defining  $R^*(v')$  and  $R(x)$ . Note that  $R^*(v') \cup R(w_K) \cup R(x)$  encodes the reduced expression  $\mathbf{w}$ .

Note that  $R^*(v')$  is defined by the path  $L_{v'^{-1}([k])}^\swarrow$  rotated clockwise 90 degrees and then reflected across a vertical axis, while  $R(x)$  is defined by the path  $L_{x([k])}^\nearrow$ . Finally we define the region  $R(v')$  to be the subset of boxes of  $D$  below  $L_{v'^{-1}([k])}^\swarrow$  (up to a rotation and and reflection, it agrees with  $R^*(v')$ ). Note that  $v'^{-1}([k]) = v^{-1}([k])$ , so  $R(x) \cap R(v') = \emptyset$  by Lemma 5.10.

Let  $J, L$  be lattice paths from  $(0,0)$  to  $(n-k, k)$  taking steps north and east and suppose  $V^\nearrow(J) = \{j_1 < \dots < j_k\}$  and  $V^\nearrow(L) = \{l_1 < \dots < l_k\}$ . We say  $J \leq L$  if  $j_r \leq l_r$  for all  $r$ ; that is,  $J$  “lies above”  $L$  when drawn in the plane (see Figure 13). We leave the proof of Lemma 5.10 to the reader.



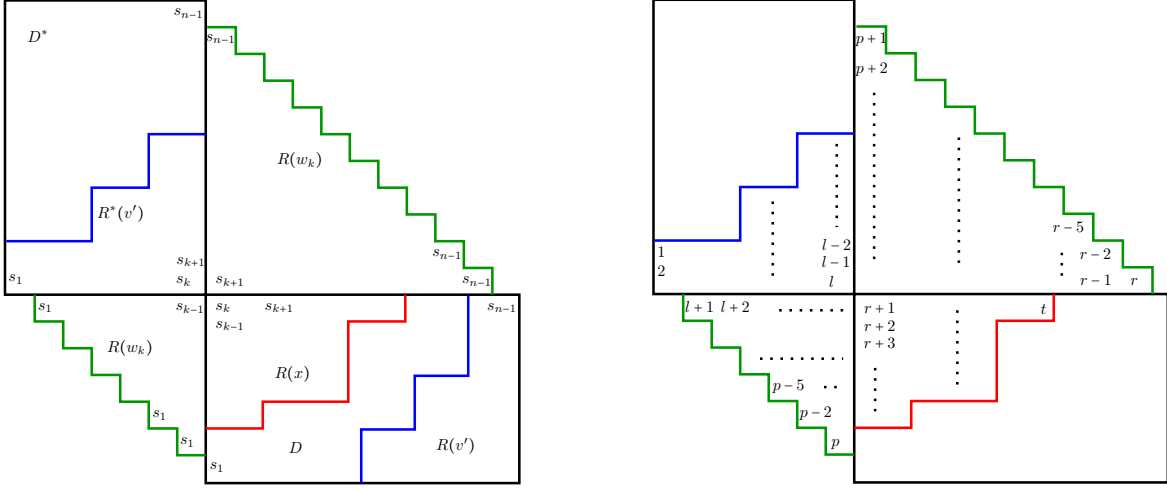


FIGURE 12. Diagram  $\mathcal{D}_{v,w}$  (left) and reading order in each region (right).

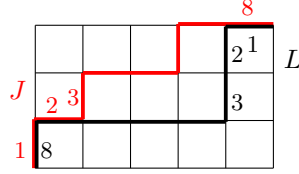


FIGURE 13. Let  $k = 3$  and  $n = 7$ . Let  $x = (1, 3, 6, 2, 4, 5, 7, 8) \in {}^K W$ ,  $v = (8, 3, 2, 7, 6, 5, 4, 1) \in W_{\max}^K$  and  $w = xv$ . The upper lattice path  $J$  is  $L_{x([k])}^\nearrow$ , with  $V^\nearrow(J) = x([3]) = \{1, 3, 6\}$ ; the lower lattice path  $L$  is  $L_{v^{-1}([k])}^\swarrow$ , with  $V^\swarrow(L) = v^{-1}([3]) = \{2, 3, 8\}$ . Since  $w = xv$  is length-additive, the bijection of Lemma 5.10 sends  $(v, w)$  to  $(J, L)$ .

**Lemma 5.10.** *Let  $\mathcal{A} = \{(v, w) \mid v \in W_{\max}^K, w \in W \text{ with length-additive factorization } w = xv\}$ . Then the following map is a bijection:*

$$\begin{aligned} \mathcal{A} &\rightarrow \{(J, L) \mid J \leq L \text{ lattice paths from } (0, 0) \text{ to } (n - k, k)\} \\ (v, xv) &\mapsto (L_{x([k])}^\nearrow, L_{v^{-1}([k])}^\swarrow). \end{aligned}$$

In particular, if  $(v, xv) \in \mathcal{A}$  then  $L_{x([k])}^\nearrow \leq L_{v^{-1}([k])}^\swarrow$ .

Next, we associate specific regions  $D_j^*, D_j$  in  $\mathcal{D}_{v,w}$  to the modules  $V_j, U_j$ .

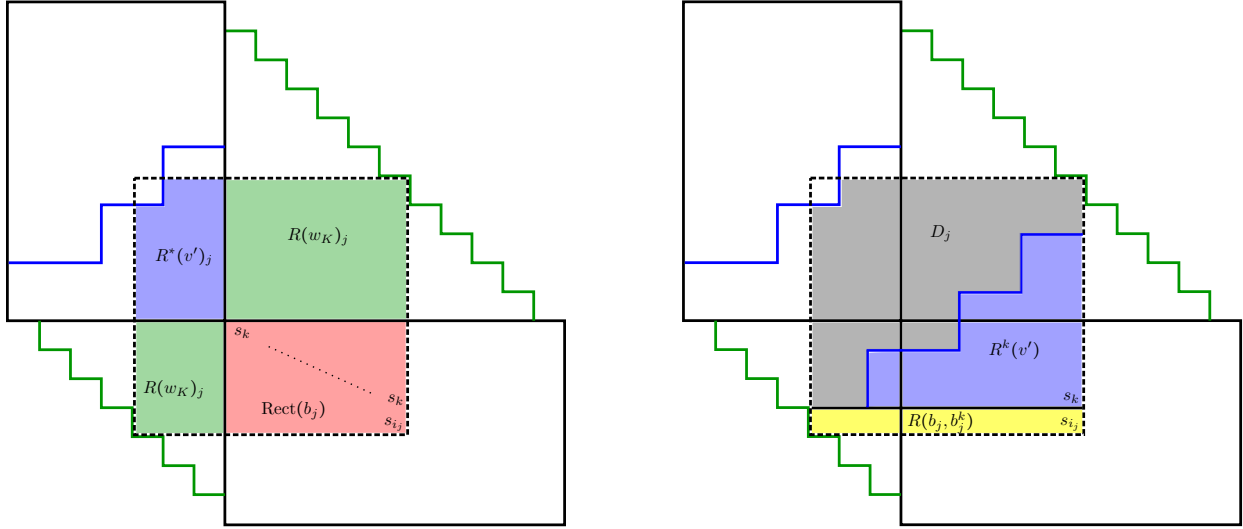
**Construction of  $D_j^* \subset \mathcal{D}_{v,w}$ .** Given  $j \in J$  there exists a corresponding box  $b_j \in R(x)$  filled with the simple generator  $s_{i_j}$ .

By Definition 5.2,  $V_j = \text{Soc}_{w_{(j)}}(Q_{i_j})$ ; we will construct a subdiagram  $D_j^*$  of  $\mathcal{D}_{v,w}$  that yields a composition diagram for the module  $V_j$ . See Figure 14.

We can write  $w_{(j)} = x_{(j)} w_K v'$ , where  $\mathbf{x}_{(j)}$  comes from entries in  $R(x)$  to the left and above  $b_j$ . In the definition of  $V_j$ , we begin with the injective module  $Q_{i_j}$ . Note that  $Q_{i_j}$  corresponds to the maximal rectangle  $R(Q_{i_j})$  in  $\mathcal{D}_{v,w}$  whose lower right corner is  $b_j$ . Next, consider the subdiagram associated to the module  $\text{Soc}_{x_{(j)}}(Q_{i_j})$ . The columnar expression for  $x_{(j)}$  can be written as follows

$$x_{(j)} = s_{i_j} s_{i_j+1} s_{i_j+2} \dots s_a s_{i_j-1} s_{i_j} s_{i_j+1} \dots s_{a-1} \dots s_b s_{b+1} s_{b+2} \dots s_k$$

where  $s_a$  (resp.  $s_b$ ) is the filling of the box in the first row (resp. column) of  $D$  and in the same column (resp. row) as  $b_j$ . It is compatible with the structure of  $Q_{i_j}$  depicted in Section 5.1 in the following sense.

FIGURE 14. Construction of subdiagrams  $D_j^*$  (left) and  $D_j$  (right).

$$\begin{aligned} \text{Soc}_{s_{i_j}}(Q_{i_j}) &= i_j & \text{Soc}_{s_{i_j+1}s_{i_j}}(Q_{i_j}) &= \begin{matrix} i_j+1 \\ i_j \end{matrix} & \text{Soc}_{s_a \dots s_{i_j+2}s_{i_j+1}s_{i_j}}(Q_{i_j}) &= \begin{matrix} a & \dots & i_j+1 \\ & & i_j \end{matrix} \\ \text{Soc}_{s_{i_j-1}s_a \dots s_{i_j+2}s_{i_j+1}s_{i_j}}(Q_{i_j}) &= \begin{matrix} a & \dots & i_j+1 & i_j-1 \\ & & i_j & \end{matrix} & \text{Soc}_{s_{a-1} \dots s_{i_j}s_{i_j-1}s_a \dots s_{i_j+2}s_{i_j+1}s_{i_j}}(Q_{i_j}) &= \begin{matrix} a & a-1 & a-2 & \dots & i_j+1 & \dots & i_j-1 \\ & & & & i_j & & \end{matrix} \end{aligned}$$

Continuing in this way, we see that the module  $\text{Soc}_{x_{(j)}^{-1}}(Q_{i_j})$  is given by the rectangle  $\text{Rect}(b_j) \subseteq D$ , whose southeast box is  $b_j$ . Next, in the definition of  $V_j$  we need to compute  $\text{Soc}_{w_K x_{(j)}^{-1}}(Q_{i_j})$ . First, observe that  $s_k$  does not appear in a reduced expression for  $w_K$ , therefore the subdiagram of  $\mathcal{D}_{v,w}$  associated to  $\text{Soc}_{w_K x_{(j)}^{-1}}(Q_{i_j})$  has trivial intersection with  $D^*$ . Recall that the boxes in  $R(w_K)$  yield a reduced expression for  $w_K$ . Thus, we see that the subdiagram for  $\text{Soc}_{w_K x_{(j)}^{-1}}(Q_{i_j})$  is obtained by extending  $\text{Rect}(b_j)$  to the north and west as much as possible, while avoiding boxes with entries  $s_k$ . In particular, we have

$$R(\text{Soc}_{w_K x_{(j)}^{-1}}(Q_{i_j})) = \text{Rect}(b_j) \cup R(w_K)_j$$

where  $R(w_K)_j = R(w_K) \cap R(Q_{i_j})$ . Finally,  $D_j^*$  is obtained from  $R(\text{Soc}_{w_K x_{(j)}^{-1}}(Q_{i_j}))$  by adding as many boxes in  $R^*(v')$  as possible, such that the result is still contained in  $R(Q_{i_j})$ . Let  $R^*(v')_j = R(Q_{i_j}) \cap R^*(v')$ . Then

$$(5.3) \quad D_j^* = \text{Rect}(b_j) \cup R(w_K)_j \cup R^*(v')_j.$$

**Remark 5.11.** The subdiagram  $D_j^*$  can also be obtained as follows. Given the box  $b_j$ , let  $R$  be the maximal rectangle contained in  $\mathcal{D}_{v,w}$  with  $b_j$  as its southeast corner. Then  $D_j^*$  results from  $R$  by removing boxes of  $R \cap D^*$  which are not in  $R^*(v')$ .

**Construction of  $D_j \subset \mathcal{D}_{v,w}$ .** By Definition 5.2,  $U_j = \mathcal{E}_{v_{(j)}^{-1}}^\dagger V_j$  is obtained by removing simple modules from the socle of  $V_j$  according to the simple reflections appearing in a reduced expression for  $v_{(j)}^{-1}$ . Note that in this case  $v_{(j)} = w_K v'$ . Again since  $w_K$  does not have  $s_k$  in its reduced expression and it is the longest element of  $W_K$ , we see that  $\mathcal{E}_{w_K}^\dagger V_j$  is obtained from  $V_j$  by quotienting out the largest submodule of  $V_j$  not supported at vertex  $k$ . In particular, if  $i_j = k$  then  $\mathcal{E}_{w_K}^\dagger V_j = V_j$ . If  $i_j < k$  then there exists a unique box

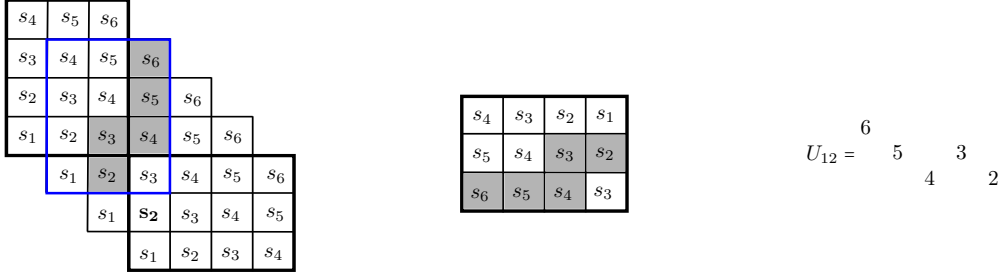


FIGURE 15.  $D_{12}$  from Example 5.4.

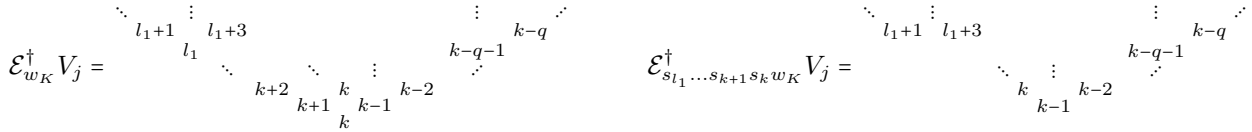
$b_j^k \in \text{Rect}(b_j)$  with entry  $s_k$  located above  $b_j$  and in the same column as  $b_j$ . Let  $R(b_j, b_j^k)$  be the maximal rectangle in  $D_j^*$  with lower right corner  $b_j$  and height  $k - i_j$  (see Figure 14). That is, the upper right corner of  $R(b_j, b_j^k)$  is the box directly below  $b_j^k$ . We see that the module associated to  $R(b_j, b_j^k)$  is the largest submodule of  $V_j$  not supported at vertex  $k$ . Therefore,  $R(\mathcal{E}_{w_K}^\dagger V_j) = D_j^* \setminus R(b_j, b_j^k)$ . Similarly, if  $i_j > k$  then there exists a unique box  $b_j^k \in \text{Rect}(b_j)$  with entry  $s_k$  located to the left of  $b_j$  and in the same row as  $b_j$ . Let  $R(b_j, b_j^k)$  be the maximal rectangle in  $D_j^*$  with lower right corner  $b_j$  of width  $i_j - k$ . That is, the lower left corner of  $R(b_j, b_j^k)$  is the box directly to the right of  $b_j^k$ , and as before we obtain  $R(\mathcal{E}_{w_K}^\dagger V_j) = D_j^* \setminus R(b_j, b_j^k)$ .

Finally, it remains to compute  $\mathcal{E}_{v^{-1}}^\dagger \mathcal{E}_{w_K}^\dagger V_j$ . Note that the columnar expression for  $v'$  is again compatible with the structure of  $\mathcal{E}_{w_K}^\dagger V_j$ , see the computations below. We have

$$v' = s_k s_{k+1} \dots s_{l_1} s_{k-1} s_k \dots s_{l_2} \dots s_{k-q-1} s_{k-q} \dots s_{t_q}$$

where  $s_{l_i}$  is the filling of the upper-most box in column  $i$  of region  $R^*(v') \subset \mathcal{D}_{v,w}$ , if we label the columns of  $R^*(v')$  by  $1, 2, \dots, q$  right to left.

The socle of  $\mathcal{E}_{w_K}^\dagger V_j$  is precisely  $S_k$ , and  $s_k$  is the first reflection in  $v'$ . Thus,  $\mathcal{E}_{s_k w_K}^\dagger V_j$  is obtained from  $\mathcal{E}_{w_K}^\dagger V_j$  by removing the simple module  $S_k$  from the socle. Similarly,  $S_{k+1}$  is in the socle of  $\mathcal{E}_{s_k w_K}^\dagger V_j$ , and  $s_{k+1}$  is the second reflection in  $v'$ , provided the first column of  $R^*(v')$  has at least two boxes. Therefore,  $\mathcal{E}_{s_{l_1} \dots s_{k+1} s_k w_K}^\dagger V_j$  is obtained from  $\mathcal{E}_{w_K}^\dagger V_j$  by removing a portion of the left-most diagonal between labels  $k$  and  $l_1$  from the composition diagram for  $\mathcal{E}_{w_K}^\dagger V_j$ .



Continuing in this way, we see that  $D_j$ , the subdiagram associated to  $U_j$ , results from  $R(\mathcal{E}_{w_K}^\dagger V_j)$  by removing the diagram  $R^k(v')$ , where  $R^k(v')$  is obtained from  $R^*(v')$  by shifting  $R^*(v')$  southeast until its bottom right corner box is  $b_j^k$  (see Figure 14). This completes the construction of the region

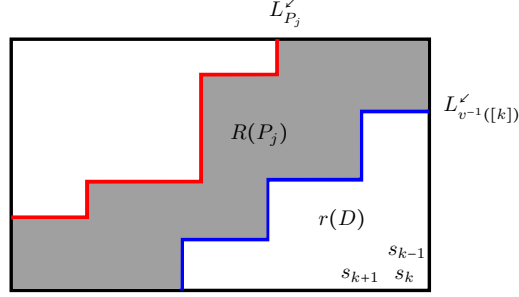
$$(5.4) \quad D_j = D_j^* \setminus (R(b_j, b_j^k) \cup R^k(v')).$$

Now, we use the above constructions to find a simple description of  $D_j$  as a subdiagram of  $D$ . See Figure 15 for an example of such a transformation.

Let  $b_j$  be a box in  $\lambda^\vee(x([k]))$  (or equivalently a box in  $R(x)$ ). This box corresponds to the module  $U_j$  and by Corollary 5.7 the associated Plücker coordinate is  $\Delta_{P_j}$  where  $P_j = v^{-1}(J(b_j))$  (see Definition 3.1).

Let  $r(D)$  be the  $k \times (n - k)$  diagram obtained by rotating  $D$  clockwise 180 degrees. Define  $R(P_j)$  to be the region in  $r(D)$  bounded by the lattice paths  $L_{P_j}^\vee$  and  $L_{v^{-1}([k])}^\vee$  (see Figure 16).

**Theorem 5.12.** *Let  $w = xv$  where  $v \in W_{max}^K$  and  $\ell(w) = \ell(x) + \ell(v)$ . Given a pair  $(v, \mathbf{w})$ , where  $\mathbf{w}$  is a standard reduced expression for  $w$ , for each  $j \in J$  the region  $R(P_j)$  gives the composition diagram for  $U_j$ .*

FIGURE 16. Region  $R(P_j)$ 

*Proof.* In (5.4) we defined a region  $D_j$  in  $\mathcal{D}_{v,w}$  that yields the desired module  $U_j$ , and we want to realize it as a region in  $r(D)$ .

Let  $r(D)_j^*$  be a diagram in  $\mathcal{D}_{v,w}$ , that has the same shape as  $D^*$  but whose southeast corner box coincides with the box  $b_j^k$  (Figure 14)

We see that  $D_j$  is contained in  $r(D)_j^*$ . Moreover, by construction, region  $D_j \subset r(D)_j^*$  is determined by two contours, see Figure 14. Next, we provide an explicit formula for these contours, and then realize them as lattice paths in the diagram  $r(D)$ . Note that the bottom contour of  $D_j$  is always below or at most coincides with the top contour of  $D_j$ , therefore we can consider them separately.

*The bottom contour of  $D_j$ .* By (5.4) the bottom contour of  $D_j$  is determined by the Young diagram  $R^k(v')$  associated to  $v'$  (see Figure 14). Observe that the bottom contour of  $D_j$  can be realized as a northeast lattice path in  $r(D)_j^*$ . By Lemma 2.21 the horizontal steps of this path are labeled by  $(v')^{-1}([k])$ . Since  $(v')^{-1}([k]) = v^{-1}([k])$ , we obtain a desired description of the horizontal steps of the bottom contour of  $D_j$  in  $r(D)_j^*$ .

*The top contour of  $D_j$ .* We proceed by induction on the length of  $v'$ . Let  $L_{r(D)_j^*}^{\rightarrow}$  denote the lattice path in  $r(D)_j^*$  resulting in the top contour of  $D_j$ . First, we consider the base case. If  $v' = e$ , then by construction  $R^*(v') = R^k(v') = \emptyset$ , therefore by (5.4)

$$D_j = \text{Rect}(b_j) \cup R(w_K)_j \setminus R(b_j, b_j^k).$$

We depict  $D_j$  in Figure 17, where we consider the case  $i_j \leq k$ . The remaining case can be proved similarly. Recall that  $\text{Rect}(b_j)$  is a rectangle in  $D$ , with entries at the corners being  $s_{i_j}, s_k, s_a, s_b$  for some  $k \leq a \leq n-1$  and  $1 \leq b \leq i_j$ . We see that the horizontal steps of  $L_{r(D)_j^*}^{\rightarrow}$  consist of three intervals

$$P = \{1, 2, \dots, e-1\} \cup \{d+1, d+2, \dots, k\} \cup \{c+1, c+2, \dots, n\}.$$

We claim that  $P_j = P$ , where  $\Delta_{P_j}$  denotes the Plücker coordinate associated to the box  $b_j$ .

By Lemma 5.6, the lattice path  $L_{v(P_j)}^{\rightarrow}$  in  $D$  cuts out a rectangle in the northwest corner of  $D$ . In our case, this statement implies that

$$v(P_j) = w_K(P_j) = \{1, 2, \dots, b-1\} \cup \{i_j+1, i_j+2, \dots, a+1\}.$$

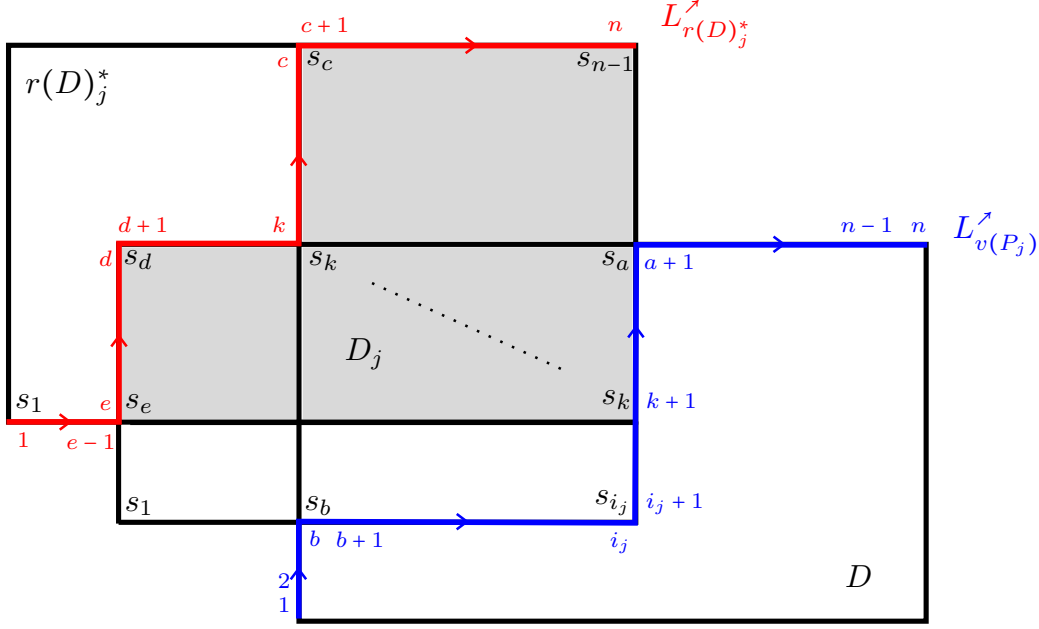
Applying  $w_K$  to this set where

$$w_K = \begin{pmatrix} 1 & 2 & \dots & i & \dots & k & k+1 & \dots & j & \dots & n-1 & n \\ k & k-1 & \dots & k+1-i & \dots & 1 & n & \dots & n-(j+k-1) & \dots & k+2 & k+1 \end{pmatrix}$$

we see that

$$P_j = \{k, k-1, \dots, k-b+2\} \cup \{k-i_j, k-i_j-1, \dots, 1\} \cup \{n, n-1, \dots, n-a+k\}.$$

It follows from Figure 17 that  $e = k - i_j + 1, d = k - b + 1, c = n - a + k - 1$ , which implies that  $P_j = P$ . This completes the proof that the top contour of  $D_j$  given by  $L_{r(D)_j^*}^{\rightarrow}$  has horizontal steps  $P_j$  in the case  $v' = e$ .


 FIGURE 17. Base case  $v' = e$ 

Now, consider the pair  $(v, \mathbf{w})$  and some  $(vs_t, \mathbf{ws}_t)$  such that the length of each element increases by one. By induction hypothesis assume that the horizontal steps of top contour of  $D_j$ , coming from the pair  $(v, \mathbf{w})$ , are given by  $P_j$ .

Let  $U'_j$  be the module associated to the box  $b_j$  and coming from the pair  $(vs_t, ws_t)$ . Let  $P'_j$  denote the corresponding element of  $\binom{[n]}{k}$  for the pair  $(vs_t, ws_t)$ . Observe that by changing  $v$  to  $vs_t$  the top contour of  $D'_j$  is obtained from the top contour of  $D_j$  by adding a box  $b'$  with entry  $s_t$  to  $R^*(v')_j$  provided that this box lies in  $R(Q_{i_j})$ ; otherwise the top contour does not change. If the box  $b' \in R(Q_{i_j})$  then the south and east edges of  $b'$  are part of the top contour for  $D_j$ . The south edge of  $b'$  is a horizontal step of  $L_{r(D)_j}^*$  with label  $t$ , while the east edge is a vertical step with label  $t+1$ . By induction hypothesis,  $t \in P_j$  and  $t+1 \notin P_j$ . At the same time since the contour of  $D'_j$  changes by adding this box  $b'$ , we see that  $t+1 \in P'_j$  and  $t \notin P'_j$ . On the other hand, we have  $P'_j = s_t(P_j)$ , which precisely interchanges  $t \in P_j$  for  $t+1$ . Thus, we see that the two agree and in the case  $b' \in R(Q_{i_j})$  the claim holds.

Now, suppose that the box  $b' \notin R(Q_{i_j})$ . Then we know that by construction  $D_j$  and  $D'_j$  have the same top contour, and we want to show  $P_j = P'_j$ . Clearly, if  $t, t+1 \in P'_j$  or  $t, t+1 \notin P'_j$  then  $P'_j = s_t(P_j) = P_j$  as desired. The remaining possibility is that  $t+1 \in P_j$  but  $t \notin P_j$ . Thus, we must be in the situation as depicted in Figure 18. Note that  $R^*(v's_t)$ , considered as a region of  $D^*$ , must contain a rectangle of height at least  $b$  and of width at least  $n-a$ . Similarly,  $R(x) \in D$  must contain a rectangle of height at least  $k+1-b$  and width at least  $a+1-k$ . Since  $D$  has height  $k$  and width  $n-k$ , this contradicts Lemma 5.10 saying that  $R(v's_t) \cap R(x) = \emptyset$  in  $D$ . Therefore, it is not possible that  $t+1 \in P_j$ ,  $t \notin P_j$ , and  $b' \notin R(Q_{i_j})$ . This completes the proof of the induction step for the top contour of  $D_j$ .

Thus, we showed that the bottom and top contour of  $D_j \subset r(D)_j^*$  has horizontal steps given by  $v^{-1}[k]$  and  $P_j$  respectively. Moreover, after rotating  $r(D)_j^*$  clockwise 90 degrees and reflecting it across a vertical axis, we obtain the desired region  $R(P_j)$ , that yields the composition factor diagram for  $U_j$ , as a subset of  $r(D)$ . For an example of this transformation see Figure 15. Note that in this way a northeast lattice path  $L^\nearrow$  in  $r(D)_j^*$  becomes a southwest path  $L^\swarrow$  in  $r(D)$ . Also, horizontal steps of  $L^\nearrow$  become vertical steps of  $L^\swarrow$ . This completes the proof of the theorem.  $\square$

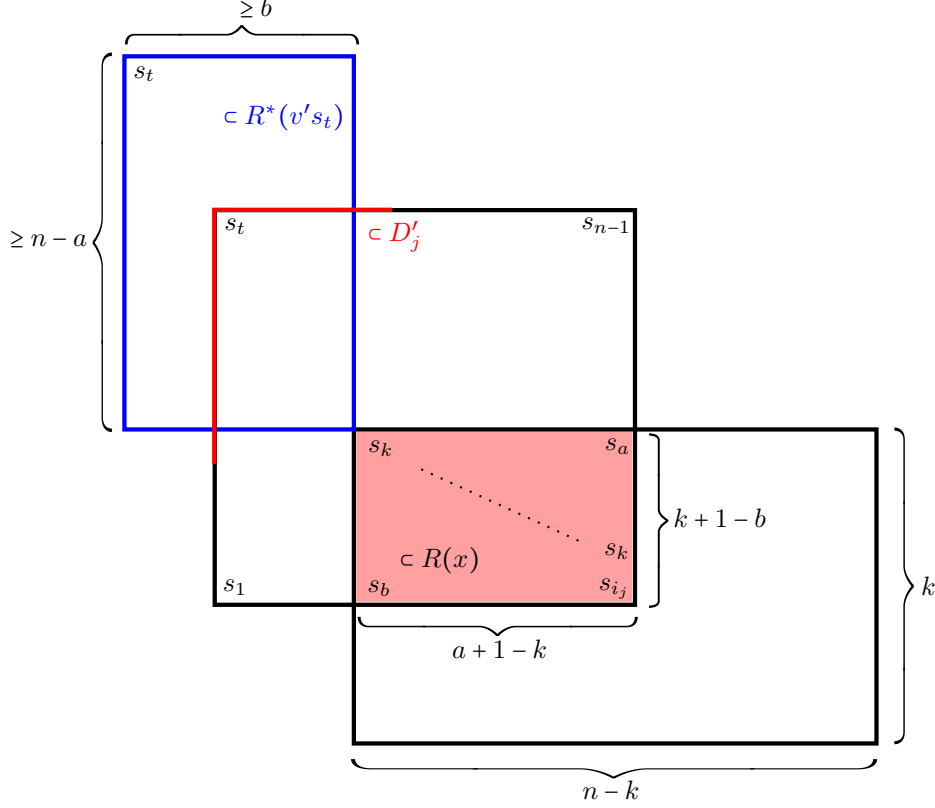


FIGURE 18. Inductive step for the top contour

**Remark 5.13.** Note the module  $U_j$  is actually indecomposable because by construction of the diagram  $D_j$  its bottom and top contour do not intersect, except on the boundary of  $r(D)_j^*$ , and  $R(P_j) \subset R(Q_k)$ . In particular, the cluster-tilting module  $U_{v,w}$  is basic and the Plücker coordinate  $\Delta_{P_j}$  is irreducible.

**5.4. An explicit description of the endomorphism quiver  $\Gamma_{U_{v,w}}$ .** In order to understand the endomorphism quiver, we need to analyze morphisms between indecomposable summands of  $U_{v,w}$ .

Recall that for a box  $b_i \in R(x)$ ,  $U_i$  denotes the associated summand of  $U_{v,w}$ . Also, recall that  $\text{Rect}(b_i)$  is the maximal rectangle in  $D$  whose southeast corner is  $b_i$ .

**Theorem 5.14.** Consider  $(v, w)$  where  $v \in W_{\max}^K$  and  $w = xv$  is length-additive. Let  $\mathbf{w} = \mathbf{xv} = \mathbf{xw}_k \mathbf{v}'$  be a standard reduced expression for  $w$ . For any pair of modules  $U_i, U_j \in \text{ind } U_{v,w}$  there exists an irreducible morphism  $U_i \rightarrow U_j$  in  $\text{add } U_{v,w}$  if and only if one of the following conditions holds:

- (i)  $\text{Rect}(b_j)$  is obtained from  $\text{Rect}(b_i)$  by removing a row
- (ii)  $\text{Rect}(b_j)$  is obtained from  $\text{Rect}(b_i)$  by removing a column
- (iii)  $\text{Rect}(b_j)$  is obtained from  $\text{Rect}(b_i)$  by adding a hook shape.

Moreover, there exists at most one irreducible morphism between  $U_i$  and  $U_j$ .

Before proving Theorem 5.14, we make the following key observation.

**Remark 5.15.** Let  $f : U_i \rightarrow U_j$  be a homomorphism, and suppose that  $N$  is an indecomposable direct summand of  $\text{im } f$ . Then because  $\text{im } f$  is a submodule of  $U_j$  and is (isomorphic to) a quotient of  $U_i$ , the composition diagram for  $N$  embeds into those for  $U_i, U_j$ . Moreover,  $N$  is closed under predecessors in  $U_i$ : for all vertices  $x$  and  $y \in I$  in the composition diagrams for  $N$  and  $U_i$ , respectively, such that  $y$  lies immediately above  $x$  in  $U_i$  (that is  $\begin{smallmatrix} y \\ x \end{smallmatrix}$  or  $\begin{smallmatrix} x \\ y \end{smallmatrix}$ ) we have that  $y$  is also in the composition diagram for  $N$ .

Similarly,  $N$  is *closed under successors* in  $U_j$ : for all vertices  $x, y \in I$  in the diagrams for  $N, U_j$  such that  $y$  lies immediately below  $x$  in  $U_j$  (that is  $\begin{smallmatrix} x \\ y \end{smallmatrix}$  or  $\begin{smallmatrix} y \\ x \end{smallmatrix}$ ), we have that  $y$  is also in the diagram for  $N$ .

Conversely, for any  $N$  that is closed under predecessors in  $U_i$  and closed under successors in  $U_j$  we get a morphism  $f : U_i \rightarrow U_j$  with image  $N$ .

We will prove Theorem 5.14 in two steps. First we treat the case  $v' = e$ , i.e.  $v = w_K$ .

**Proposition 5.16.** *Theorem 5.14 is true when  $v = w_K$ , i.e.  $v' = e$ .*

*Proof.* By the proof of Theorem 5.12 all indecomposable summands of  $U = U_{v, \mathbf{w}}$  are of the form given in Figure 19. Moreover, we must have  $S_k = \text{Soc } U_i = \text{Soc } U_j$  and either  $c_i + r_i = k$  or  $a_i + r_i = n - k$  for any  $U_i \in \text{ind } U$ . Thus, we can rephrase the statement of the theorem in terms of these new parameters  $a_i, c_i, r_i$  that define a given summand of  $U$ . Here both (ia) and (ib) correspond to case (i) of the theorem, depending if  $b_i$  is above or below the main diagonal. Similar correspondences hold for the remaining cases.

- (ia)  $r_i = r_j + 1$ ,  $a_i = a_j$ , and  $c_i + r_i = c_j + r_j = k$
- (ib)  $r_i = r_j$ ,  $c_i = c_j - 1$ , and  $a_i + r_i = a_j + r_j = n - k$

- (iia)  $r_i = r_j$ ,  $a_i = a_j - 1$ , and  $c_i + r_i = c_j + r_j = k$
- (iib)  $r_i = r_j + 1$ ,  $c_i = c_j$ , and  $a_i + r_i = a_j + r_j = n - k$

- (iiia)  $r_i = r_j - 1$ ,  $a_i = a_j + 1$ , and  $c_i + r_i = c_j + r_j = k$
- (iiib)  $r_i = r_j - 1$ ,  $c_i = c_j + 1$ , and  $a_i + r_i = a_j + r_j = n - k$ .

By the construction of the region  $D_j \subset \mathcal{D}_{v, w}$  (see Figure 17), given  $U_i \in \text{add } U$  defined by  $a_i, r_i, c_i$  a module  $U_z$  defined by  $a_z, r_z, c_z$  is also in  $\text{add } U$  if  $r_z \leq a_z$  and either  $a_z = a_i, c_z \geq b_i$  or  $c_z = c_i, a_z \geq a_i$ . Indeed, every module in  $\text{add } U$  corresponds to a unique box in  $R(x)$ . Given a box  $b_i \in R(x)$  associated to the module  $U_i$ , all the boxes  $b_z \in D$  above and to the left of  $b_i$  are also in  $R(x)$ . The module  $U_z$  with the above properties is precisely the one coming from such a box  $b_z \in R(x)$ . Thus,  $U_z \in \text{add } U$  as claimed.

Below we consider an arbitrary morphism  $f : U_i \rightarrow U_j$ , and using the particular structure of the modules we show that it factors through another summand  $U'$  of  $U$ . Moreover, we obtain two maps  $U_i \rightarrow U'$  and  $U' \rightarrow U_j$  whose composition is  $f$  together with additional conditions on the structure of  $U'$ . Since we are interested in the case when  $f$  is irreducible, we can reduce  $f$  to the case  $U_i \rightarrow U' = U_j$  or  $U' = U_i \rightarrow U_j$ . We then continue in the same way replacing  $f$  by one of the two morphisms. At every step we obtain more information about the particular structure of  $U_i$  and  $U_j$  until we recover the case listed in the theorem.

Let  $f : U_i \rightarrow U_j$  be a nonzero nonidentity morphism in  $\text{mod } \Lambda$ . Since  $U_j$  has a one-dimensional socle it follows that  $\text{im } f$ , which is a submodule of  $U_j$ , is indecomposable. Let  $N = \text{im } f$ . By Remark 5.15 it is closed under predecessors in  $U_i$  and closed under successors in  $U_j$ . Moreover, the socle of  $N$  is also  $S_k$ , and we obtain the configuration depicted in Figure 20. Here,  $r_z \leq r_i, r_j$ ,  $r_z + c'_z \leq r_j + c_j$ , and  $r_z + a_z \leq r_j + a_j$ . Conversely, for every such  $N$  as in the figure we obtain a nonzero morphism  $U_i \rightarrow U_j$ .

First, we consider the case  $r_i + c_i = k$  and  $r_j + c_j = k$ . Note that  $N$  is not necessarily in  $\text{add } U$ . Thus, we construct a module  $U_z \in \text{ind } \Lambda$  of the same structure as  $U_i, U_j$  defined by  $a_z = a_i, r_z$ , and  $c_z$  such that  $c_z + r_z = k$ . Since  $r_z \leq r_i$  and  $c_z \geq c_i$  it follows that  $U_z \in \text{ind } U$ . We also obtain maps  $g : U_i \rightarrow U_z$  and  $h : U_z \rightarrow U_j$  such that  $f = hg$ . This implies that  $f$  is reducible in  $\text{add } U$  unless  $g = 1$  or  $h = 1$ .

As we are interested in irreducible morphisms  $f$ , suppose first that  $h = 1$ . Thus,  $U_z = U_j$  and  $f = g$ . If  $r_z = r_i$ , then  $U_i = U_z$  and  $g = f = 1$  contrary to our original assumption that  $f$  is not the identity morphism. Now, if  $r_z < r_i$  consider a module  $U_t$  defined by  $a_t = a_i, r_t = r_z + 1$  and  $c_t$  such that  $c_t + r_t = k$ . In particular,  $c_t = c_z - 1$ . Since  $r_t \leq r_i$  and  $c_t > c_i$  it follows that  $U_t \in \text{add } U$ . In this case, we note that  $f$  factors through  $U_t$ . That is, there exist maps  $\rho, \pi$  as below

$$\begin{array}{ccc} U_i & \xrightarrow{f=g} & U_z \\ & \searrow \rho & \nearrow \pi \\ & U_t & \end{array}$$

such that  $f = \pi\rho$ . Note that by definition  $\pi \neq 1$  as  $c_t \neq c_z$ . Since we are interested in irreducible morphisms  $f$ , we consider the case  $\rho = 1$  and  $f = \pi$ . If  $f = \pi$  then we have  $U_i = U_t$  and  $U_j = U_z$ . By construction,

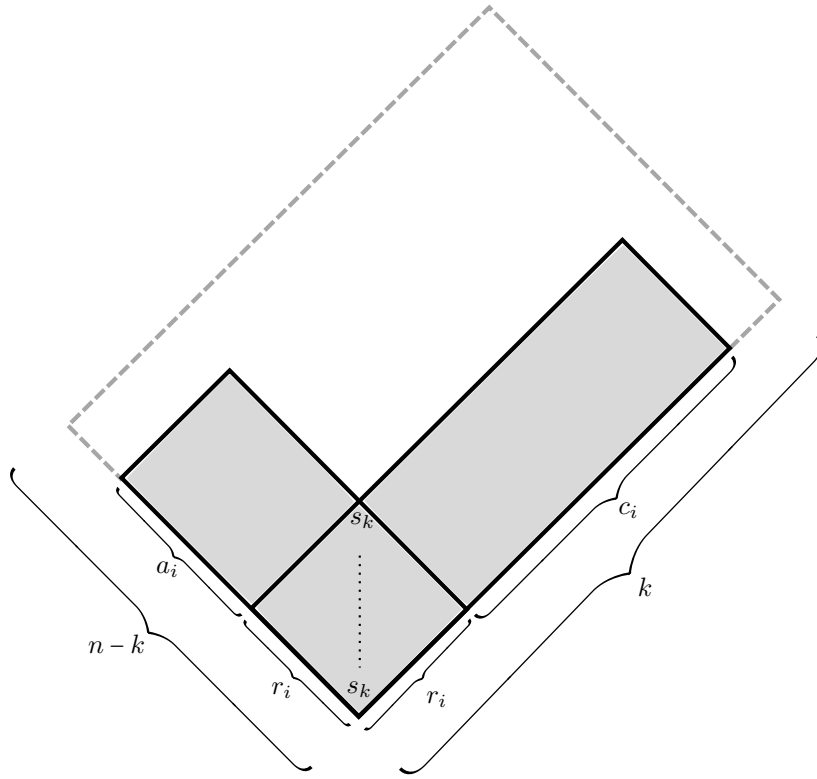


FIGURE 19. Module  $U_i$

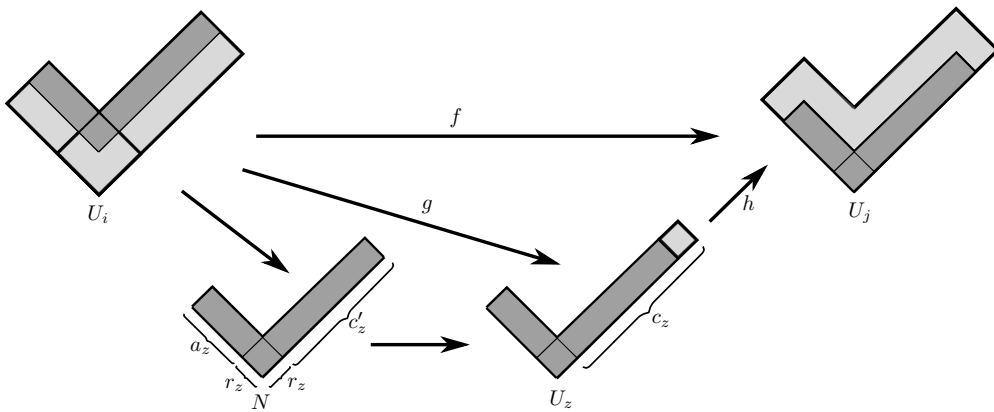


FIGURE 20. Morphism  $f : U_i \rightarrow U_j$  with image  $N$

$a_i = a_j$ ,  $r_i = r_j + 1$  and  $c_i + r_i = c_j + r_j = k$ , which agrees with case (ia). Conversely, by the structure of  $U_i$  and  $U_j$  it is easy to see that such  $f$  is indeed irreducible in  $\text{add } U$ .

Now, consider the case  $g = 1$ . Thus,  $h = f$  and  $U_z = U_i = X$ . Let  $U_q$  be the module defined by  $a_q = a_z + 1$ ,  $r_q = r_z$ ,  $c_q = c_z$ , provided that  $a_z + r_z < n - k$ . Observe that  $U_q \in \text{add } U$  because  $r_q = r_z$  and  $c_q > a_z$ . If



$a_q + r_q \leq a_j + r_j$ , we see that  $f$  factors through  $U_q$ . In particular, there exist morphisms  $\sigma, \delta$  as below

$$\begin{array}{ccc} U_z & \xrightarrow{f=h} & U_j \\ & \searrow \sigma & \nearrow \delta \\ & U_q & \end{array}$$

where  $f = \delta\sigma$ . Since we are looking for irreducible maps we take  $\delta = 1$ . Note that  $\sigma \neq 1$  as  $a_z < a_q$ . In the case  $\delta = 1$  we have  $f = \sigma$  is injective, and  $U_z = U_i, U_q = U_j$ . Therefore,  $r_i = r_j, a_i = a_j - 1$ , and  $r_i + c_i = r_j + c_j = k$ , which is precisely the conditions of case (iia). Also, because  $f$  is injective, we can see by the particular structure of  $U_i$  and  $U_q$  that it is actually irreducible in  $\text{add } U$ .

It remains to consider the the case  $f = h$  and  $a_z + r_z = a_j + r_j$ . First, we observe that  $r_z \neq r_j$ , as otherwise  $U_i = U_z = U_j$  and  $f$  is the identity map. Thus, let  $U_p$  be the module defined by  $r_p = r_z + 1, a_p = a_z - 1, c_p = c_z - 1$ , provided  $a_z, c_z$  are both nonzero. In this case,  $U_p \in \text{add } U$  because  $r_p \leq r_j$  and  $a_p \geq a_j$ . Thus, we see that  $f = h$  factors through  $U_p$

$$\begin{array}{ccc} U_z & \xrightarrow{f=h} & U_j \\ & \searrow \epsilon & \nearrow \theta \\ & U_p & \end{array}$$

where  $f = \theta\epsilon$ . Note that  $\epsilon \neq 1$  by construction, therefore we consider the case  $\theta = 1$ . Thus,  $f = \epsilon$  and  $U_z = U_i, U_j = U_p$ , where  $r_i = r_j - 1, a_i = a_i + 1$ , and  $c_i + r_i = c_j + r_j = k$ . In particular, this agrees with case (iiia) of the lemma. Again, since  $f$  is injective it is easy to see that it is irreducible in  $\text{add } U$ .

Finally, suppose that  $f = h$  and  $a_z + r_z = a_j + r_j$  as above, but  $a_z = 0$  or  $c_z = 0$ . If  $a_z = 0$  then  $r_z = a_j + r_j$ . We also know that  $U_z$  maps injectively into  $U_j$  via  $f$ . Therefore,  $r_z \leq r_j$  which implies that  $a_j = 0$ . We obtain  $U_z = U_i = U_j$  and  $f$  is the identity morphism. This is a contradiction. On the other hand, if  $c_z = 0$  then  $r_z = k$ . Since  $r_z \leq r_j \leq k$ , we obtain  $r_j = k$ . Also,  $a_j + r_j \leq k$  implies that  $a_j = 0$  and we deduce a contradiction as above.

This completes the proof when  $c_i + r_i = c_j + r_j = k$ . A similar argument applies in the case  $a_i + r_i = a_j + r_j = n - k$ . Therefore, it remains to consider the situation when  $r_i + c_i = k$  and  $a_j + r_j = n - k$  while  $r_i + a_i < n - k$  and  $c_j + r_j < k$  and vice versa. In particular, we want to show that every morphism in this case is reducible. Suppose that  $f : U_i \rightarrow U_j$  where  $r_i + c_i = k$  and  $r_j + c_j = n - k$  while  $r_i + a_i < n - k$  and  $c_j + r_j < k$ . The other case follows similarly. Now, obtain a module  $U_u$  defined by  $r_u = r_i, a_u + r_u = n - k, c_u + r_u = k$ . Note that  $U_u$  is different from both  $U_i$  and  $U_j$ . Moreover,  $U_u \in \text{add } U$  because  $r_u = r_i$  and  $a_u > a_i$ . We obtain that  $f$  factors through  $U_u$ . In particular,  $f$  is reducible in  $\text{add } U$  and the resulting maps  $U_i \rightarrow U_u$  and  $U_u \rightarrow U_j$  are between types of modules that we considered earlier. This shows that such  $f$  does not yield any new irreducible morphisms, as desired.  $\square$

In the second step in the proof of Theorem 5.14, we relate morphisms between summands of  $U_{v,w}$ , and morphisms between summands of  $U_{w_K, \mathbf{x}w_K}$  where  $w = xv$  and  $v \in W_{\max}^K$ .

**Lemma 5.17.** *Let  $w = xv$ , where  $v \in W_{\max}^K$  and  $\ell(w) = \ell(x) + \ell(v)$ . Denote the cluster-tilting modules coming from a standard reduced expressions for the pairs  $(w_K, xw_K)$  and  $(v, w)$  by  $U, U'$  respectively. Let  $U_i, U_j \in \text{ind } U$  and let  $U'_i, U'_j \in \text{ind } U'$  be the corresponding summands of  $U'$ . Then, there exists a bijection between irreducible morphisms  $U_i \rightarrow U_j$  in  $\text{add } U$  and irreducible morphisms  $U'_i \rightarrow U'_j$  in  $\text{add } U'$ .*

*Proof.* By [BKT14, Proposition 5.16] there are equivalences of categories  $\mathcal{C}_x \xrightarrow{\sim} \mathcal{C}_{v,w}$  and  $\mathcal{C}_x \xrightarrow{\sim} \mathcal{C}_{w_K, xw_K}$ . In particular, the categories  $\mathcal{C}_{v,w}$  and  $\mathcal{C}_{w_K, xw_K}$  are also equivalent. By [Lec16, Remark 5.2] this equivalence identifies the two cluster-tilting modules  $U$  and  $U'$ . In particular, this implies that there is a bijection between irreducible morphisms  $U_i \rightarrow U_j$  in  $\text{add } U$  and irreducible morphisms  $U'_i \rightarrow U'_j$  in  $\text{add } U'$ .  $\square$

Together Proposition 5.16 and Corollary 5.17 prove Theorem 5.14. Next, we present the main theorem of this section.

**Theorem 5.18.** *Let  $w = xv$  be a length additive factorization and  $v \in W_{\max}^K$ . For a standard reduced expression  $\mathbf{w}$  of  $w$ , the labeled quiver  $\Gamma_{U_{v,w}}$  coincides with  $Q_{v,w}$ .*

*Proof.* By Definition 3.1 and Theorem 5.14, the quivers coincide. And by the construction of  $\Delta_{P_j}$  and Lemma 5.6, the labels of the vertices coincide as well.  $\square$

As a corollary, we obtain Proposition 3.3.

## 6. THE PROOFS OF THEOREM 1.5 AND THEOREM 1.6

In this section we first prove Theorem 1.6, and then deduce Theorem 1.5 from it.

**6.1. The proof of Theorem 1.6.** Let  $v \leq w$  be permutations where  $v \in W_{\max}^K$  and  $w = xv$  is a length-additive factorization. Let  $\mathbf{w}'$  be a standard reduced expression for  $w' := xw_K$  and let  $G_{v,w}$  be the graph obtained from the bridge graph  $B_{w_K, \mathbf{w}'}$  by applying  $v^{-1}$  to the boundary vertices. We label the faces of  $G_{v,w}$  using the target labeling and let  $Q_{v,w}$  be the labeled dual quiver of  $G_{v,w}$  with the vertex labeled  $v^{-1}([k])$  removed. So far, we have shown that  $Q_{v,w}$  is the rectangles seed (Proposition 4.11), and that  $Q_{v,w}$  agrees with  $\Gamma_{U_{v,w}}$  (Theorem 5.18).

Now, let  $G$  be a plabic graph obtained from  $G_{v,w}$  by a sequence of moves (M1)-(M3). The boundary faces of  $G$  have the same labels as the boundary faces of  $G_{v,w}$ . Let  $Q$  be the dual quiver of  $G$ , with the vertex labeled  $v^{-1}([k])$  removed. Recall that a square move at a face of a plabic graph changes the dual quiver via mutation at the corresponding vertex. So we can obtain  $Q$  from  $Q_{v,w}$  by a sequence of mutations. On the other hand, this same sequence of mutations can be performed on the corresponding cluster-tilting module  $U_{v,w}$  and its labeled quiver  $\Gamma_{U_{v,w}}$  resulting in a new module  $U$  and its labeled quiver  $\Gamma_U$ . Now, labeling  $Q$  with target labels, we claim that  $Q = \Gamma_U$ . The two quivers are clearly equal if we ignore the labels, so we only need to show that the labelings coincide. In order to do so, we first establish that  $G_{v,w}$  has the following property.

**Definition 6.1.** [KW14, Definition 10.3] Let  $G$  be a generalized plabic graph. For each trip  $T_{i \rightarrow j}$ , label each edge in the trip with  $j$ . We say  $G$  has the *resonance property* (resp. *anti-resonance property*) if for every vertex  $v$  there are numbers  $i_1 < i_2 < \dots < i_r$  such that when we read the labels of the edges around  $v$  going counterclockwise (resp. clockwise) from the edge labeled  $\{i_1, i_2\}$ , we see  $\{i_1, i_2\}, \{i_2, i_3\}, \dots, \{i_{r-1}, i_r\}, \{i_1, i_r\}$  in that order.

Note that if  $G$  is a generalized plabic graph with vertices of degree at most 3, the resonance (anti-resonance) property reduces to the following: for each vertex  $v$  of degree 3, when we read the labels of edges around  $v$  counterclockwise (clockwise) they are lexicographically decreasing. The (anti-)resonance property is preserved by plabic graph moves [KW14, proof of Theorem 10.5], and gives the following information about the trips coming in to square faces of  $G$ .

**Lemma 6.2.** *Let  $G$  be a generalized plabic graph with the resonance property, and let  $f$  be a square face of  $G$  whose vertices are all of degree 3. Suppose the trips coming into the vertices of  $f$  are  $T_{i \rightarrow a}, T_{j \rightarrow b}, T_{k \rightarrow c}$ , and  $T_{l \rightarrow d}$  reading clockwise around  $f$  (see Figure 22). Then  $a, b, c, d$  are cyclically ordered.*

*Proof.* By symmetry we can assume that either  $a$  or  $b$  is the minimum of  $\{a, b, c, d\}$ . We will show only the case when  $a$  is the smallest of the 4 numbers, as the other case is similar.

Let  $v_a$  be the vertex of  $f$  where  $T_{i \rightarrow a}$  enters the square. Reading counterclockwise, the labels of edges around  $v_a$  are  $\{b, c\}, \{a, c\}, \{a, b\}$ . By the resonance property, this sequence is lexicographically decreasing, so we have that  $b < c$ . Similarly, if  $v_c$  is the vertex of  $f$  where  $T_{k \rightarrow c}$  enters the square, the labels of edges around  $v_c$  are  $\{c, d\}, \{a, d\}, \{a, c\}$  reading counterclockwise. Thus  $c < d$  and  $a < b < c < d$ .  $\square$

**Remark 6.3.** Lemma 6.2 and its proof also hold if you replace “resonance” with “anti-resonance” and “clockwise” with “counterclockwise” throughout. If  $G$  has the (anti-)resonance property when you label edges with sources of trips, rather than targets, then an identical argument shows that in the setting of Lemma 6.2,  $i, j, k, l$  are cyclically ordered.

**Proposition 6.4.** *Let  $v \leq w$  where  $v \in W_{\max}^K$  and  $w$  has length-additive factorization  $w = xv$ . Then  $G_{v,w}$  has the resonance property.*

*Proof.* Let  $\mathbf{w}'$  be a standard expression for  $w' := xw_K$ . Taking into account convention differences, [KW14, Theorem 10.5] implies that  $B_{w_K, \mathbf{w}'}$  has the anti-resonance property. So to show that  $G_{v, w}$  has the resonance property, it suffices to show that if  $x, y, z$  appear in the edges around a trivalent vertex with  $x < y < z$ , then  $x, y, z$  is “reversed” by  $v^{-1}$ ; that is  $v^{-1}(z) < v^{-1}(y) < v^{-1}(x)$  or  $v^{-1}(y) < v^{-1}(x) < v^{-1}(z)$  or  $v^{-1}(x) < v^{-1}(z) < v^{-1}(y)$ . A triple that is not reversed is “preserved”.

A triple  $x < y < z$  is preserved if when we write  $v$  in list notation, we see the substrings  $(\dots, x, \dots, y, \dots, z, \dots)$ ,  $(\dots, y, \dots, z, \dots, x, \dots)$ , or  $(\dots, z, \dots, x, \dots, y, \dots)$ . Since the numbers  $[k]$  and  $[k+1, n]$  appear in decreasing order in  $v$ , the first substring is impossible, the second can occur only if  $x, y \leq k$  and  $z > k$ , and the third can occur only if  $x \leq k$  and  $y, z > k$ .

Let  $L$  denote the lattice path  $L_{v^{-1}([k])}'$  labeled as follows: number the vertical steps of  $L_{v^{-1}([k])}'$  with  $[k]$  from southwest to northeast and number the horizontal steps with  $[k+1, n]$  from southwest to northeast. Recall that reading  $L$  from northeast to southwest gives  $v$  in list notation. It is not hard to see from the preceding paragraph that a triple  $x < y < z$  is preserved exactly when the steps labeled  $x, y, z$  in  $L$  alternate between vertical and horizontal as you walk along  $L$ .

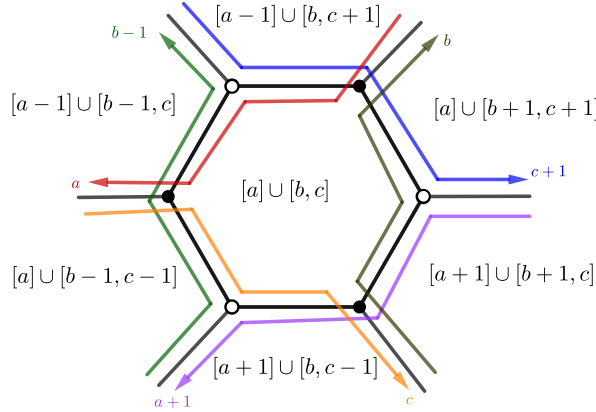


FIGURE 21. The configuration of trips around a hexagonal face  $f$  in  $B_{w_K, \mathbf{w}'}$ . The label indicates the target of the trip. Let  $\lambda$  be the partition such that  $V^\lambda(\lambda) = [a] \cup [b, c]$ . Then starting from the face above  $f$  and moving clockwise, the partitions corresponding to the faces adjacent to  $f$  are obtained from  $\lambda$  by: adding a hook, adding a column, removing a row, removing a hook, removing a column, and adding a row.

We first consider the vertices in an internal hexagonal face  $f$  of  $B_{w_K, \mathbf{w}'}$ . Let  $I := [a] \cup [b, c]$  be the label of  $f$  ( $0 \leq a < b < c \leq n$ ). Since  $f$  is hexagonal,  $\lambda^\vee(I)$  contains a  $2 \times 2$  rectangle, so  $a \leq k-2$  and  $c \geq k+2$ . It follows from the description of  $B_{w_K, \mathbf{w}'}$  in Corollary 4.10 and Proposition 4.11 that the faces adjacent to  $f$  and the trips involving edges of  $f$  are as shown in Figure 21. The edges coming in to vertices are labeled by the two element subsets of one of the following triples:

$$(6.1) \quad \{a, b-1, c\}, \{a, b-1, c+1\}, \{a, b, c+1\}, \{a+1, b-1, c\}, \{a+1, b, c\}, \{a+1, b, c+1\}.$$

Note that in  $L$ , the vertical step labeled  $a$  is to the right of the horizontal step labeled  $c+1$ . Indeed, let  $\lambda = (\lambda_1, \dots, \lambda_k)$  be the partition above  $L$ . Since  $xv$  is length-additive,  $\lambda^\vee(x([k])) \subseteq \lambda$  by Lemma 5.10, so  $\lambda^\vee(I) \subseteq \lambda$  and is not frozen for  $\lambda$ . This implies that  $\lambda_{k-a+1} > b-a$ , the width of  $\lambda^\vee(I)$ . That is, the vertical step labeled  $a$  (which is in row  $k-a+1$ ) appears to the right of the horizontal step labeled  $b-a+k$  (which is in column  $b-a$ ). We also know that  $a+(c-b)+1 = k$ , so we have that the step labeled  $a$  appears to the right of the step labeled  $c+1$ .

This observation is enough to tell us that all triples in Equation (6.1) are reversed. Indeed, all horizontal steps with labels at most  $c+1$  appear to the left of the step labeled  $a$  and all vertical steps with labels at

least  $a$  appear to the right of the step labeled  $c + 1$ , so the steps labeled with triples from Equation (6.1) will not alternate between vertical and horizontal as you walk along  $L$ .

Now, suppose  $\lambda^\vee(I)$  is a single row which is not frozen for  $\lambda^\vee(x([k]))$ . Then  $a = k - 1$  and  $b = c$ . Removing a hook or a row from  $\lambda^\vee(I)$  both result in the empty partition, so the faces adjacent to  $f$  look like Figure 21 with the edge between the lowest and lower right faces removed. The vertex of degree two satisfies the resonance condition. It is not difficult to see that the edges coming in to trivalent vertices are still labeled by the two-element subsets of one of the triples in Equation (6.1), and by the same argument these triples are reversed.

The case when  $\lambda^\vee(I)$  is a single column which is not frozen for  $\lambda^\vee(x([k]))$  is entirely analogous. We have  $b = a + 2$  and  $c = k + 1$ , so the faces adjacent to  $f$  look like Figure 21 with the edge between the lowest and lower left faces removed. Again, the triples whose 2-element subsets label edges around vertices appear in Equation (6.1), so these triples are reversed.

It remains to check the trivalent vertices that are not in any internal face. Such vertices arise when there is more than one  $\lambda$ -frozen rectangle with a single row (column). Let  $v$  be such a vertex. Then it follows from the proof of Proposition 4.11 that  $v$  is in two boundary faces corresponding to  $\lambda$ -frozen rectangles with a single column (resp. row) and is in the boundary face corresponding to the empty partition. The vertex  $v$  is in the unique  $(j, j + 1)$ -bridge used in the construction of  $B_{w_K, \mathbf{w}'}$ . Let  $f$  be the boundary face containing the edges of this bridge. Note that  $v$  is adjacent to the boundary vertex  $j + 1$  (resp.  $j$ ).

If  $f$  corresponds to a rectangle with a single column, its label is  $[j - 1] \cup [j + 1, k + 1]$ ; if  $f$  corresponds to a rectangle with a single row, its label is  $[k - 1] \cup [j + 1, j + 1]$ . Then by a suitable modification of Figure 21, we conclude that the edges around  $v$  are labeled with the two-element subsets of  $\{j, j + 1, k + 1\}$  in the first case and with the two-element subsets of  $\{j, j + 1, k\}$  in the second. In the first case,  $\{j, j + 1, k + 1\}$  is a reversed triple:  $j$  is not a fixed point, so the horizontal step labeled  $k + 1$  in  $L$  (in the first row) precedes the vertical step labeled  $j$ . By an almost identical argument,  $\{k, j, j + 1\}$  is a reversed triple in the second case. □

As an immediate corollary, we have that each of the plabic graphs in Lemma 4.12 has either the resonance or the anti-resonance property.

**Corollary 6.5.** *Let  $x, v$  and  $w = xv$  be as in Proposition 6.4 and let  $\mathbf{w}'$  be a standard reduced expression for  $w' := xw_K$ . Then*

- (1) *the graph obtained from  $B_{w_K, \mathbf{w}'}$  by applying  $w^{-1}$  to the boundary vertices has the resonance property if you label the edges by the sources of trips, rather than targets;*
- (2) *the graph obtained from  $B_{w_K, \mathbf{w}'}$  by applying  $v^{-1}$  to the boundary vertices and “reflecting in the mirror” has the anti-resonance property if you label the edges by the sources of trips;*
- (3) *the graph obtained from  $B_{w_K, \mathbf{w}'}$  by applying  $w^{-1}$  to the boundary vertices and “reflecting in the mirror” has the anti-resonance property.*

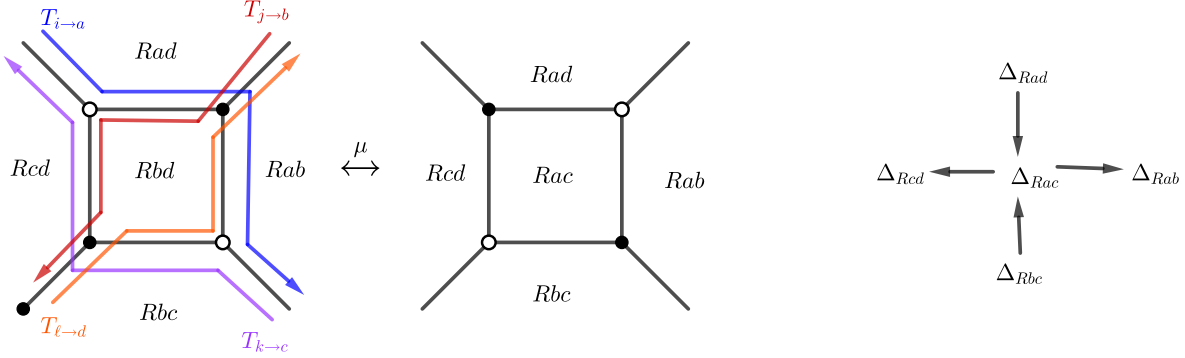
*Proof.* With the labeling indicated, the edges of each of these graphs are labeled with exactly the same sets as the edges of  $G_{v, w}$ . Anti-resonance in 2) and 3) is because “reflecting in the mirror” takes counterclockwise to clockwise. □

We can now show that if  $G$  is a generalized plabic graph move-equivalent to  $G_{v, w}$ , square moves on  $G$  agree with the categorical mutation of modules in  $\mathcal{C}_{v, w}$ . This, together with Theorem 5.18, completes the proof of Theorem 1.6.

**Lemma 6.6.** *Let  $G$  be a reduced plabic graph that is move-equivalent to  $G_{v, w}$ . Suppose that the (target) labeled quiver  $Q(G) = \Gamma_U$ , for some cluster-tilting module  $U \in \mathcal{C}_{v, w}$ . If  $G'$  is obtained from  $G$  by performing a square move at some face  $F$  of  $G$ , then*

$$Q(G') = \Gamma_{U'}$$

*as labeled quivers, where  $U'$  denotes the mutation of  $U$  at the corresponding indecomposable summand  $U_F$  of  $U$ .*


 FIGURE 22. Plabic graphs  $G$  and  $G'$  respectively, and the labeled quiver  $Q(G')$ 

*Proof.* Note that  $G$  has the resonance property, since the resonance property is preserved by moves.

The label of the square face  $F$  and its surrounding faces are given in Figure 22. Here,  $R$  is a  $(k-2)$ -element subset of  $[n]$  and  $Rac$  stands for  $R \cup \{a, c\}$ . Thus,  $F$  has label  $Rac$  in  $G$  and after the mutation it has label  $Rbd$ . By Lemma 6.2,  $a, b, c, d$  are cyclically ordered. Now, consider the local configuration in  $\Gamma_U$  around the vertex  $\Delta_{Rac}$  corresponding to the summand  $U_F$  of  $U$ . By definition of mutation,  $U' = U/U_F \oplus U'_F$ , where  $U'_F$  is defined by the two short exact sequences as follows.

$$0 \longrightarrow U'_F \longrightarrow U_{Rbc} \oplus U_{Rad} \longrightarrow U_F \longrightarrow 0 \quad 0 \longrightarrow U_F \longrightarrow U_{Rab} \oplus U_{Rcd} \longrightarrow U'_F \longrightarrow 0$$

where we identify summand of  $U$  with the labels of the corresponding faces in  $G$ . By the properties of the cluster-character map  $\varphi$  this yields the relation

$$\varphi_{U_F} \varphi_{U'_F} = \varphi_{U_{Rbc}} \varphi_{U_{Rad}} + \varphi_{U_{Rab}} \varphi_{U_{Rcd}}.$$

Note that if one of the faces adjacent to  $F$  has label  $v^{-1}([k])$  then the associated module  $U_{v^{-1}([k])}$  is the zero module and  $\varphi_{U_{v^{-1}([k])}} = \Delta_{v^{-1}([k])} = 1$  by Remark 4.13. In this case, the relation above still holds. Since the two labeled quivers  $Q(G)$  and  $\Gamma_U$  coincide, each function  $\varphi_{U_E} \in \mathbb{C}[\mathcal{R}_{w_k, w}]$ , where  $E$  is a face in  $G$ , is simply a Plücker coordinate coming from the label of the face. In particular, we have the following.

$$\varphi_{U_F} = \varphi_{Rac} = \Delta_{Rac} \quad \varphi_{U_{Rab}} = \Delta_{Rab} \quad \varphi_{U_{Rbc}} = \Delta_{Rbc} \quad \varphi_{U_{Rcd}} = \Delta_{Rcd} \quad \varphi_{U_{Rad}} = \Delta_{Rad}$$

Therefore, the relation above becomes

$$\Delta_{Rac} \varphi_{U'_F} = \Delta_{Rbc} \Delta_{Rad} + \Delta_{Rab} \Delta_{Rcd}$$

which is precisely a three-term Plücker relation in the corresponding skew Schubert variety. Thus, we conclude that  $\varphi_{U'_F} = \Delta_{Rbd}$ . This shows that the two labeled quivers  $Q(G')$  and  $\Gamma_{U'}$  agree.  $\square$

**Remark 6.7.** Since both graphs in Lemma 4.12 give rise to the same labeled seed (up to reversing all arrows in the quiver, which does not affect mutation), and all have the resonant or anti-resonant property by Corollary 6.5, Lemma 6.6 shows that any reduced plabic graph move-equivalent to a graph in Lemma 4.12 gives rise to a seed for  $\pi_k(\mathcal{R}_{v, w})$ .

**6.2. The proof of Theorem 1.5.** We now explain how to deduce Theorem 1.5 from Theorem 1.6.

Recall that for  $v \in W_{\max}^K$ ,  $\pi_k(\mathcal{R}_{v, w_0}) = X_\lambda^\circ$ , where  $V^\vee(\lambda) = v^{-1}([k])$ . The decorated permutation corresponding to  $\pi_k(\mathcal{R}_{v, w_0})$  is  $v^{-1}w_0$ . Recall also that we can obtain  $v^{-1}$  in list notation from  $\lambda$  by labeling the southeast border of  $\lambda$  with  $1, \dots, n$  going southwest and first reading the labels of vertical steps going northeast and then reading the labels of the horizontal steps going northeast. So to obtain  $v^{-1}w_0$ , we reverse the order in which we read the border of  $\lambda$ , first reading the labels of horizontal steps going southwest and then reading the labels of the vertical steps going southwest. Let  $\pi_\lambda^\vee := v^{-1}w_0$ .

Let  $x := w_0 v^{-1}$ , so  $xv = w_0$ . This factorization is length-additive. Let  $\mathbf{w}'$  be a standard reduced expression for  $w' := xw_K$ . If we take  $B_{w_K, \mathbf{w}'}$ , apply  $w_0^{-1}$  to the boundary vertices, and “reflect in the mirror”, we obtain a graph  $G'_{v, w_0}$  which has trip permutation  $\pi'_\lambda$  and whose boundary vertices are labeled with  $1, \dots, n$  clockwise. According to Theorem 5.18 and Lemma 4.12, if we label the dual quiver of  $G'_{v, w_0}$  using target labels, we obtain a seed for the coordinate ring of (the affine cone over)  $X_\lambda$ . And by Remark 6.7, if  $G$  is any reduced plabic graph move-equivalent to  $G'_{v, w_0}$  (that is, with boundary vertices labeled  $1, \dots, n$  clockwise and trip permutation  $\pi'_\lambda$ ), then the (source) labeled dual quiver  $Q(G)$  gives a seed.

## 7. APPLICATIONS

In this section we give applications of Theorem 1.5 and Theorem 1.6.

**7.1. The coordinate rings of Schubert and skew-Schubert varieties.** Combining Theorem 1.5 and Theorem 1.6 with [MS16b, Theorem 3.3] and [Mul13], we obtain the following corollary.

**Corollary 7.1.** *Let  $v \leq w$ , where  $v \in W_{\max}^K$  and  $w = xv$  is length-additive. Then the cluster algebra  $\mathbb{C}[\pi_k(\overline{\mathcal{R}_{v,w}})]$  is locally acyclic, and thus is finitely generated, normal, locally a complete intersection, and equal to its own upper cluster algebra.*

Combining our result with [FS18, Theorem 1.2], we find that the quivers giving rise to the cluster structures for Schubert and skew Schubert varieties admit *green-to-red sequences*, which by [GHKK14] implies that the cluster algebras have *Enough Global Monomials*. Hence, we have the following corollary.

**Corollary 7.2.** *Let  $v \leq w$ , where  $v \in W_{\max}^K$  and  $w = xv$  is length-additive. Then the cluster algebra  $\mathbb{C}[\pi_k(\overline{\mathcal{R}_{v,w}})]$  has a canonical basis of theta functions, parameterized by the lattice of  $g$ -vectors.*

**7.2. Skew Schubert varieties whose cluster structure has finite type.** In [Sco06], Scott classified the Grassmannians whose coordinate rings have a cluster algebra of finite type. He showed that in general the cluster algebras have infinite type, except in the following cases: the coordinate ring of  $Gr_{2,n}$  has a cluster algebra of type  $A_{n-3}$ , while the coordinate rings of  $Gr_{3,6}$ ,  $Gr_{3,7}$ , and  $Gr_{3,8}$  have cluster algebras of types  $D_4$ ,  $E_6$ , and  $E_8$ , respectively.

It is straightforward to classify for which skew Schubert varieties  $\pi_k(\mathcal{R}_{v,w})$  the cluster structure described here is finite type. It depends only on  $wv^{-1}$ . We will need the following two facts.

**Proposition 7.3** ([CK06]). *Let  $Q$  and  $Q'$  be orientations of trees  $T$  and  $T'$ , respectively. If  $Q$  can be obtained from  $Q'$  by a sequence of mutations, then  $T$  and  $T'$  are isomorphic.*

**Lemma 7.4** ([FWZ17, Remark 5.10.9]). *Let  $Q$  be a quiver and let  $Q'$  be a subquiver of  $Q$  consisting of some vertices of  $Q$ , which inherit being frozen or mutable from  $Q$ , and all arrows between them. Then if  $Q$  is mutation equivalent to a (disjoint union of) type ADE Dynkin diagram, so is  $Q'$ .*

**Proposition 7.5.** *Let  $v \leq w$ , where  $v \in W_{\max}^K$  and  $w = xv$  is length-additive. Let  $\lambda = \lambda^\vee(x([k]))$  and let  $\lambda'$  be the diagram obtained from  $\lambda$  by removing all boxes that touch the southeast boundary of  $\lambda$ . Then the cluster algebra  $\mathcal{A} = \mathbb{C}[\pi_k(\overline{\mathcal{R}_{v,w}})]$  given in Theorem 1.6 is*

- (1) *type A if and only if  $\lambda'$  does not contain a  $2 \times 2$  rectangle;*
- (2) *type D if and only if  $\lambda' = (i, 2)$  or its transpose for  $i \geq 2$ ;*
- (3) *type  $E_6$ ,  $E_7$ , or  $E_8$  if and only if  $\lambda'$  or its transpose is one of  $(3, 3)$ ,  $(3, 2, 1)$ ,  $(4, 3)$ ,  $(4, 2, 1)$ ,  $(3, 3, 1)$ ,  $(5, 3)$ ,  $(5, 2, 1)$ ,  $(4, 4)$ ,  $(4, 2, 2)$ .*

*In particular, the cluster algebra associated to the Schubert variety  $X_\lambda$  is of finite type if and only if  $\lambda'$  is in the above list.*

*Proof.* (1) The backwards direction follows from the fact that if  $\lambda'$  does not contain a  $2 \times 2$  rectangle, then  $Q_{v,w}$  is an orientation of a path. For the other direction, recall that the mutable part of all type A quivers can be obtained from a triangulation of a polygon [FWZ17, Lemma 5.3.1]. It is not hard to see that there is no arrangement of 4 arcs in a triangulation that gives the quiver we draw

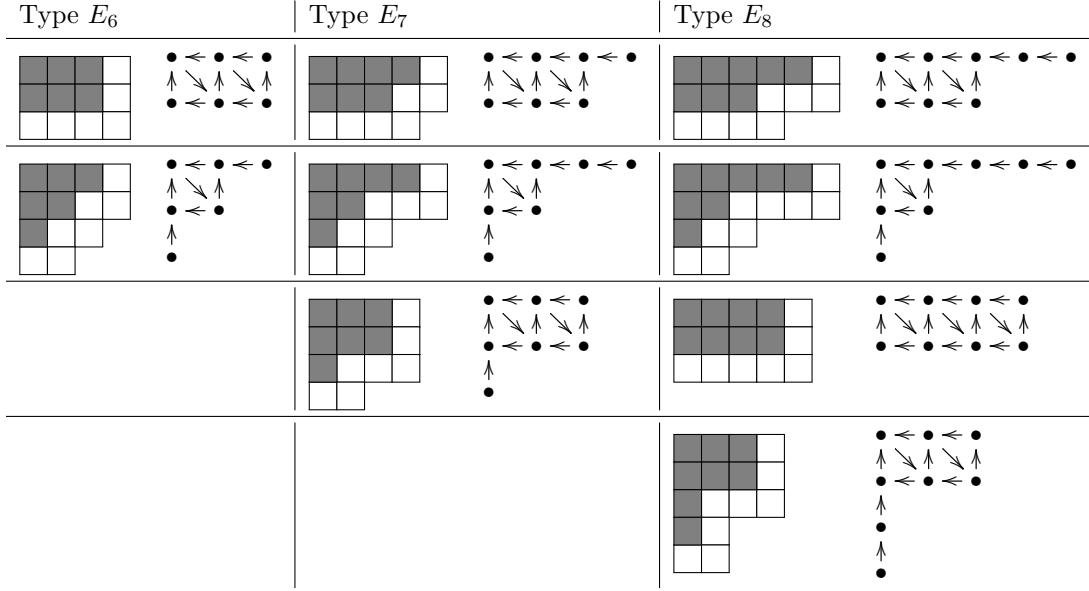


FIGURE 23. Up to transposition, the smallest partitions giving rise to quivers of types  $E_6, E_7, E_8$ , whose mutable parts are shown on the right. The boxes corresponding to mutable vertices are shaded. Adding any number of boxes to the first row or column of these partitions only adds isolated frozen vertices to the quiver, and so also gives rise to a quiver of type  $E_6, E_7, E_8$ .

from a  $2 \times 2$  rectangle according to Definition 3.1, so if  $\lambda'$  contains a  $2 \times 2$  rectangle as a subdiagram,  $\mathcal{A}$  is not type  $A$ .

- (2) The backwards direction follows from inspection of the associated quivers; if one mutates at the vertex in the northwest box, one obtains an orientation of a type  $D$  Dynkin diagram. If  $|\lambda'| \leq 8$ , then necessity follows from direct computation and Proposition 7.3. Four partitions of 8 are not finite type (see Figure 24), so by Lemma 7.4 any partition containing one of these four will not be finite type. The partitions of 9 that are not of type  $A$ , are not  $(7, 2)$  or its transpose, and do not contain a partition of 8 that is infinite type are shown in Figure 24; they are all infinite type. Thus, the only partitions of 9 that are finite type and not type  $A$  are  $(7, 2)$  and its transpose. From this, we can conclude that  $\mathcal{A}$  is type  $D$  only if  $\lambda' = (i, 2)$  or its transpose. Indeed,  $\mathcal{A}$  is infinite type if  $\lambda'$  is not type  $A$  and contains any partition of 9 that is not  $(7, 2)$  or its transpose, or, equivalently, if  $\lambda' \neq (i, 2)$  or its transpose.
- (3) By direct computation, using Proposition 7.3.

□

**7.3. Applications to the preprojective algebra.** As an application of Theorem 5.12, we obtain an explicit way to compute the summands of a cluster-tilting module  $U_{v,w}$ , whereas Leclerc's definition is constructive. This provides a novel connection between Plücker coordinates and the structure of the summands of  $U_{v,w}$ . It is an interesting problem to determine whether this correspondence extends beyond the case of Schubert and skew-Schubert varieties. Such a combinatorial interpretation of the modules would be useful in computing morphisms between the summands of  $U_{v,w}$  for arbitrary  $(v, \mathbf{w})$ . Moreover, given two modules  $U, U' \in \mathcal{C}_{v,w}$  that correspond to Plücker coordinates  $\Delta_P, \Delta_{P'}$  on the positroid variety  $\pi_k(\mathcal{R}_{v,w})$ , it is natural to ask whether we can detect an extension between  $U$  and  $U'$  in terms of the corresponding lattice paths  $L_P^\vee, L_{P'}^\vee$ . In particular, this would tell us whether two cluster variables  $\Delta_P, \Delta_{P'}$  are compatible

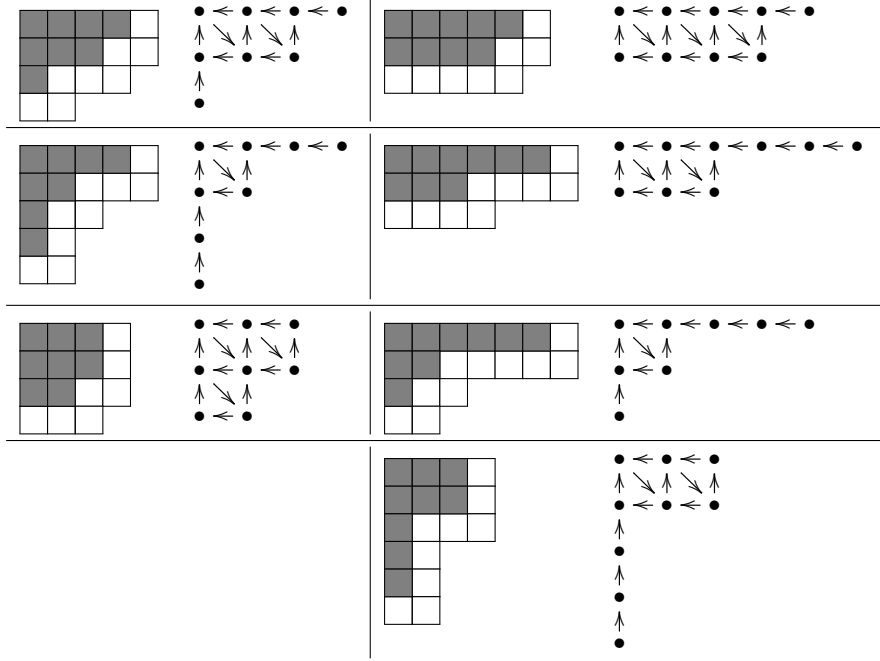


FIGURE 24. These partitions (and their transposes) are the smallest partitions giving rise to quivers of infinite type, whose mutable parts are shown on the right. The boxes corresponding to mutable vertices are shown in green. Adding any number of boxes to the first row or column of these partitions only adds isolated frozen vertices to the quiver, and so also gives rise to a quiver of infinite type.

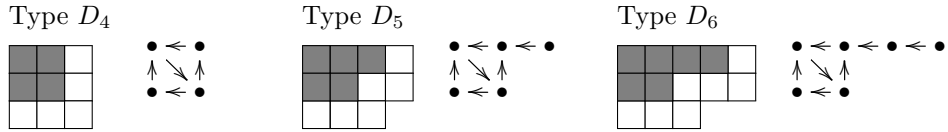


FIGURE 25. A series of Schubert varieties which yield the type  $D_n$  cluster algebras.

in the cluster algebra  $\mathbb{C}[\pi_k(\widehat{\mathcal{R}}_{v,w})]$ . This could provide new insights into the representation theory of preprojective algebras.

Moreover, when  $w = xv$  is length additive and  $v \in W_{max}^K$ , we can explicitly write down many of the seeds for the pair  $(v, w)$  using the combinatorics of plabic graphs. Thus we find that these cluster algebras have all the nice properties mentioned in Section 7.1 (they are locally acyclic, equal to their upper cluster algebra, admit green-to-red sequences, have a canonical basis of theta functions, etc).

#### APPENDIX A. SKEW SCHUBERT VARIETIES

Besides decorated permutations,  $\mathbb{J}$ -diagrams are another combinatorial object indexing positroid varieties. In this section we will give a recipe for the  $\mathbb{J}$ -diagrams of the *skew Schubert varieties*, i.e. the positroids of the form  $\pi_k(\mathcal{R}_{v,w})$ , where  $v \in W_{max}^K$  and  $w$  has a length-additive factorization  $xv$ . Recall that in this case,  $x \in {}^K W$ . The trip permutation of such a positroid is  $v^{-1}xv$ . While we do not know a combinatorial characterization of these trip permutations, we can describe the corresponding  $\mathbb{J}$ -diagrams.

**A.1. The  $\mathbb{J}$ -diagrams associated to skew Schubert varieties.** We first need some preliminary notions, following [LW08].



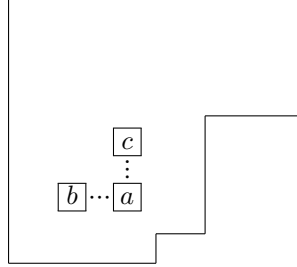


FIGURE 26. The  $\mathcal{J}$ - property: if  $b, c = +$  then  $a = +$ .

For a Young diagram  $\lambda$  that fits inside of a  $k \times (n - k)$  rectangle, let  $u_\lambda^\nearrow \in {}^K W$  be the Grassmannian permutation of type  $(k, n)$  with  $u_\lambda^\nearrow([k]) = V^\nearrow(\lambda)$ .

**Definition A.1.** An  $\oplus$ -diagram (“o-plus diagram”)  $O$  of shape  $\lambda$  is a Young diagram  $\lambda$  that has been filled with 0’s and +’s. We say  $O$  is of type  $(k, n)$  if  $\lambda$  fits into a  $k \times (n - k)$  rectangle. An  $\oplus$ -diagram is a  $\mathcal{J}$ -diagram (“Le-diagram”) if the “ $\mathcal{J}$ -property” holds: there is no 0 such that there is a + above it in the same column and a + to its left in the same row (see Figure 26).

Suppose  $\lambda$  fits inside of a  $k \times (n - k)$  rectangle. By Lemma 2.21, given a reading order, we can obtain a reduced expression  $\mathbf{u}$  for  $u_\lambda^\nearrow$  from  $\lambda$ . Fixing a reading order, each  $\oplus$ -diagram  $O$  of shape  $\lambda$  gives a subexpression  $\mathbf{r}$  of  $\mathbf{u}$ , obtained by replacing each simple transposition in a box filled with a + by a 1. The permutation  $r$  given by this subexpression does not depend on the reading order [LW08, Proposition 4.6], so we will denote it by  $r(O)$  (for the “reading word” of  $O$ ).

Note that by [Pos, Lemma 19.3],  $O$  is a  $\mathcal{J}$ -diagram if and only if  $\mathbf{r}$  is a *positive distinguished subexpression* of  $\mathbf{u}$  (see Definition B.1).

**Proposition A.2.** Let  $M$  be a  $\mathcal{J}$ -diagram of shape  $\lambda$  with reading word  $r$ , and let  $u = u_\lambda^\nearrow$ . Then  $M$  corresponds to the positroid variety  $\pi_k(\mathcal{R}_{u^{-1}w_0, r^{-1}w_0})$

*Proof.* By [Pos, Theorem 19.1],  $M$  corresponds to  $\pi_k(\mathcal{R}_{r^{-1}, u^{-1}})$ . Note that in the complete flag variety, the map  $Bx \rightarrow Bxw_0$  gives an isomorphism between  $\mathcal{R}_{v, w}$  and  $\mathcal{R}_{wv_0, v w_0}$ . The proposition follows immediately.  $\square$

**Remark A.3.** Let  $v \in W_{\max}^K$  and  $u \in W_{\min}^K$ . The  $\mathcal{J}$ -diagram of  $\pi_k(\mathcal{R}_{v, w_0}) \cong X_{v^{-1}([k])}^\circ$  has shape  $\lambda^\vee(v^{-1}([k]))$  and every box contains a +. For  $u \in W_{\min}^K$ , the  $\mathcal{J}$ -diagram of  $\pi_k(\mathcal{R}_{w_K, w_K u}) \cong (X^{u^{-1}([k])}^\circ)^\circ$  is the  $k \times (n - k)$  rectangle where all boxes above  $L_{u^{-1}([k])}^\vee$  contain 0’s and all boxes below contain +’s.

We can use  $\mathcal{J}$ -moves to change  $\oplus$ -diagrams into  $\mathcal{J}$ -diagrams.

**Definition A.4.** [LW08, Section 5] Suppose  $O$  is an  $\oplus$ -diagram containing a rectangular subdiagram where all non-corner boxes are filled with zeros and the northeast and southwest corners are filled with pluses (shown below). If  $b$  is 0, a  $\mathcal{J}$ -move changes  $b$  to + and changes  $a$  either from 0 to + or from + to 0.

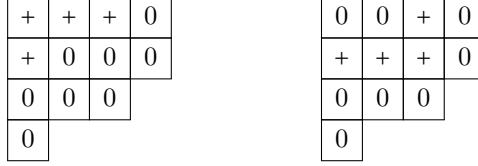
$a$	0	0	0	+
0	0	0	0	0
+	0	0	0	$b$

Note that these are actually the *rectangular*  $\mathcal{J}$ -moves of [LW08, Definition 4.11].

See Figure 27 for examples of  $\mathcal{J}$ -moves.

The key properties of  $\mathcal{J}$ -moves are as follows.

**Lemma A.5.** [LW08, Lemma 4.13, Proposition 4.14] *Let  $O$  be an  $\oplus$ -diagram.*

FIGURE 27. Two  $\mathbb{I}$ -moves.FIGURE 28. On the left,  $O_{x,v}$  and on the right,  $M(O_{x,v})$  for  $x = (1, 2, 4, 7, 3, 5, 6, 8)$  and  $v = (4, 3, 8, 2, 7, 6, 1, 5)$ .

- (1)  $O$  can be made into a  $\mathbb{I}$ -diagram  $M$  (“ $\mathbb{I}$ -ified”) by a finite sequence of  $\mathbb{I}$ -moves.
- (2) If  $O'$  is related to  $O$  by a sequence of  $\mathbb{I}$ -moves, then  $r(O) = r(O')$ .
- (3)  $M := M(O)$  does not depend on the sequence of  $\mathbb{I}$ -moves.

Now, consider  $x \in {}^K W$  and  $v \in W_{max}^K$  such that  $\ell(xv) = \ell(x) + \ell(v)$ . Recall from Lemma 5.10 that  $L_{x([k])}^{\nearrow}$  lies above  $L_{v^{-1}([k])}^{\swarrow}$ . Let  $\lambda_x$  and  $\lambda_v$  be the partitions above  $L_{x([k])}^{\nearrow}$  and  $L_{v^{-1}([k])}^{\swarrow}$ , respectively.

**Definition A.6.** Let  $O_{x,v}$  be the  $\oplus$ -diagram of shape  $\lambda_v$  with the boxes in  $\lambda_x$  filled with +’s and all other boxes filled with 0’s (see Figure 28).

**Proposition A.7.**  $M(O_{x,v})$ , the  $\mathbb{I}$ -ification of  $O_{x,v}$ , is the  $\mathbb{I}$ -diagram of  $\pi_k(\mathcal{R}_{v,xv})$ .

**Remark A.8.** Proposition A.7, together with the definition of  $O_{x,v}$  (which is determined by two noncrossing lattice paths in a rectangle, i.e. a skew Young diagram), is the reason that we refer to these positroid varieties as *skew Schubert varieties*.

*Proof.* Let  $M := M(O_{x,v})$ . Note that  $u_{\lambda_v}^{\nearrow}$  (that is, the Grassmannian permutation of type  $(k, n)$  which maps  $[k]$  to  $V^{\nearrow}(\lambda_v)$ ) is equal to  $w_0 v^{-1}$ . The reading word of  $O_{x,v}$ , and thus of  $M$ , is  $w_0 v^{-1} x^{-1}$ ; this follows from the fact that there is a reading order for  $\lambda_v$  which reads the boxes of  $\lambda_v \setminus \lambda_x$  before the boxes of  $\lambda_x$ . So by Proposition A.2,  $M$  corresponds to  $\pi_k(\mathcal{R}_{v,xv})$ .  $\square$

## APPENDIX B. A CLUSTER STRUCTURE NOT REALIZABLE BY GENERALIZED PLABIC GRAPHS

If  $\pi_k(\mathcal{R}_{v,w})$  is not a skew Schubert variety, it is in general impossible to realize the seeds from Leclerc’s construction (Theorem 5.3) as labeled quivers coming from (generalized) plabic graph. Indeed, this can fail even in  $Gr_{2,5}$ . Before giving an example, we briefly review Leclerc’s construction for the pair  $(v, \mathbf{w})$ , where  $v \in W_{max}^K$ ,  $v < w$  and  $\mathbf{w}$  is a reduced expression for  $w$ .

**Definition B.1.** Let  $v \leq w$  be permutations and  $\mathbf{w} = s_{i_t} \cdots s_{i_1}$  a reduced expression for  $w$ . The *positive distinguished subexpression* for  $v$  in  $\mathbf{w}$  is a reduced expression  $\mathbf{v} = v_t \cdots v_1$  where  $v_j \in \{s_{i_j}, e\}$ . We give  $\mathbf{v}$  in terms of the products  $v_{(j)} := v_j \cdots v_2 v_1$ . We set  $v_{(0)} = e$  and

$$v_{(j)} = \begin{cases} s_{i_j} v_{(j-1)} & \text{if } v v_{(j)}^{-1} s_{i_j} < v v_{(j)}^{-1} \\ v_{(j-1)} & \text{otherwise.} \end{cases}$$

In other words, the positive distinguished subexpression for  $v$  is the rightmost subexpression for  $v$  in  $\mathbf{w}$ , working from right to left.

Let  $\mathbf{v}$  be the positive distinguished subexpression for  $v$  in  $\mathbf{w} = s_{i_t} \cdots s_{i_2} s_{i_1}$ . Let  $w_{(j)} = s_{i_j} \cdots s_{i_2} s_{i_1}$  for  $1 \leq j \leq t$  and let  $v_{(j)} = v_j \cdots v_1$  be as in the above definition. Let  $J \subset \{1, \dots, t\}$  be the collection of indices  $j$  such that  $v_j = e$ . According to Theorem 5.3, the cluster variables in the seed corresponding to  $(v, \mathbf{w})$  are the distinct irreducible factors of  $\prod_{j \in J} \Delta_{v_{(j)}^{-1} \{[i_j]\}, w_{(j)}^{-1} \{[i_j]\}}$ .

**Example B.2.** Consider  $v = (2, 5, 1, 4, 3)$ ,  $w = (5, 3, 4, 2, 1)$  and the following reduced expression  $\mathbf{w}$  for  $w$ , where the positive distinguished subexpression for  $v$  is in bold:

$$\mathbf{w} = s_1 s_2 \mathbf{s_1 s_3 s_2 s_4 s_3 s_2 s_1}.$$

Note that  $w$  does not have a length-additive factorization ending in  $v$ .

If one computes the generalized minors  $\Delta_{v_{(j)}^{-1}([i_j]), w_{(j)}^{-1}([i_j])}$  coming from Theorem 5.3, they are not all irreducible. However, if we associate Plücker coordinates to the irreducible factors of these generalized minors (as in Section 5.2), we obtain  $\Delta_{13}, \Delta_{23}, \Delta_{14}, \Delta_{45}, \Delta_{15}$ .

However,  $\{13, 23, 14, 45, 15\}$  cannot be the set of face labels of a generalized plabic graph for  $Gr_{2,5}$ . This comes from the fact that the number 2 appears only once among the set  $\{13, 23, 14, 45, 15\}$ . In more detail, suppose  $G$  were such a generalized plabic graph.  $G$  has no internal faces and no lollipops. Without loss of generality,  $G$  is source-labeled. The face  $f$  labeled 23, is adjacent to one other face, labeled 13. So consider the trip  $T$  beginning at 2 and ending at  $j$ . We know that  $f$  is the only face to the left of this trip, and that  $T$  must pass through vertices of degree 2 only. Then the trip beginning at  $j$  is again  $T$ , traveled in the opposite direction. Thus,  $j$  must be in the label of every face besides  $f$ , a contradiction.

On the other hand,  $\{13, 23, 14, 45, 15\}$  is a subset of the face labels of a plabic graph for the top cell in  $Gr_{2,5}$ , since it is a weakly separated collection. Further, variables in the rectangles seed for the skew-Schubert varieties is always a subset of the face labels of a plabic graph  $G$  for the top cell (and the quiver for the rectangles seed is obtained from  $Q(G)$  by deleting some vertices and freezing others). One might ask if the seeds given in Leclerc's construction can always be obtained from a plabic graph for the top cell in this way. The following example will show that this is not the case.

**Example B.3.** Consider  $v = (3, 2, 7, 6, 1, 5, 4)$ ,  $w = (7, 6, 4, 2, 5, 3, 1)$ , and the following reduced expression  $\mathbf{w}$  for  $w$ , where the positive distinguished subexpression for  $v$  is in bold:

$$\mathbf{w} = \mathbf{s_1 s_2 s_3 s_2 s_1 s_4 s_5 s_4 s_3 s_2 s_6 s_5 s_4 s_3 s_2 s_1 s_5 s_2}$$

The irreducible factors of the generalized minors  $\Delta_{v_{(j)}^{-1}([i_j]), w_{(j)}^{-1}([i_j])}$  are  $\Delta_{135}, \Delta_{126}, \Delta_{235}, \Delta_{345}, \Delta_{145}, \Delta_{467}, \Delta_{127}$ , and  $\Delta_{125}$  (the first variable is mutable and the others are frozen). Note that 467 and 235 are not weakly separated, so this set of Plücker coordinates cannot be a subset of the face labels of a plabic graph for the top cell.

## REFERENCES

- [ASS06] Ibrahim Assem, Daniel Simson, and Andrzej Skowroński. *Elements of the representation theory of associative algebras. Vol. 1*, volume 65 of *London Mathematical Society Student Texts*. Cambridge University Press, Cambridge, 2006. Techniques of representation theory.
- [BIRS09] A. B. Buan, O. Iyama, I. Reiten, and J. Scott. Cluster structures for 2-Calabi-Yau categories and unipotent groups. *Compos. Math.*, 145(4):1035–1079, 2009.
- [BKT14] Pierre Baumann, Joel Kamnitzer, and Peter Tingley. Affine Mirković-Vilonen polytopes. *Publ. Math. Inst. Hautes Études Sci.*, 120:113–205, 2014.
- [Che12] N. Chevalier. *Algèbres amassées et positivité*. 2012. Thesis (Ph.D.)—Université de Caen.
- [CK06] Philippe Caldero and Bernhard Keller. From triangulated categories to cluster algebras. II. *Ann. Sci. École Norm. Sup. (4)*, 39(6):983–1009, 2006.
- [Fra16] Chris Fraser. Quasi-homomorphisms of cluster algebras. *Adv. in Appl. Math.*, 81:40–77, 2016.
- [FS18] Nicolas Ford and Khrystyna Serhiyenko. Green-to-red sequences for positroids. *J. Combin. Theory Ser. A*, 159:164–182, 2018.
- [FSB19] Chris Fraser and Melissa Sherman-Bennett. Quasi-isomorphic cluster structures on positroid varieties, 2019. In preparation.
- [FWZ17] Sergey Fomin, Lauren Williams, and Andrei Zelevinsky. Introduction to cluster algebras. Chapters 4-5, 2017. preprint, [arXiv:1707.07190](https://arxiv.org/abs/1707.07190).

- [FZ02] Sergey Fomin and Andrei Zelevinsky. Cluster algebras. I. Foundations. *J. Amer. Math. Soc.*, 15(2):497–529 (electronic), 2002.
- [GHKK14] Mark Gross, Paul Hacking, Sean Keel, and Maxim Kontsevich. Canonical bases for cluster algebras, 2014. preprint, [arXiv:1411.1394](https://arxiv.org/abs/1411.1394).
- [GLS08] Christof Geiss, Bernard Leclerc, and Jan Schröer. Partial flag varieties and preprojective algebras. *Ann. Inst. Fourier (Grenoble)*, 58(3):825–876, 2008.
- [GLS11] Christof Geiss, Bernard Leclerc, and Jan Schröer. Kac-Moody groups and cluster algebras. *Adv. Math.*, 228(1):329–433, 2011.
- [Kar16] Rachel Karpman. Bridge graphs and Deodhar parametrizations for positroid varieties. *J. Combin. Theory Ser. A*, 142:113–146, 2016.
- [KL79] David Kazhdan and George Lusztig. Representations of Coxeter groups and Hecke algebras. *Invent. Math.*, 53(2):165–184, 1979.
- [KLS13] Allen Knutson, Thomas Lam, and David E. Speyer. Positroid varieties: juggling and geometry. *Compos. Math.*, 149(10):1710–1752, 2013.
- [KW14] Yuji Kodama and Lauren Williams. KP solitons and total positivity for the Grassmannian. *Invent. Math.*, 198(3):637–699, 2014.
- [Lec16] B. Leclerc. Cluster structures on strata of flag varieties. *Adv. Math.*, 300:190–228, 2016.
- [LS15] Kyungyong Lee and Ralf Schiffler. Positivity for cluster algebras. *Ann. of Math. (2)*, 182(1):73–125, 2015.
- [LW08] Thomas Lam and Lauren Williams. Total positivity for cominuscule Grassmannians. *New York J. Math.*, 14:53–99, 2008.
- [MS16a] G. Muller and D. Speyer. The twist for positroids, 2016. preprint, [arXiv:1606.08383](https://arxiv.org/abs/1606.08383) [math.CO].
- [MS16b] Greg Muller and David E. Speyer. Cluster algebras of Grassmannians are locally acyclic. *Proc. Amer. Math. Soc.*, 144(8):3267–3281, 2016.
- [Mul13] Greg Muller. Locally acyclic cluster algebras. *Adv. Math.*, 233:207–247, 2013.
- [OPS15] Suho Oh, Alexander Postnikov, and David E. Speyer. Weak separation and plabic graphs. *Proc. Lond. Math. Soc. (3)*, 110(3):721–754, 2015.
- [Pos] A. Postnikov. Total positivity, Grassmannians, and networks. Preprint. Available at <http://www-math.mit.edu/~apost/papers/tpgrass.pdf>.
- [Ric92] R. W. Richardson. Intersections of double cosets in algebraic groups. *Indag. Math. (N.S.)*, 3(1):69–77, 1992.
- [Rie98] K. Rietsch. *Total positivity and real flag varieties*. ProQuest LLC, Ann Arbor, MI, 1998. Thesis (Ph.D.)–Massachusetts Institute of Technology.
- [Rin98] Claus Michael Ringel. The preprojective algebra of a quiver. In *Algebras and modules, II (Geiranger, 1996)*, volume 24 of *CMS Conf. Proc.*, pages 467–480. Amer. Math. Soc., Providence, RI, 1998.
- [Sch14] Ralf Schiffler. *Quiver representations*. CMS Books in Mathematics/Ouvrages de Mathématiques de la SMC. Springer, Cham, 2014.
- [Sco06] Joshua S. Scott. Grassmannians and cluster algebras. *Proc. London Math. Soc. (3)*, 92(2):345–380, 2006.
- [Ste96] John R. Stembridge. On the fully commutative elements of Coxeter groups. *J. Algebraic Combin.*, 5(4):353–385, 1996.
- [Wil07] Lauren K. Williams. Shelling totally nonnegative flag varieties. *J. Reine Angew. Math.*, 609:1–21, 2007.

DEPARTMENT OF MATHEMATICS, UNIVERSITY OF CALIFORNIA AT BERKELEY, BERKELEY, CA USA  
*E-mail address:* [khrystyana.serhiyenko@berkeley.edu](mailto:khrystyana.serhiyenko@berkeley.edu)

DEPARTMENT OF MATHEMATICS, UNIVERSITY OF CALIFORNIA AT BERKELEY, BERKELEY, CA USA  
*E-mail address:* [m.shermanbennett@berkeley.edu](mailto:m.shermanbennett@berkeley.edu)

DEPARTMENT OF MATHEMATICS, HARVARD UNIVERSITY, CAMBRIDGE, MA USA  
*E-mail address:* [williams@math.harvard.edu](mailto:williams@math.harvard.edu)